2011

Analysis and Fingerprinting of Glycosaminoglycans

Joseph King
Virginia Commonwealth University

ANALYSIS AND FINGERPRINTING OF GLYCOSAMINOGLYCANS

A dissertation submitted in partial fulfillment of the requirements for the degree of Doctor of Philosophy at Virginia Commonwealth University.

by

JOSEPH TIMOTHY KING

Director: UMESH R. DESAI
Professor, Department of Medicinal Chemistry

Virginia Commonwealth University
Richmond, VA
July, 2011

Acknowledgements

I owe a great deal to many individuals for helping me through my graduate studies. First and foremost, I thank my advisor Dr. Umesh Desai for his mentorship and support. Who would have thought that a small summer project on low molecular weight heparins would have become a dissertation! This would have never succeeded without Dr. Desai's mentorship and support. The knowledge and skills that I have learned from him with respect to technical writing and scientific thinking are invaluable.

I have been privileged to work with some amazing people in the Desai lab group and in the Institute for Structural Biology and Drug Discovery. Whether I was trying to resolve a tough organic chemistry issue and needed guidance or if I just wanted a laugh, there was always someone to talk to. I especially thank Dr. Aiye Liang and Dr. Jay Thakkar for our many conversations whether scientific or not in their content. I will never forget the two long trips we took as a team to Nashville and Orlando. It made for a very interesting car ride! Special thanks goes to Akul Mehta for his advice concerning NMR and for his ability to smile or laugh at almost anything I say or do. Thanks also to all the other Desai lab group members that I have been privileged to interact with. You guys are the best! Thanks also to Justin Elenewski, Phil Mosier, Chengxiao Da, Meng Zhang, and Maria Palesis for being there on the late night shift. It would not have been the same without you.

The faculty and administration of the VCU School of Pharmacy have been outstanding. Thanks to Dr. Karnes, Dr. Safo, Dr. Westkaemper, and Dr. Brophy for serving on my committee. I also thank Dr. Wu-Pong, Dr. Reinders, and Karen Bryant for career advice and guiding me through the entire graduation process. I also thank my pharmacy clerkship mentors for giving me much needed experience in the realm of pharmacy as working day and night in a lab can make one lacking in such skills!

Finally, there many individuals outside of the School of Pharmacy who have been instrumental in successful bringing me through the last six years that I should acknowledge. I owe a great deal of gratitude to my parents who have continually supported me with their love and prayers. Thanks also to my friends from the bible study groups I have participated in and to Calvary Baptist Church. Special thanks also goes out to JoAnna Talbott and her family as they have been a source of great encouragement, blessing, and joy to me in the last months of my time at VCU. Most of all, I thank Christ Jesus my Lord who has guided me with loving kindness and abundant grace through this time of my life. Words could never express my gratitude.

Table of Contents

List of Tables

List of Figures

List of Equations

List of Abbreviations

aPTT, activated partial thromboplastin time; CE, capillary electrophoresis; COSY,correlation spectroscopy; CS,chondroitin sulfate; DS, dermatan sulfate; DVT, deep vein thrombosis; ELSD, evaporative light scattering detection; ESI, electrospray ionization; FDA, food and drug administration; GAG, glycosaminoglycan; Glc, glucuronic acid; GlcNAc, N-acetyl-glucosamine; HIT, heparin induced thrombocytopenia; HMBC, heteronuclear multiple bond correlation; HMQC, heteronuclear multiple quantum coherence; HPLC, high performance liquid chromatography; HS, heparan sulfate; KS, keratan sulfate; LMWH, low molecular weight heparin; LOD, limit of detection; LOQ, limit of quantitation; MEKC, micellar electrokinetic chromatography; MS, mass spectrometry; NMR, nuclear magnetic resonance; NOESY, nuclear overhauser effect spectroscopy; OSCS, oversulfated chondroitin sulfate; PAGE, polyacrylamide gel electrophoresis ; PCA, principle component analysis ; PLS-DA, partial least square - discriminant analysis; ROESY, rotational nuclear overhauser effect Spectroscopy; SAX, strong anion exchange; SDS, sodium dodecylsulfate; TOCSY, total correlation spectroscopy; UFH, unfractionated heparin; UPLC, ultra performance liquid chromatography; USP, US pharmacopeia; UV, ultraviolet.

Abstract

ANALYSIS AND FINGERPRINTING OF GLYCOSAMINOGLYCANS

By Joseph Timothy King, PhD

A dissertation submitted in partial fulfillment of the requirements for the degree of Doctor of Philosophy at Virginia Commonwealth University.

Virginia Commonwealth University, 2011

Major Director: Umesh R. Desai
Professor, Department of Medicinal Chemistry

Heparin is a complex mixture of sulfated polysaccharides derived from animals and one of the oldest drugs in use. While an efficacious anticoagulant, heparin is beset by side effects and pharmacokinetic difficulties. Low molecular weight heparins (LMWH) are made by depolymerizing unfractionated heparin (UFH) and have made improvements in these areas. However, they still retain a phenomenally high level of complexity due to their polydispersity and the introduction of non-native structural features. This makes the structural characterization LMWHs a daunting task.

This work details the development of a novel capillary electrophoretic (CE) method for fingerprinting LMWHs. Since their complexity normally results in a nearly featureless electropherogram, polyalkylamines were used as a resolving agents to yield highly resolved and reproducible fingerprints characteristic of the LMWH being investigated.

Linear polyamines of resolved LMWH in a manner dependent on chain length and charge density, while cyclic polyamines were incapable of resolution. Longer length glycosaminoglycans such as UFH and chondroitin sulfate were not successfully fingerprinted as they lacked run to run consistency. Further investigation into the mode of polyamine binding showed that they bound to LMWH via a two site binding model, indicating the presence of specific sites on LMWH that tightly bind polyamines. Upon the saturation of these sites, the polyamines continue to interact via general electrostatic binding. Pentaethylenehexamine was also able to separate the known contaminant oversulfated chondroitin sulfate from UFH.

In July of 2010, the US food and drug administration approved a generic for the widely used LMWH enoxaparin, a questionable move due to the difficulties of proving the equivalence of such a complex mixture. A comparison of the brand and generic batches of enoxaparin using the fingerprinting method revealed striking similarities, bolstering the generic's claim of equivalency and providing a protocol for the evaluation of other biosimilar LMWHs.

This is the first work utilizing CE in developing high resolution fingerprints of LMWH. It presents a noteworthy method for quality assessment of LMWH and provides the basis for designing other small molecule probes for the analysis of complex glycosaminoglycans.

Introduction

1.1 The Structure, Source, and Pharmacological Properties of Heparin

Heparin is a heterogeneous, polydisperse, highly sulfated natural polysaccharide that is widespread among species ranging from invertebrates, such as shrimp and clams, to mammals, such as cows and humans [1-2]. Part of the larger family of carbohydrates, known as glycosaminoglycans (GAGs), it is the oldest anticoagulant in use and one of the longest serving pharmaceuticals [3]. Along with its closely related cousin heparan sulfate (HS), it has been shown to interact with a myriad of proteins such as antithrombin, granulocyte-colony stimulating factor, fibroblast growth factors, chemokines such as interleukins, cellular adhesion proteins such as selectins and fibronectin, pathogen proteins from herpes-simplex and human immunodeficiency viruses, and many others [4-6]. The structural diversity of heparin and HS makes them among the most difficult substances to analyze, but also gives them a rich biological profile as evidenced by the numerous review articles detailing heparin/HS interactions with proteins that have been published to date [2,4,6,7]. These promise much in the area of drug discovery [7].

The biosynthesis of these polymers differs enormously from that of proteins in that there is no template that codes for them. Instead, the synthesis of heparin, HS, and related sugars is carried out by a host of enzymes that yield a complicated mixture of molecules. The synthetic process begins with the building of a specific tetrasaccharide sequence on a serine residue of a core protein. In the crucial step that follows, an

acetylated glucosamine (GlcNAc) is added to the tetrasaccharide, ensuring that the resulting molecule will be heparin or HS rather than another GAG. The chain is extended by adding glucuronic acid (GlcA) and GlcNAc in an alternating manner by the work of GlcA/GlcN transferases, with GlcNAc(1→4)GlcA as the sequence. This is followed by the N-deacetylation and subsequent N-sulfation of GlcNAc and then by the epimerization of many glucuronic acids to iduronic acid by C-5 epimerase. Finally, 2-O, 3-O, and 6-O sulfotransferases extensively sulfate the sugar, making it one of the strongest acids in nature. However, none of these enzymes modify the GAG backbone to completion or in an equivalent manner. The resulting hodgepodge, appropriately called unfractionated heparin (UFH), is a mixture of millions of structurally distinct polysaccharides with an average molecular weight of ~15 kDa and an average chain length of ~50 residues when harvested, yielding a astonishingly heterogeneous and polydisperse mixture of molecules [6,8,9].

While heparin and HS are closely related, there are a number of key differences between them. First, heparin chains are freed from the proteoglycan core by *endo*-β-D-glucuronidase after synthesis and are subsequently stored in the granules of mast cells along with various positively charged proteases and histamine. In contrast, HS is found on the surfaces of many cells and interacts with many proteins in the body [4,5]. HS is also larger then heparin with a molecular weight range of 5-50 kDa and an average of 30 kDa, while heparin ranges from 5-40 kDa with an average of 12 kDa. Heparin is extensively sulfated and most glucuronic acid residues are converted to iduronic acid during synthesis (~90%,) while HS is less sulfated with a lesser degree of epimierization. Thus, HS is more complex than heparin, having a higher degree of

polydispersity and heterogeneity [5,9]. Related GAGs include chondroitin sulfate (CS), dermatan sulfate (DS), and Keratan sulfate (KS), and hylauronic acid that differ from heparin with relation to sugar conformation and composition, degree of sulfation, the type of linkages between sugars, molecular weight, their location in the body, and their functions. Representitive structures of several GAGs are pictured in **figure 1** [6].

Heparin was discovered almost a century ago and began to see use as an anticoagulant in the 1930's [10]. Since then much has been discovered with respect to the structure and mechanism responsible for this activity. Heparin inhibits blood coagulation by binding to a highly positively charged site on antithrombin, a serpin, specifically by a sequence known as the H5 pentasaccharide. While antithrombin is always present in the blood, it is relatively inactive. The binding of H5 causes a conformational change in the serpin that increases its ability to inhibit by several hundred fold a number of coagulation proteases, but most notably factor Xa and factor IIa (thrombin). This maintains normal hemostasis by preventing unwanted thrombosis [11].

UFH's longevity is a testimony to its therapeutic efficacy, but it is not without problems. The drug exhibits irregular pharmacokinetics due to extensive protein binding which makes routine monitoring of activated partial thromboplastin time (aPTT) necessary if therapeutic anticoagulation is to be acheived and maintained. UFH and may also cause osteoporosis with long term use [12]. The most alarming problem with UFH is heparin-induced thrombocytopenia (HIT). HIT manifests itself by a precipitous drop in platelets and is caused by antibodies that form against heparin-platelet factor 4 complexes. While it is an efficacious anticoagulant, these drawbacks make UFH an

expensive and often risky drug to administer and largely limit its use to inpatient settings.

1.2 The Structure and Pharmacological Properties of Low Molecular Weight Heparin

Low molecular weight heparins (LMWH) were developed in the 1990's by depolymerizing UFH by various methods to yield a mixture of compounds between 2,000 and 9,000 daltons. While they share many chemical and therapeutic features with UFH, LMWHs are distinct in a number of ways. They inhibit factor Xa to a greater extent than thrombin because longer GAG chains are needed for this to occur [13,14]. LMWHs generally exhibit better pharmacokinetics due to less binding to plasma proteins and platelets resulting in substantially fewer monitoring requirements. Less binding to proteins, platelets, and osteoblasts decreases many of the undesirable side effects, such as HIT and osteoporosis [12,13]. The risk of bleeding between LMWH and UFH is similar as shown in a recent meta-analysis comparing UFH and enoxaparin in patients receiving deep vein thrombosis (DVT) prophylaxis [15]. These features represent a significant improvement over UFH and their prominence in the prevention and treatment of venous thromboembolic disease and is even used in outpatient settings [16,17].

One thing that has long been apparent concerning LMWHs is the diversity that exists between varying brands and formulations. This diversity is determined by a number of factors including: 1) the source of the crude heparin extract, 2) the quality and rigor of the post extraction purification yielding clinical UFH, 3) the method by which UFH is depolymerized to yield LMWH. The latter is the most critical in

contributing to LMWH identity and in the introduction of novel structural features [2]. The three brands of LMWH available in the US are tinzaparin (Innohep^{TM}, M_r: 4500), dalteparin (Fragmin^{TM}, M_r:6000) and enoxaparin (Lovenox^{TM}, M_r:4200). Tinzaparin is manufactured via heparinase digestion to yield a smaller GAG chain with an unsaturated uronate residue on the non-reducing end. Dalteparin is formed by treating UFH with nitrous acid to yield LMWH molecules with a five-membered anhydromannitol residue at the reducing end. Enoxaparin is manufactured under basic conditions yielding a chain with an unsaturated uronate residue in a manner similar to tinzaparin but with chains also containing a 1,6-anhydromannose on the reducing end (**figure 2**) [2,18,19]. Because our ability to analyze these complex mixtures is limited, other chemical features not found in UFH may also be present. This makes each brand on the US and world market to be considered a distinct pharmacological entity that is not interchangeable according to the FDA [13].

The uncertainty surrounding the structure of LMWHs has come to forefront in recent years with the introduction of generic enoxaparin formulations. These are often referred to as biosimilar LMWHs [20]. Several of these have appeared around the world in the last decade, raising concerns over their chemical and therapeutic equivalence [21]. Maddineni et al. compared two generic enoxaparin formulations from India and one from Brazil with Lovenox^{TM} using a battery of enzymatic, chemical, and pharmacodynamic tests. While the activated partial thromboplastin time and prothrombin time of all four were similar, the molecular weight varied from 3905 to 4339 daltons. Lovenox^{TM} and the Indian brands were readily digested by heparinase, but the Brazilian formulation was resistant to breakdown. Since these enzymes are highly

dependent on the structural nuances of heparin, its inability to degrade it indicates a manufacturing process that differs from that which yield the trade name product.

The immunogenic potential of these LMWHs is also of great concern especially with regard to HIT. Gomes et al. compared Lovenox™ to Cutenox™, a generic version manufactured by Gland-Pharma in India in an open label study in Brazil. 110 healthy volunteers were given 40 mg Lovenox™ and 110 were given 40 mg Cutenox™ daily for 10 days. Interestingly, there was a slight difference in antibody composition between the groups at 10 days, with Lovenox™ having slightly more IgA with Cutenox™ leading to more IgG. While very close to one another, the differences in antibody profiles may be indicative of structural deviation caused by differing conditions of manufacture. It also raises concerns over the possibility that these LMWHs interact differently with other proteins in our body and lead to unforeseen side effects [22]. Since a generic LMWH would not be required to go through the rigorous safety and efficacy trials as the innovator, these may only be detected after it has seen wide usage. Yet, the cost of developing a new drug provides a powerful incentive to move generics onto the market.

1.3 Current Issues in the Analysis of Heparin and Low Molecular Weight Heparin

In early 2008, an outbreak of hypersensitivity reactions to UFH manufactured by Baxter Pharmaceuticals was reported in the US. Symptoms typically began a few minutes from initiation of treatment and included hypotension, shortness of breath, and edema. In the US, 81 U.S. fatalities were reported [23-25]. Analysis of these samples revealed that they were contaminated with the oversulfated chondroitin sulfate (OSCS), a product of the chemical oversulfation of CS [26]. This highly anionic, non-natural GAG is able to mimic the anticoagulant effects of UFH and difficult to distinguish due to

structural similarities due to its structural similarities (**figure 1a**). OSCS has been shown to activate the plasma contact system beginning with factor XIIa. Factor XIIa is part of the intrinsic coagulation pathway, but also converts prekallikrein to kallikrein when activated. Kallikrein stimulates the production to bradykinin, a powerful vasodilator and inflammatory promoter [23,27,28]. This tragedy has spawned the development of a wide spectrum of analytical techniques for the detection of OSCS in heparin and has prompted the FDA to revise its analytical protocol [29,30]. Given the complex nature of UFH and the possibility of other contaminants, the need for rapid, high powered protocols for heparin analysis is likely to continue.

On July 23, 2010 the food and drug administration (FDA) approved the first generic version of enoxaparin for the US [31]. Manufactured by Momenta Pharmaceuticals and marketed by Sandoz, it was approved by the FDA from an abbreviated new drug application and did not undergo the extensive clinical trials of the innovator product. Instead, the FDA examined physiochemical properties such as molecular weight distribution, disaccharide composition, and the presence of the 1,6-anhydromannose ring. In addition, “the FDA required not only biological and biochemical assay data to demonstrate equivalent anticoagulant activity *in vitro* and *in vivo* but also pharmacodynamic data from healthy human volunteers.” [32] While achieving equivalence in these areas is notable, the fine structure of the drug remains a mystery.

The staggering chemical complexity of heparin means that there are boundless opportunities for biochemical studies. The 2008 contamination crisis along with the development and approval of generic LMWHs has created a renewed sense of urgency

in developing robust methods for the detection of contaminants and characterization of the GAGs themselves. Nuclear magnetic resonance (NMR) methods, various spectroscopic techniques, electrophoretic protocols, chromatographic methods, mass spectrometry, and hyphenated techniques have appeared in increasing number. What follows in sections 1.4-1.7 is a survey of the techniques used in the analysis of UFH and LMWH with special attention to the fingerprinting of and purity of these drugs. Emphasis is given to the ease of use of the assay, the time required to complete it, the cost of equipment and materials, sensitivity, specificity, and overall usefulness of the methods.

1.4 Nuclear Magnetic Resonance of Heparins

Nuclear magnetic resonance (NMR) spectroscopy has been extensively used to characterize heparins, Proton NMR (^{1}H-NMR) was the first to be used to probe the sugar backbone and the functional groups that decorate it in the 1960's [33,34]. In addition to ^{1}H-NMR, ^{13}C-NMR and various 2-dimensional NMR methods have given us substantial insight into GAG structure, meaning that NMR has been utilized in the study of heparin far more than other spectroscopic techniques such as infrared or raman. Disaccharides obtained after enzymatic digestion of heparin were first characterized by ^{1}H-NMR in 1971 by Perlin and Mackie [35]. Since then, ^{13}C-NMR and 2-D NMR techniques including heteronuclear multiple quantum coherence (HMQC) [36], correlation spectroscopy (COSY), total correlation spectroscopy (TOCSY), nuclear overhauser enhancement spectroscopy (NOESY), and rotating frame nuclear Overhauser enhancement spectroscopy (ROESY), have confirmed the structures of these GAG building blocks as well as oligosaccharides [37-39]. These powerful techniques have enabled elucidation of the structure of many heparin oligosaccharides,

but efforts are hampered by the inherent randomness of sulfation and chain length. The most extensive effort to characterize heparin oligosaccharides was performed by Pervin et al. in 1995. This mammoth effort involved depolymerizing and fractionating massive amounts of heparin to yield 50 grams of oligosaccharides of M_w<5,000. Fourteen homogeneous GAGs were isolated ranging from disaccharide to tetradecasaccharide and characterized using COSY. However, the internal uronic residues were distinguishable only up to octasaccharide length sugars [35]. Given that heparin contains chains far larger than tetradecasaccharide, even the most powerful NMR techniques would be unable to establish the structures of full length heparin chains even if purified to homogeneity.

Though NMR was previously shown to detect contaminants in heparin preparations [40-42], the 2008 heparin contamination crisis has brought NMR into fresh focus. Rather than complete structural elucidation, efforts have been focused on identifying glycosaminoglycan contaminants in UFH by observing subtle differences in NMR spectra. Most analyses since 2008 have relied on the presence of a downfield shift of the N-acetyl signal in ^{1}H-NMR. This results due to the change in electronic character of the local carbon as a result of the increase in negative charge. Guerrini et al. was the first to identify the OSCS contaminant in 2008 using ^{1}H-NMR. The contaminating OSCS was differentiated from UFH and the natural impurity DS by a downfield shift of the N-acetyl signal from 2.04 to 2.16 ppm in the ^{1}H-NMR spectrum. DS showed a chemical shift of 2.08 [26]. This confirmed the work previously published by Maryuna et al. in 1998 [43]. Since then, the results of more than one hundred heparin batches have been tested [44,45,30]. Beyer et al. quantitatively determined the

amount OSCS and DS present in 108 samples of UFH with OSCS having an LOD of 0.1% of a 25 mg sample of UFH [44]. The protocol has been applied to crude UFH and to the active pharmaceutical ingredient (API) [46]. It should be noted that many other peaks beside the N-acetyl signal are indicative of OSCS contamination, but their proximity to other signals makes reliable distinction difficult especially at low OSCS concentrations [44,45]. The robustness and low limit of detection of this method caused the FDA and U.S. Pharmacopia (USP) to mandate the use of ^{1}H-NMR in the testing of individual UFH batches [29,30].

^{1}H-NMR has also been coupled to other powerful analytical and chemometric techniques. In 2005, Korir et al. characterized a pair of dissacharides and a tetrasaccharide with tandem capillary electrophoresis-NMR (CE-NMR) using capillary isotachophoresis, a mechanism allowing for sampe . Though the large amount of sample required for NMR makes CE-NMR largely impractical at this point, further technological advances may allow them to regularly be used in tandem [47]. Limtiaco et al. used weak anion exchange high performance liquid chromatography (HPLC) coupled to ^{1}H-NMR to study OSCS, UFH, CS, and DS. Run conditions were optimized to allow for a nearly 8 minute baseline separation of OSCS and UFH using a 0.1-1 M NaCl gradient. Using D_2O based buffer, distinctive on flow ^{1}H-NMR profiles of UFH and OSCS could be acquired. Stopped flow NMR allowed the GAGs a much longer residence in the flow cell and yielded a far more detailed spectra in which many peak assignments were possible for UFH, CS A, DS, and OSCS with enough resolution and sensitivity to assign protons from within and in between individual sugars. Additional sensitivity was gained by repeatedly injecting OSCS contaminated UFH samples into

the column. Since UFH eluted at 0.6 M NaCl and OSCS at 0.8 M NaCl, the UFH was washed away after each injection and the OSCS was retained on the column. After 10 injections, the concentrated OSCS was eluted using 0.8 M NaCl and analyzed using flow NMR to yield highly resolved spectra. HPLC-NMR has the potential to signal the presence of impurities in UFH as well as identify them even when present in small amounts [48].

Data from ^{1}H-NMR has also proven useful in chemometric analyses [44,49-52]. Zang et al. utilized several techniques including principle component analysis (PCA) and partial least squares discrminant analysis (PLS-DA). PCA is a method for reducing large numbers of variables into a smaller number of “principle components” that account for variation. The component accounting for the most variation in the sample is designated PC1, while the next is PC2 and so on. When plotted in two or three dimensions, enormously complex data sets can be analyzed using only a few variables. PCA was able to sharply distinguish UFH and OSCS, but not DS. PLS-DA provided even better seperation and could predict the presence of significant amounts of OSCS in test samples with few misclassifications [51].

Two dimensional NMR and ^{13}C-NMR were instrumental in chemically identifying the heparin contaminant in 2008. Seven peaks unique to OSCS were seen in the contaminated UFH using ^{13}C-NMR while HMBC and HSQC identified oversulfated monosaccharides [26]. Diffusion Ordered Nuclear Magnetic Resonance Spectroscopy (DOSY) has been used to characterize LMWH and UFH formulations and distinguished OSCS in LMWH [54,55]. DOSY makes use not only of ^{1}H-NMR chemical shifts, but the ditransaltional diffusion coefficient (D_t in m^2/s) which is dependent on molecular weight

rather than structural subtleties. Since OSCS chains are on average much larger than LMWH, the presence of this contaminant is made most apparent. Such a technique however, would be of little use if the contaminant were of a similar molar mass. Rudd et al. used 2-D correlation spectroscopy to identify a variety of oversulfated polysaccharide contaminants. This was done by subtracting standard UFH data sets from UFH samples contaminated with OSCS, oversulfated dextran sulfate, and oversulfated agarose sulfate, leaving the peaks characteristic of the contaminant available for unhindered study [56]. NOESY has also been used to identify OSCS in UFH by taking into account the environments of the ring protons [57].

The power of two dimensional NMR is such that it is able to provide accurate structural information for GAGs far to complex for one dimensional NMR [36]. The chief limitation is that the complexity of GAG spectra often requires highly skilled interpretation. UFH and LMWH would prove much more difficult than a homogeneous sample because of their heterogeneity. However, it would prove most useful for confirming the identity of a contaminant that had been isolated especially when used alongside mass spectrometry.

1.5 Other Spectroscopic Techniques in the Analysis of Heparins

Infrared (IR) and Raman spectroscopies have been used to highlight suspected OSCS contaminated UFH lots using chemometric techniques [58]. Circular dichromism is useful in distinguishing between GAGs as it measures the absorption of polarized light in non-racemic samples [59]. The conformation of uronic acid in particular is distinguishable since glucuronic and iduronic acids are opposite enantiomers. It has also shown characteristic spectra of heparin when bound to different cations (Na^+, Mg^{2+},

K^+, Ca^{2+}, Mn^{2+}, Cu^{2+}, Fe^{3+}) [60]. Since cations other than sodium may shift the N-acetyl group of OSCS, NMR spectra, circular dichromism may be used in complimentary to NMR in explaining deviant signal shifts [61]. Circular dichromism was recently reported to give a clear differentiation of UFH and OSCS [62].

Jagt et al. published one of the most innovative heparin analysis protocols using self assembling fluorescent receptors. The positively charged β-CD derivative heptakis-[6-deoxy-6-(2-aminoethylsulfanyl)]-β-CD was derivatized with a number of amino and guanadino groups and allowed to form an inclusion complex with various lithocholic acid derivatives which bind with strong affinity. A number of lithocholic acid compounds derivatized with a quinolinium flourophore were complexed with the functionalized CD. The result was a complex with a dense positive charge and a fluorescent compound sensitive to its local environment. This work yielded a complex showing a change in fluorescence with OSCS that was far above UFH, LMWH, HS, DS, and CS. This work is of great importance in that it proves that small to medium sized molecules or complexes can distinguish between remarkably similar GAGs, which would be of great potential in detecting specific contaminants. It also provides a simple pathway for designing relatively complicated probes for the wider study of GAGs [63].

1.6 Electrophoretic Analysis of Heparins

Electrophoresis is a time tested approach for separating and studying heparin and heparin-like GAGs. Preparative scale agarose gels was used to separate and isolate four HS oligosaccharides [64]. Gradient polyacrylamide gel electrophoresis (PAGE) is useful in resolving heparin species with a similar degree of polymerization but differing internal structure and sulfation density [65]. In spite of the ubiquity of gel

electrophoresis in laboratories, capillary electrophoresis (CE) is used more often with GAGs as evidenced by the number of literature reviews in the last decade [66-68]. Several types of CE exist including capillary zone elcectrophoresis [66], capillary isotachophoresis [69], micellar electrokinetic chromatography (MEKC) [70], capillary gel electrophoresis [71], capillary isoelectric focusing [72], and capillary electrochromatography [73]. Of these, capillary zone electrophoresis (hereafter designated simply as CE) and MEKC are most commonly employed in the analysis of heparins because of their simplicity and effectiveness in seperating GAGs.[67].

In CE, a sample is injected into narrow, buffer filled, fused silica capillaries with an inner diameter of 20-100 μm and an electric field is applied that will draw the analytes toward the oppositely charged electrode as seen in **figure 3**. **Figure 3a** shows CE with basic (pH~7) in normal polarity mode. Under these conditions, the silanol groups on the wall are deprotonated, causing the cations of the buffer to coat to the wall forming an immovable “stern” layer. Ions in the layer outside of this coating are electrostatically pulled towards the cathode as a result of the zeta potential generated by the electric field when applied to the layer. Because these cations drag their shells of hydration, a powerful electroosmotic force is exerted in the direction of the cathode that is able to pull even oppositely charged molecules toward the cathode, enabling the separation of all ionic species and extending the length of the capillary. Under acidic conditions, the silanol groups are largely protonated, suppressing the electroosmotic force and allowing separation solely on the basis of charge-mass-ratio. Depending on the charge of the analytes, either normal or reverse polarity can be used at low pH (**figure 3b**) [67,74,75]. MECK utilizes is a form of CE in which a surfactant is added to

the buffer at a concentration that allows for the formation of micelles. These act as a kind of stationary phase that differentially interacts with analytes, altering their mobility and enabling their separation [70]. A maintained CE instrument in capable hands is able to produce highly resolved electropherograms using only nanoliters of sample in a rapid fashion [68].

Multiple CE protocols have been used to separate heparin disaccharides and oligosaccharides. Pervin et al. separated eight heparin/heparin sulfate dissacharides along with eight CS/UFH dissachardes with an unsaturated double bond and varying sulfation levels using reverse polarity CE with 20 mM phosphate buffer, pH 3.48, while13 heparin oligosaccharide standards ranging from 2-14 monosaccharides were separated using MECK (10 mM sodium borate, 50 mM SDS, pH 8.8, normal polarity). Baseline separation was achieved between the di- and tetrasaccharides with resolution decreasing at longer chain lengths [76]. These results were consistent with that obtained previously by Desai et al. for a mixture of 17 heparin chains ranging from di to hexasaccharide. Compositional fingerprinting of several LMWHs were also achieved, but only after significant depolymerization with heparin lyase enzymes [77]. Laser induced fluorescence [78] and copper sulfate [79] have also been employed in the detection of GAGs via CE.

The resolution of intact UFH and LMWH presents a major hurdle for CE because of the phenomenal complexity of these mixtures since millions of GAG molecules are present with only infinitesimal differences. Ramasamy et al. fingerprinted four LMWHs using reverse polarity CE with both fused silica and neutral hydrophilic capillaries. While there were noticeable differences between the products, most of the GAG remained in a

relatively broad, featureless peak [80]. Patel et al. analyzed intact and decomposed dalteparin and enoxaparin using reverse polarity CE. A comparison of two batches of enoxaparin showed differences among the fine features of the electropherogram. While enoxaparin resolution was better than that obtained by Ramasamy et al., the bulk of enoxaparin remained locked in a featureless peak [81].

The heparin contamination crisis has incited great interest in electrophoretic protocols in detection of heparin contaminants with special focus on OSCS. PAGE was used to analyze heparins depolymerized by treatment with nitrous acid. Heparin is far more sensitive to nitrous acid than most other GAGs including CS and OSCS because of the presence of numerous N-sulfate groups (as opposed to N-acetyl groups). UFH contaminated with 25% w/w OSCS was clearly distinguishable after nitrous acid depolymerization with the small UFH fragments mostly migrating to the end of the gel. The LOD of a 100 µg sample was approximately 0.5% w/w. Other GAGs such as DS, OSDS, hyaluronic acid, dextran sulfate as well as other heparinoids were also readily distinguishable from UFH, showing the utility of PAGE in detecting a variety of potential contaminants [45]. Cellulose acetate plate electrophoresis was also employed in the detection of OSCS and DS in UFH with a DS LOD of 0.4% [82]. The ubiquity of PAGE in biochemical research makes it an attractive option for separation, but resolution is dependent on the chemical decomposition of GAGs.

While PAGE and cellulose acetate electrophoresis are capable of separating contaminants and impurities in UFH, neither is able to match the speed and resolution of CE in this application. The FDA published a CE protocol that was able to detect OSCS in UFH but only with partial resolution [83,84]. Though this protocol was later

replaced by strong anion exchange HPLC (SAX-HPLC), a number of subsequent methods were published with increasing efficiency and resolution [85]. Since then, several new CE protocols have been published. Wielgos et al used 600 mM phosphate pH 3.5 buffer with a 25 µm ID capillary with a total length of 64.5 cm. The result was a nearly baseline resolved electropherogram with OSCS visible as a sharp just ahead of UFH. Changing the counterion from sodium to lithium dramatically shortened the run time by nearly 75% with an LOD below 0.1 % w/w of the total amount GAG mass. Lithium based buffers have low conductivity relative to sodium and allow for higher field strengths, yielding shorter separations. However, such stellar sensitivity was only accomplished with extended path capillaries that are only compatible with CE systems manufactured by Agilent [84]. A modified version of this method was used alongside 1 and 2 dimensional NMR to separate OSCS as well as oversulfated “tank bottom” material considered to be waste by-products of the UFH purification process [26].

An improved method was published by Somsen et al. that resulted in the near baseline resolution of OSCS from UFH using high molarity tris buffer with an LOD of 0.019 mg/ml for OSCS. The high concentration of tris resulted in substantial sharpening of the OSCS peak, making it easy to distinguish from UFH and DS and the generation of a very sharp peak. The method did not require an extended path length capillary and used a CE system from Beckman without an extended path length capillary [86]. OSCS and UFH were separated using a capillary loaded with polymerized β-cyclodextrin and the polymer Tetronic® 1107 which contains two positive charges under acidic conditions. The mixture of the two polymers creates a cationic pseudostationary phase that sulfated polysaccharides will readily interact with. The LOD for the detection of

OSCS was an astonishing 0.07% w/w of a 0.1 mg/ml UFH sample, the best yet achieved with CE [87].

Since GAGs have low UV extension coefficients, derivitization with UV active substances would enable enhanced sensitivity. Quantitative CE was used for the resolution of galactosamine and glucosamine after acidic hydrolysis of a UFH/OSCS mixture and the derivitization of the monosaccharides with anthranilic acid. Since UFH and OSCS are composed of glucosamine and galactosamine sugars respectively, their detection and quantitation allowed for distinguishing between two GAGs. However, this was only possible if DS was previously degraded by chondroitinase since this would also give galactosamine and potentially sound a false alarm [88]. Other sources of galactosamine and glucosamine could potentially do the same.

1.7 Chromatographic Analysis of Heparins

Chromatography of glycosaminoglycans has long been used in resolving and quantitatively separating heparin and related polysaccharides. Thin layer chromatography is capable of separating sulfated other GAGs from heparin [89]. Gel filtration chromatography was used to fractionate nitrous acid depolymerised heparin into long chains (MW > 3000), shorter chains such as tetrasaccharides, and disaccharides [90]. Paper chromatography SAX-HPLC was employed in the separation, quantification, and identification of tritiated disaccharides and oligosaccharides [91]. Strong anion exchange chromatography was used in purifying 14 oligosaccharides in Pervin et al's massive study [36]. Reverse phase ion pairing chromatography acquired baseline separation of sugars ranging from disaccharide to tetradecasaccharide [92]. Hyphenated LC-MS is a an extremely effective tool for the characterization of GAG

mixtures since it can both separate and reveal structural information of GAGs [93-95]. Chromatography presents an attractive method for the separation of GAGs because of the diversity of media and techniques, the ability to collecti the resolved fractions, and the possibility of analysis via hyphenated techniques (LC-MS and LC-NMR) [47,96,97].

Due to their relative ease of analysis, chromatographic studies of disaccharide and oligosaccharide composition derived from LMWH and UFH abound in the literature [92,96]. Karamanos et al resolved all the major disaccharides of heparin and heparan sulfate using reverse phase ion pairing HPLC with tetrabutylammonium and an acetonitrile gradient. As expected, heparin contains a far greater proportion of trisulfated disaccharide (68%) than heparan sulfate (8.7%). In comparison, the depolymerization of dalteparin by heparin lyases yielded 84.2% trisulfated disaccharide [98]. UPLC coupled to ESI-MS was able to separate and quantify heparin/heparan sulfate disaccharides in under 5 minutes with heparin from porcine intestine, bovine intestine, and bovine kidney yielding different disaccharide compositional profiles [99]. However, few studies exist for the characterization of intact LMWH or UFH. Patel et al. developed a powerful isocratic reverse phase HPLC technique capable of developing high resolution fingerprints of LMWHs using both UV-vis and evaporative light scattering detection (ELSD) under optimized conditions. Buffer concentration, pH, proportion of acetonitrile, and the type and concentration of ion pairing agents were varied to optimize separation. Incredibly, the reverse phase technique allowed for baseline separation of many peaks in enoxaparin samples previously fractionated by size exclusion chromatography. Such baseline resolution as yielded by this two stage separation is typically very difficult to obtain and would facilitate LC-MS analysis of individual peaks,

giving detailed insight into the elusive structural subtleties of LMWHs [100]. Doneanu et al. produced the most highly resolved fingerprint of LMWH ever obtained using reverse phase ion pairing UPLC coupled to quadrapole time of flight mass spectrometry. The resolutive capabilities of UPLC and the analytical prowess of MS come together to yield a total ion chromatogram of tinzaparin with over 50 peaks [101]. Both of these techniques are capable of analyzing LMWHs in unprecedented detail, but are very sensitive run buffer composition and may require the use of highly complex and expensive equipment in the case of UPLC-MS.

Strong anion exchange HPLC has become one of the most effective means of detecting oversulfated contaminants in UFH. Trehy et al. separated OSCS and DS from UFH using a polymer based SAX-HPLC column and achieved a separation far superior to the initial FDA method. Using UV detection, it is one of the most sensitive methods for detecting OSCS published to date with an LOD of 6.2 µg/ml (0.03% of 20 mg/ml UFH solution) [102]. The method was further developed to detect a variety of GAGS including CS, hyaluronic acid, oversulfated hyaluronic acid, and OSDS with elution time being largely dependent on the degree of sulfation of each GAG [103]. Weak anion exchange chromatography has yielded similar results [104]. The protocol's sensitivity and resolution as well as the relative abundance of HPLC systems had led to the SAX-HPLC method's adoption in place of the CE protocol in the FDA and USP standards [46].

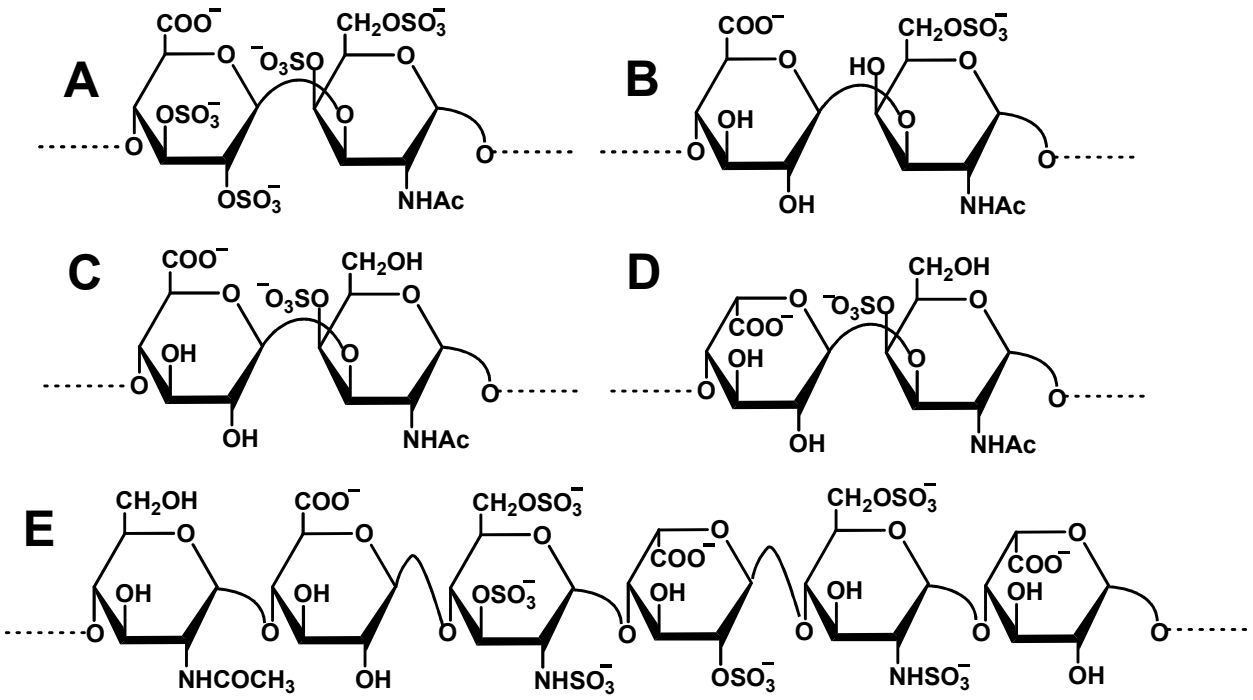

Figure 1.1 Representative structures of glycosaminoglycans. A) Fully oversulfated chondroitin sulfate B) Chondroitin-6-sulfate C) Chondroitin-4-sulfate D) Dermatan sulfate E) Unfractionated heparin.

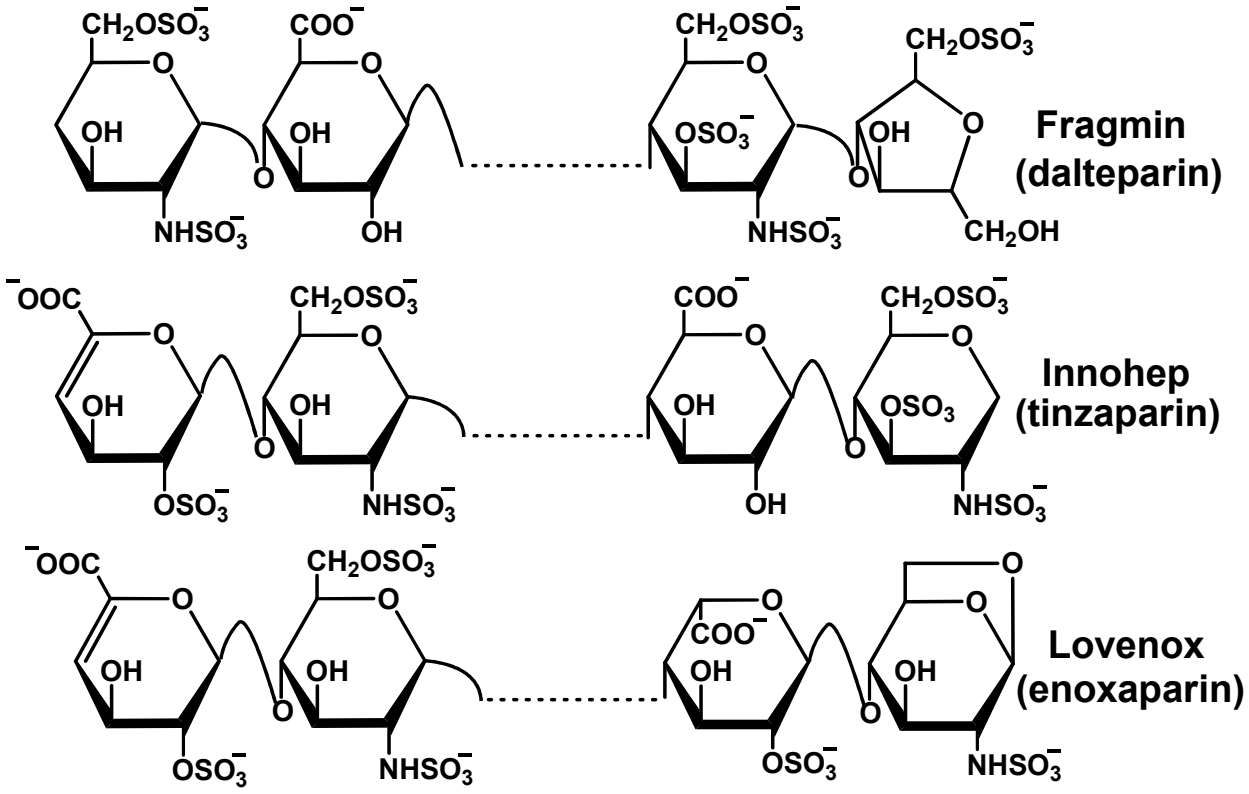

Figure 1.2: Representative structures of low molecular weight heparins. The brands listed are available in the USA.

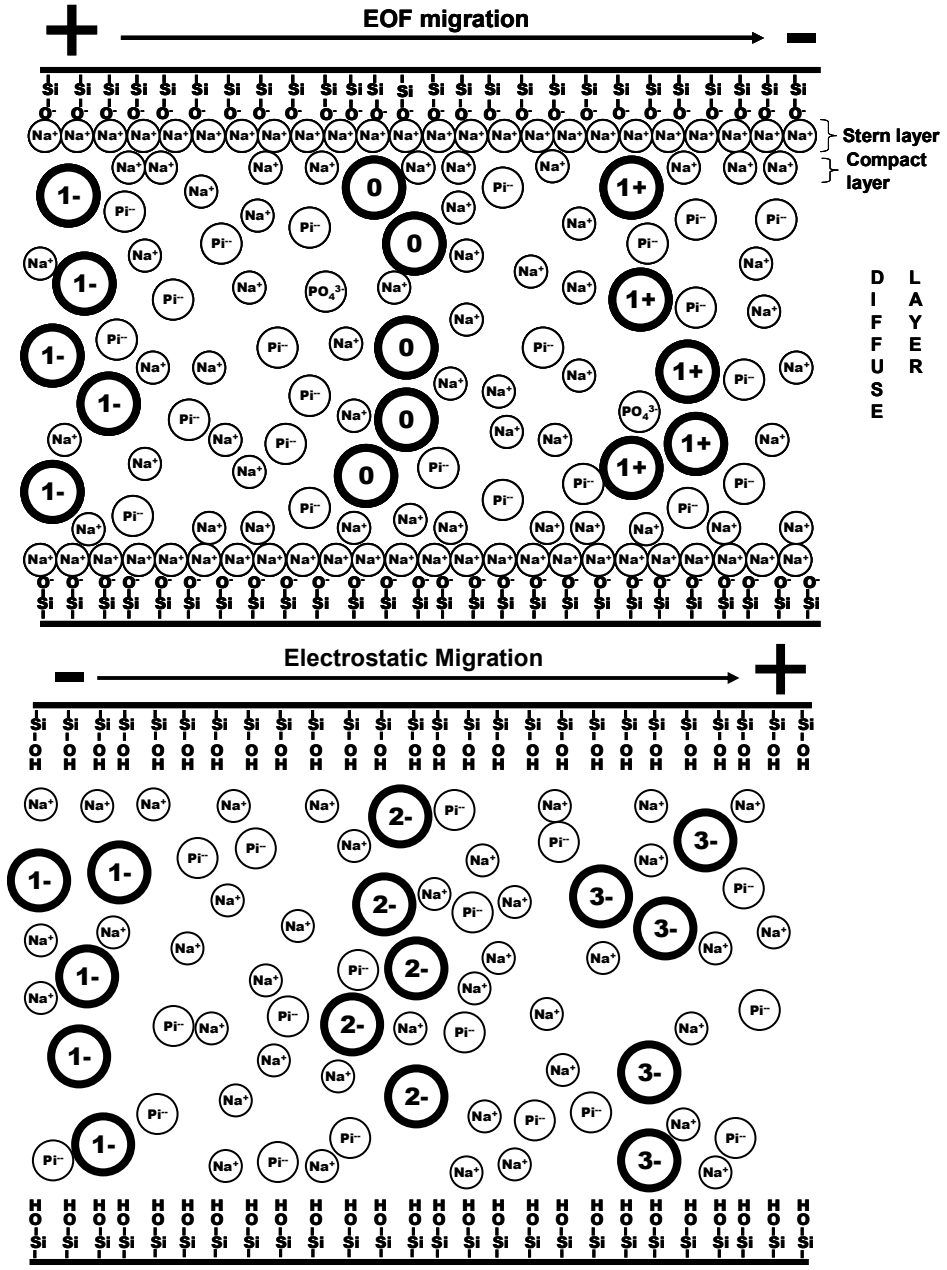

Figure 1.3: Diagram of capillary zone electrophoresis. A) normal polarity, B) reverse polarity. Adapted from Dantuluri et al [67].

Capillary Electrophoretic Fingerprinting of Low Molecular Weight Heparins

2.1 Background

A large number of biophysical techniques have been used to characterize heparins. Gel electrophoresis, especially PAGE, has been developed to analyze heparin polydispersity [105-108]. while chromatography, e.g., SEC or GPC, has been developed to assess the molecular weight and oligomeric composition [106,108-114] Other chromatographic techniques, e.g., reverse-phase, ion-pairing and strong anion exchange, have been used to prepare heparin oligosaccharides as well as perform oligosaccharide compositional analysis [36,92,115-120]. NMR spectroscopy has also been used to assess saccharide composition and sulfation pattern, while being especially useful for identifying certain non-native structures [41,121-123]. Two-dimensional diffusion ordered spectroscopy has also been reported for detecting OSCS in LMWH preparations [124]. Recently, tandem liquid chromatography-mass spectrometry (LC-MS) has been exploited to perform sequence analysis on relatively purified preparations of oligosaccharide [94,125-129]. Reverse- phase-ion-pairing ultra high performance liquid chromatography-MS (UPLC-MS) yielded a spectacularly resolved total ion chromatogram fingerprint of tinzaparin, though such hyphenated methods require intricate equipment and skilled operators making difficult to implement

for routine use [101]. While these results represent significant achievements in the analysis of LMWH, the sheer complexity of these mixtures necessitate the further development of robust, consistent, and high resolution techniques.

A technique that has gained widespread acceptance in LMWH and heparin oligosaccharides analysis is capillary electrophoresis (CE). The earliest application of CE for disaccharide compositional analysis of LMWHs [76-77,130] has now been modified to protocols with much better sensitivity and resolving power [131-132]. A significant improvement in sensitivity of CE detection has been pre-column labeling with chromophores or fluorophores [78,133]. Further advances in CE applicability have been the development of a tandem CE–MS system for elucidating structural information [134]. Unfortunately, these powerful approaches work on essentially pure oligosaccharides, enzymatically depolymerized samples, or mixtures of smaller heparin chains. Additionally, none of the methods is particularly suitable for assessing LMWH preparations on a routine basis. More importantly, the absence of a rapid and simple biophysical protocol for monitoring product quality is a major impediment for identifying LMWHs complications. We sought to develop a CE method that can be employed in high resolution fingerprinting of LMWH batches. Our hypothesis was that alkyl polyamines would be able to interact with the highly sulfated heparin chains, resulting in a highly resolved, formulation specific electrophoretic signature. We successfully established low cost, extremely simple, and robust CE method to fingerprint intact LMWHs that is especially useful for assessing product identity, quality, and batch-to-batch variability.

2.2 Experimental Procedures

2.2.1 Chemicals and Electrophoresis Supplies

Enoxaparin (Lovenox^{TM}, 40 mg syringes, Lot # 094480) and tinzaparin (Innohep^{TM}, 2 mL, 20,000U vial, Lot # DB1586) were purchased from VCU Medical Center Department of Pharmacy Services, Richmond, VA. Two different Sigma LMWH preparations (ID# H8537, lot #043K10261; and ID# H3400, lot 102K0673) from Sigma (St. Louis, MO.) 2-Aminoacridone (AMAC) and sodium cyanoborohydride were also purchased from Sigma (St. Louis, MO). Linear and cyclic polyamines were from either Aldrich (St. Louis, MO) or Acros (Geel, Belgium) All other reagents/chemicals were analytical grade and purchased from either Fisher (Fair Lawn, NJ) or Sigma-Aldrich (St. Louis, MO). Fused silica capillaries were purchased from Beckman-Coulter (Fullerton, CA).

2.2.2 AMAC-Labeling of Low Molecular Weight Heparins

The labeling of oligosaccharides at the reducing terminus with 2-aminoacridone has been described extensively in the literature [35-37]. An essentially equivalent protocol was followed herein. Briefly, clinically available enoxaparin and tinzaparin were dialyzed extensively against deionized water (MWCO 500) to eliminate excipients and lyophilized to obtain a solid. Sigma LMWH (ID# H3400) was obtained in solid form and used as such. Solid LMWH (10–15 mg) and sodium cyanoborohydride (25 mg) were dissolved in 560 µL of deionized water and mixed with a solution of AMAC (4 mg) dissolved in 158 µL of 85% (v/v) acetic acid:DMSO. The mixture was allowed to incubate at 37°C for 16 hours, then dialyzed against deionized water to remove free, unreacted AMAC, and lyophilized. The solid so obtained was dissolved in deionized water containing 10% DMSO (v/v) at 10 mg/mL and stored at -78°C until use.

2.2.3. Capillary Electrophoresis of Low Molecular Weight Heparins

CE was performed using a 75 μm fused silica capillary (40 cm to the detector window) installed in a Beckman-Coulter P/ACE MDQ capillary electrophoresis system. A fresh capillary was activated using 5 min flushes each of 1 M NaOH, deionized water, 1 M H_3PO_4, and deionized water in sequence, while between each runs the flush time was reduced to 30 sec with a final run buffer flush of 2 min. Under optimal fingerprinting conditions, the stock solution of a LMWH was diluted nearly 10-fold with 10% DMSO/water for injection into the capillary. CE run buffers used included 50 mM sodium phosphate buffer at pH 2.3 and 100 mM ammonium formate buffer, pH 3.5. Each contained 10% DMSO and appropriate resolving agent at the desired concentration. Every CE run was performed with fresh 1 mL buffer vials. The temperature of the capillary was maintained at 15°C and the run current was held constant at -75 μA under optimal fingerprinting conditions. AMAC-labeled LMWH was injected for 15 sec at 1 PSI giving a total injection amount of 150 ng and an injection volume of ~ 5–10 % of the total capillary volume. Electrophoresis was monitored at 254 nm with a data collection rate of 4 Hz. Limit of detection (LOD) and limit of quantitation (LOQ) was taken to be 3 and 10 standard deviations above the average baseline in the region where LMWH was located, as defined in the literature [135]. Deviations from these conditions are noted in the text or figure captions. Unless specified otherwise, the Sigma LMWH used is ID# H3400 and enoxaparin is lot #94480.

2.3 Results and Discussion

2.3.1 Linear Alkyl Polyamines Resolve Electrophoretic Profile of LMWHs

Analysis of unfragmented, intact LMWHs is challenging because of polydispersity and microheterogeneity, which are major impediments to resolution despite the power of CE. Typically, a wide peak with few features is observed for intact LMWH samples in normal as well as reverse polarity implying that the mixture of the millions of species cannot be resolved (**figure 2.1A**) [136-138]. Recently, Ramasamy et al. [80] and Patel et al. [81] attempted to fingerprint LMWH using a bare fused silica capillary under reverse polarity conditions. Both groups reported an essentially broad LMWH peak consisting of few shoulders in the peak front. To devise a more robust method for assessing product identity and quality, we reasoned that the presence of certain polycationic agents (**figure 2.2**), which modify the effective charge density of the highly sulfated polymeric chains in a structure-dependent manner, will generate a characteristic fingerprint pattern in CE of intact LMWHs.

Two clinically used LMWHs, enoxaparin (Lovenox^{TM}) and tinzaparin (Innohep^{TM}), and one LMWH from Sigma were chosen. To aid detection, each LMWH was reductively coupled with 2-aminoacridone (AMAC) on the reducing end. CE of AMAC-labeled tinzaparin in 50 mM sodium phosphate buffer containing 10 % DMSO at pH 2.3 gave an unsymmetrical broad peak between 16 and 24 min (**figure 2.1A**), supporting previous results on other LMWHs [80-81]. However, in the presence of 100 μM tetraethylenepentamine (4EP), a linear molecule containing five basic nitrogens separated by ethylene groups, the broad peak showed much longer migration time and displayed multiple components. Enoxaparin also exhibited a peak with few features in the absence of RA but was well resolved with 100 μM 4EP (**figure 2.1B**). Sigma LMWH featured a number of distinguishable peaks between 20 and 26 minutes but none were

baseline resolved. The addition of 50 μM 5EH transformed it into a highly resolved fingerprint (**figure 2.1C**). Among the several buffers investigated, 50 mM sodium phosphate (pH 2.3) and 100 mM ammonium formate (pH 3.5) (**figure 2.3**), provided optimal resolution without compromising sensitivity and speed of analysis. These results suggest that interaction with linear polyamines, which assume a polycationic nature in strongly acidic conditions, dramatically alters the electrophoretic mobility of LMWH chains. More importantly, the multiple peaks observed suggest that structurally different LMWH chains are affected to different extents.

A wide ranging set of electrophoretic conditions were explored in acquiring useful LMWH fingerprints. Temperature was varied from 15 to 35°C, voltage from 5 to 25 kV, and capillary diameter from 50 to 75 μm. 15°C, -75 μA constant current, and 75 μM capillary ID were chosen for the consistency of migration times, minimization of noise and joule heating, and strong signal. 20 and 50 mM phosphate buffers ranging from pH 2.17 to 3.5 were explored with the 50 mM buffer being used for later runs. 20 mM sodium citrate at pH 3.15 yielded LMWH peaks with excessive noise. Normal polarity conditions were explored with ~ pH 7 phosphate and HEPES buffers without success. Early in the project, it was noted that AMAC labeled LMWH tended to settle to the bottom of the sample vial over time. This is largely caused by tendency of the hydrophobic AMAC labels to aggregate in aqueous solutions, resulting in current irregularities and inconsistent electropherograms (**figure 2.4**). Acetonitrile, methanol, and DMSO were explored as sample additives to remedy this. A 10% DMSO additive proved to be the most effective additive as it disrupted the aggregation caused by the

hydrophobic label. DMSO had a remarkably favorable effect on run to run consistency and was used in all subsequent experiments.

2.3.2 Fingerprinting Pattern Depends on the Structure of the Resolving Agent

To assess whether the structure of the resolving agent affects the resolution of LMWHs, we screened several cyclic and linear polyamines (**figure 2.2**). We reasoned that the cyclic amines would present a dense cationic scaffold for possible interaction with closely knit polyanionic domains in LMWHs, while the linear amines would favor recognition of longer cationic domains. Also, linear polyamines containing either two-, three- or four-carbon spacers between nitrogen atoms (**figure 2.2**) were investigated to assess recognition of saccharide domains with different charge densities.

Figure 2.5 shows the electrophoretic profile of enoxaparin in 50 mM sodium phosphate buffer, pH 2.3, in the presence of 125 μM concentration of either SPM, 4EP or 5EH. As the number of nitrogen atoms increase (SPM < 4EP < 5EH), the resolving agent is able to interact with enoxaparin better resulting in slower migration times. Sigma LMWH behaves in a similar manner (**figure 2.6**). Tinzaparin also follows this pattern, but reacts much more strongly with 5EH and weakly with SPM. This indicates that tinzaparin is much more sensitive than enoxaparin and sigma LMWH to the charge density on resolving agents (**figure 2.7**). This suggests that structural domains in the chains of the two groups of LMWHs are different.

Although both 3ET and SPD (**figure 2.2**) contain four basic nitrogens, the former weakly resolved enoxaparin, while SPD was virtually ineffective at concentrations as high as 500 μM. Cyclic polyamines 3AN and 4AD were also completely ineffective. Likewise, polybrene, a longer cationic polymer, was also not effective (**figure 2.8**). This

suggests that fingerprinting is not a general property of all polyamines. More importantly, optimal distribution of basic nitrogens and chain length is necessary for good fingerprinting pattern.

The fingerprint resolution is highly sensitive to not only the structure of the resolving agent, but also its concentration. More specifically, the linear resolving agents, e.g., SPM, 4EP, and 5EH displayed a narrow range of concentrations that gave the best resolution. For example, 125 μM 5EH baseline resolves the Sigma LMWH fingerprint over a long period of time (**figure 2.5**), meaning that further increases in resolving agent concentration would only extend the run time while providing little added resolution. The same is not true for enoxaparin (**figure 2.6**), suggesting that the fingerprint pattern is characteristic with respect to both the LMWH and the resolving agent.

It is important to note that several peaks are baseline resolved in the fingerprint pattern with 5EH, especially in the region of 22 to 30 min (**figure 2.5**). It is likely that use of laser-induced fluorescence would enhance sensitivity that would allow for the decrease of LMWH concentration, potentially allowing for a fully baseline-resolved fingerprint pattern. Baseline resolution also indicates that analysis of enoxaparin using CE-MS may be possible under compatible run conditions (ammonium formate).

2.3.3 Different LMWHs Display Different Fingerprint Patterns

To assess whether the fingerprint pattern is characteristic of individual LMWHs, we compared CE runs of enoxaparin, tinzaparin and Sigma LMWH in the presence of 50 μM 4EP at pH 2.3 (**figure 2.9**). Each LMWH shows a characteristic fingerprint pattern defined primarily by the extent of interaction with the resolving agent. Whereas enoxaparin displays prominent peaks at 25 and 30 min, Sigma LMWH is devoid of the

pattern at ~30 min. In contrast, both these patterns are absent in tinzaparin. Also, tinzaparin displays much lower resolution than enoxaparin and Sigma LMWH. Equivalent results were observed for other resolving agents including SPM and 5EH (not shown). These fingerprint patterns are highly reproducible with notably low intra-day (**figure 2.10A**). The variability in migration time was investigated in more detail for several resolving agents by selecting a prominent peak from the sample (data not shown). It was observed that the protocol yields an average migration time variability of 21 seconds, which suggests the possibility of automated comparative analysis. With respect to inter-day reproducibility, the overall pattern and migration time of two enoxaparin fingerprints appeared consistant (**figure 2.10B**), though a more detailed analysis would involve several sets of runs over a period of weeks. In the absence of resolving agent, the electrophoretic response displayed good linearity over a wide range concentration with a measured limit of detection and quantitation of 140±23 and 290±47 µg/mL, respectively (see **figure 2.11** and **Table 2.1**). These limits are not as good as expected and it is likely that the use of higher sensitivity chromo- or fluorophores or laser-induced detection may improve sensitivity. Overall, the results indicate that fingerprinting pattern, especially with multiple resolving agents, and the stability of electropherograms could greatly help identify and quantitate individual LMWHs. We believe that the quality and consistency of these fingerprints will prove useful in batch to batch analysis of LMWHs.

2.4 Conclusions and Significance

Our results show that LMWHs can be readily fingerprinted using a simple capillary electrophoretic protocol. The protocol uses readily available chemicals, is

rapid, and is highly reproducible in producing distinctive fingerprint patterns. It can be exploited for identifying intact LMWHs, monitoring product quality and for checking batch to batch variability. Although the resolution achieved using a single resolving agent is sufficient, the power of fingerprinting might be expanded with multiple resolving agents or with a mixture of resolving agents. This is especially important considering that a number of LMWHs are being rapidly introduced in the world market [139].

Agent 5EH was found to be especially good at resolving enoxaparin and Sigma LMWH into several baseline-resolved peaks. It is likely that full baseline-resolution will become possible with selected modifications to the protocol, e.g., use of laser-induced fluorescence. This will enable detailed sequence analysis of nearly all LMWH chains through tandem CE-MS/MS approaches. A major advantage of the MS-based analysis is the possibility of identifying the proportion of LMWH chains containing the high-affinity pentasaccharide sequence, which governs anticoagulant activity *in vivo* [140]. Likewise, it is likely that the CE-MS/MS approach will become useful in deciphering heparin structure – activity relationships in areas other than coagulation.

Table 2.1: Limit of Detection and Limit of Quantitation for Enoxaparin.

	Absorbance *(× 10^6)*	**Concentration**
	(AU)	*(µg/mL)*
Average Noise	261 ± 42[a]	-
Limit of Detection	387 ± 62[b]	143 ± 23[c]
Limit of Quantitation	681 ± 109[d]	290 ± 47[c]

[a]Several blank runs were recorded and the noise in the baseline corresponding to the enoxaparin peak was analyzed to obtain the average noise height and its standard deviation. [b]Represents 3×SD over the baseline. [c]Obtained using the linear regression described in Figure 11. [d]Represents 10×SD over the baseline.

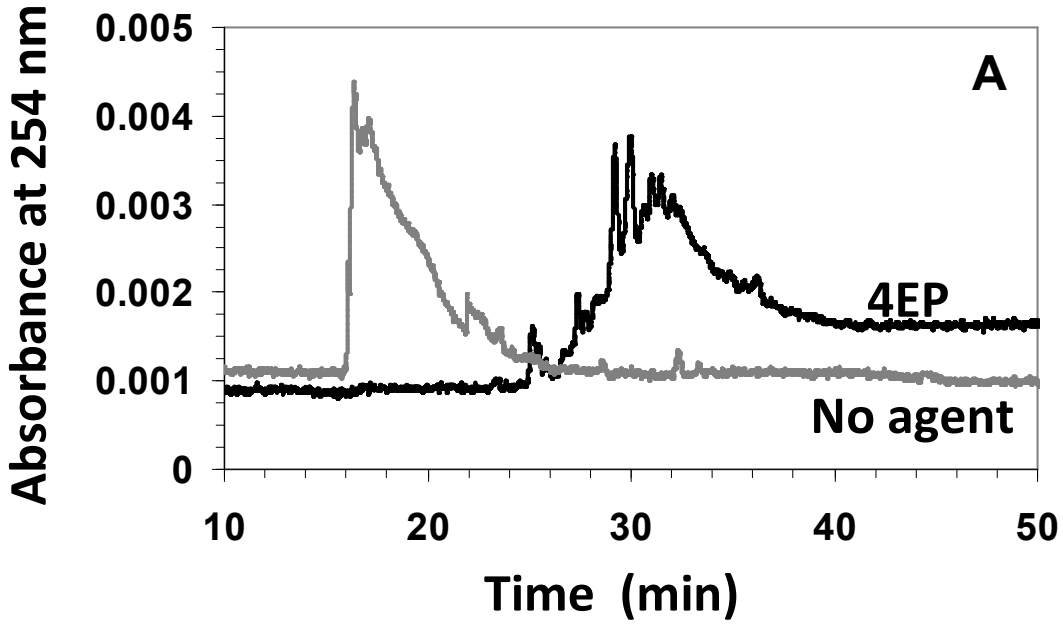

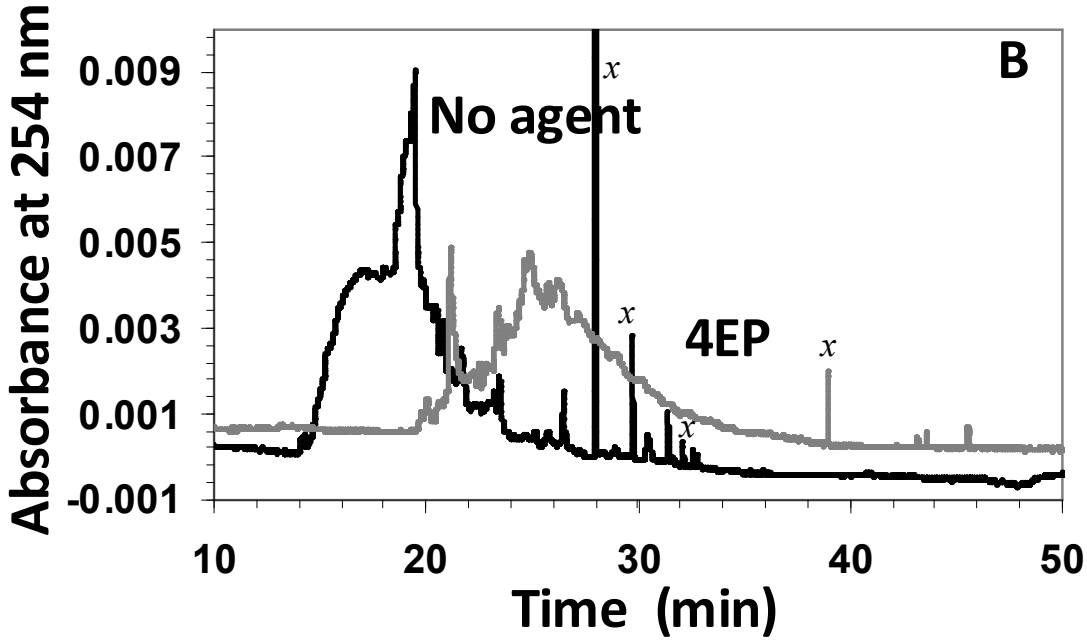

(Continued on page 36)

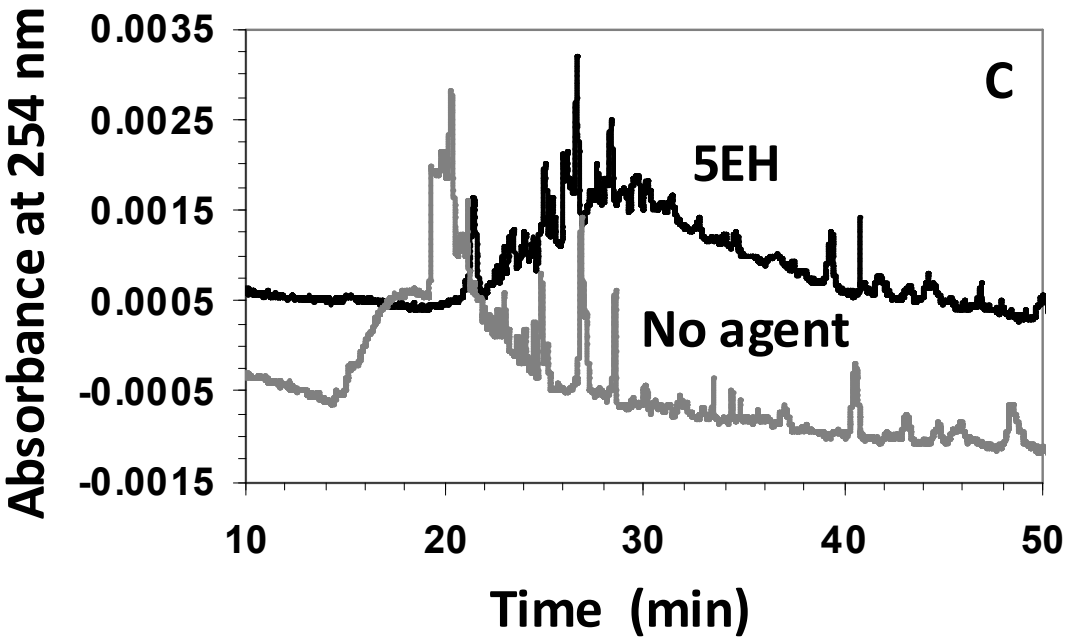

Figure 2.1: Linear alkyl polyamines turn nearly featureless peaks into highly resolved fingerprints. A) Tinzaparin with and without 100 μM 4EP, B) Enoxaparin with and without 100 μM 4EP, and C) Sigma LMWH with and without 50 μM 5EH. Peaks marked with "x" are sudden disturbances due to bubble formation during the electrophoretic run.

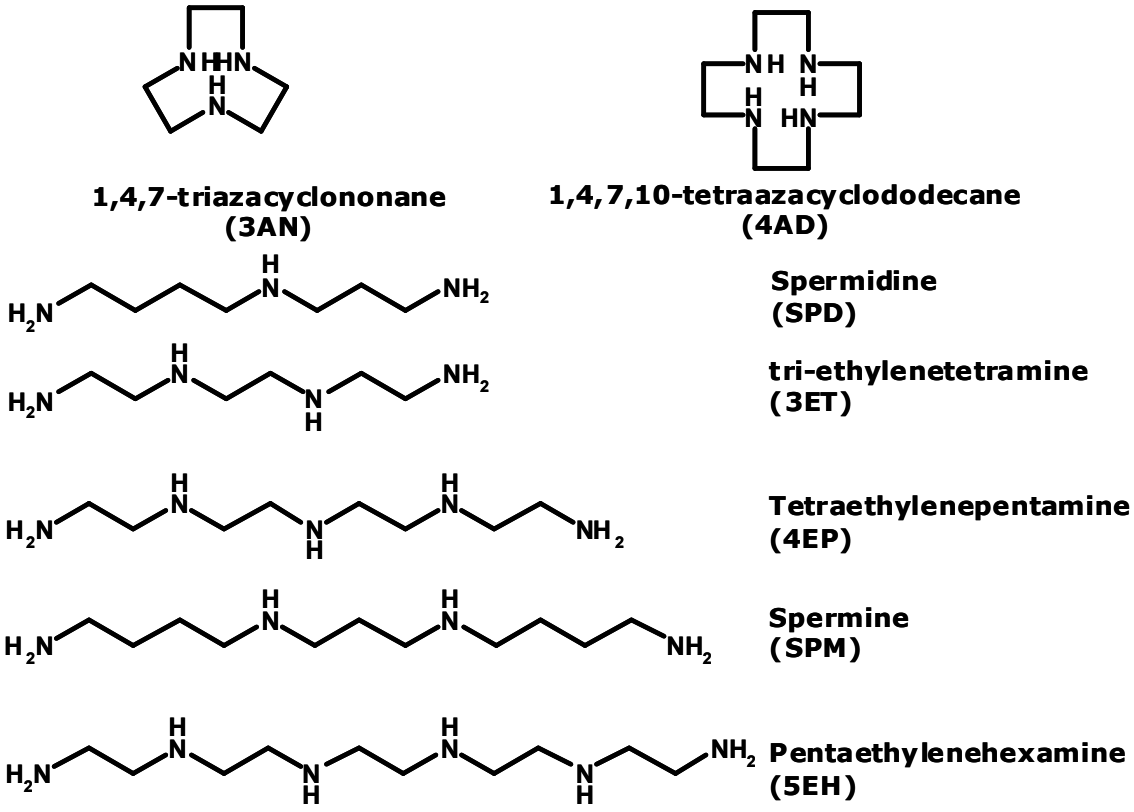

Figure 2.2: **The structures of alkyl polyamines screened for fingerprinting LMWHs.**

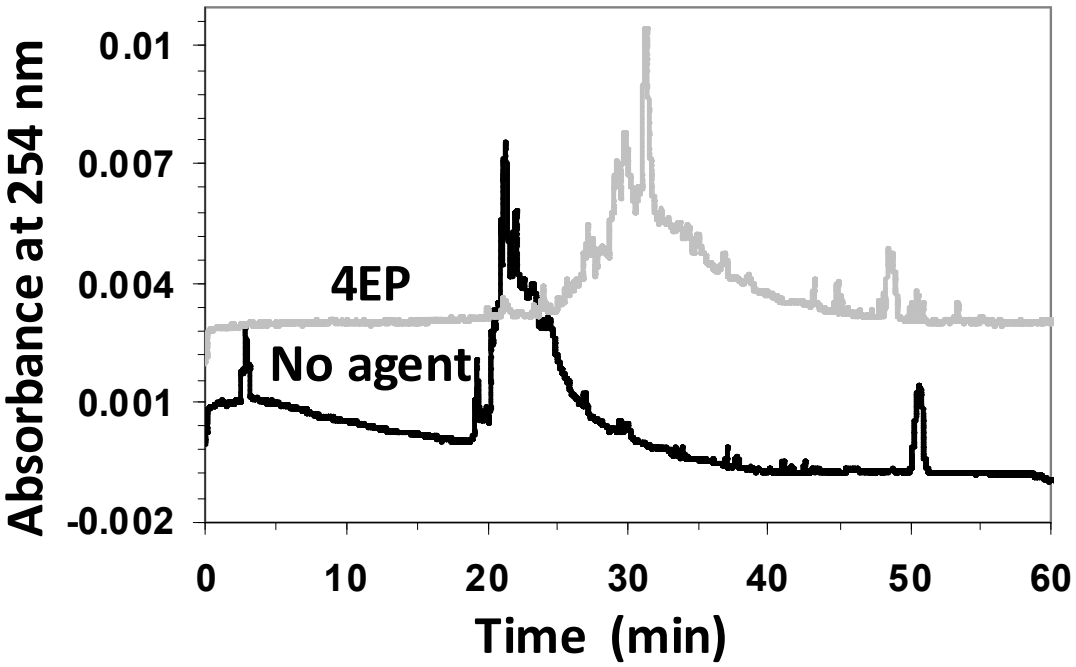

Figure 2.3: Enoxaparin is effectively fingerprinted by 100 µM 4EP in 100 mM ammonium formate.

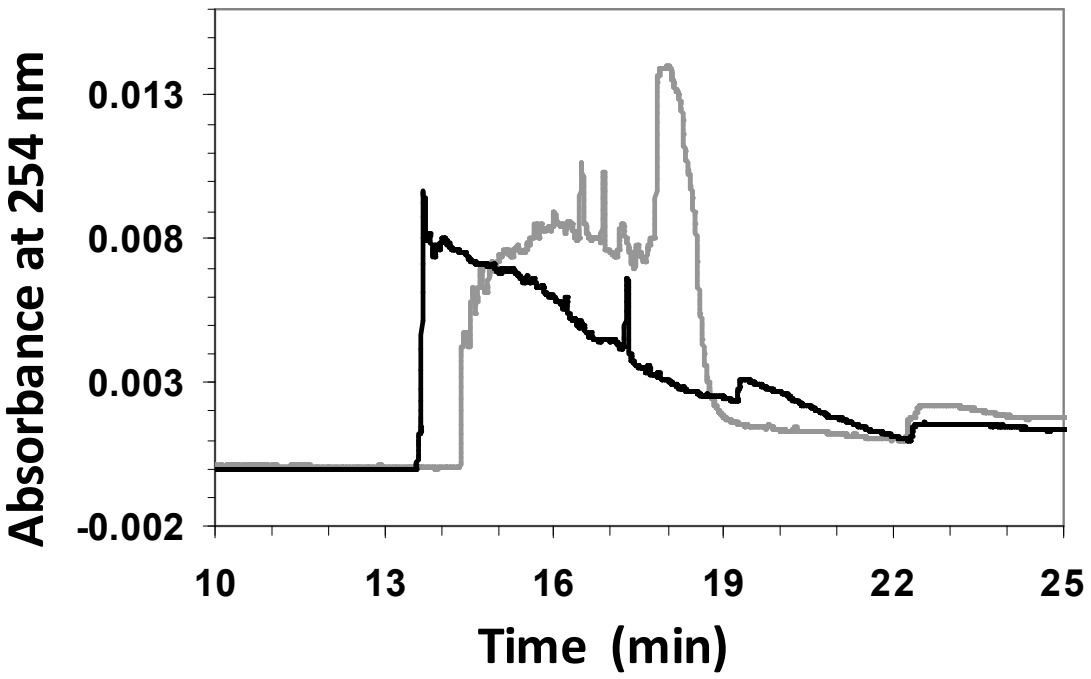

Figure 2.4: **Back to back unlabeled Sigma LMWH (H8537) runs**. Buffer contained 49 µM SPM with no DMSO in the sample and buffer. Run conditions: 20 mM sodium phosphate pH 3.3, 10 kv constant voltage, 25°C constant temperature.

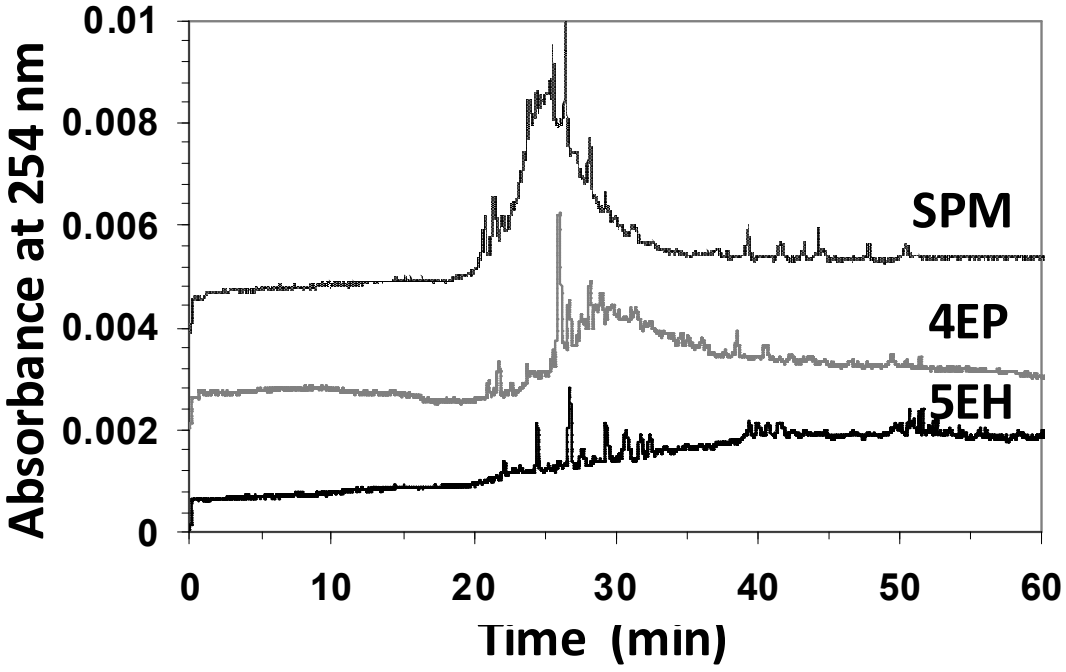

Figure 2.5: **Sigma LMWH fingerprints with 125 µM SPM, 4EP, and 5EH respectively.** Peaks marked with "x" are sudden disturbances due to bubble formation during the electrophoretic run.

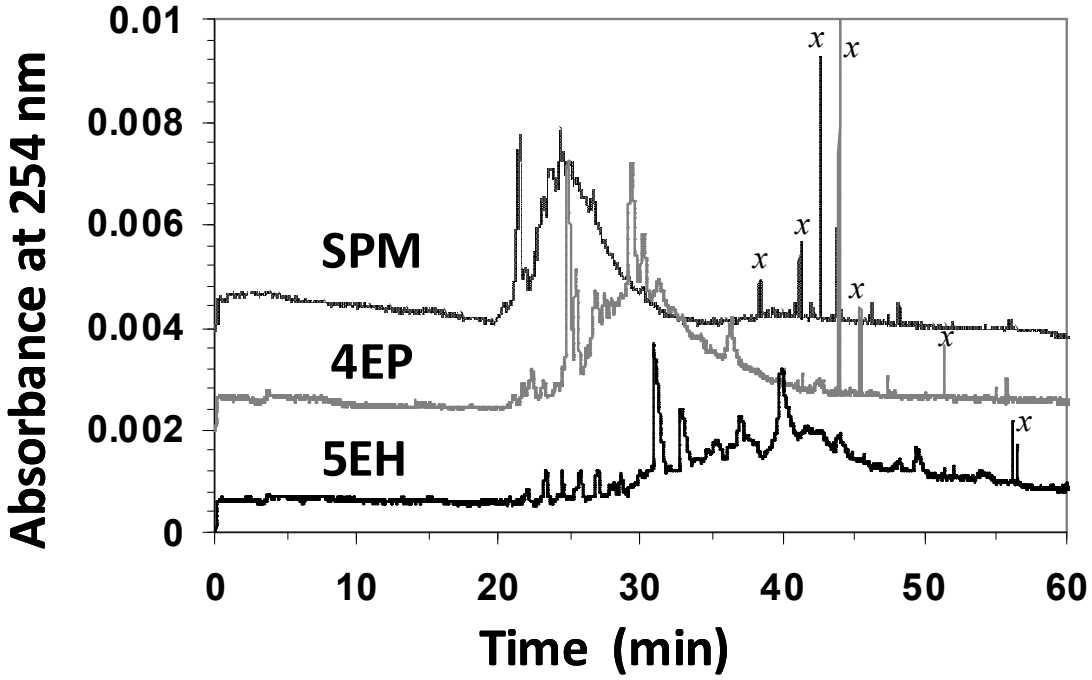

Figure 2.6: **Enoxaparin fingerprints with 125 µM SPM, 4EP, and 5EH respectively.**

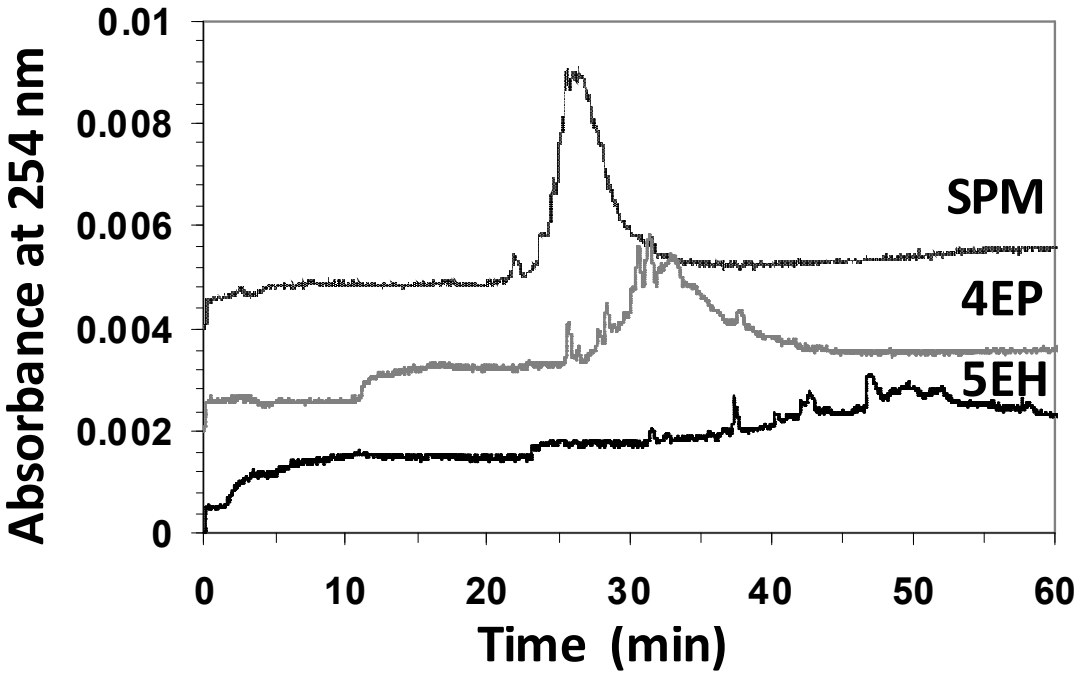

Figure 2.7: **Tinzaparin fingerprints with 125 µM SPM, 4EP, and 5EH respectively.**

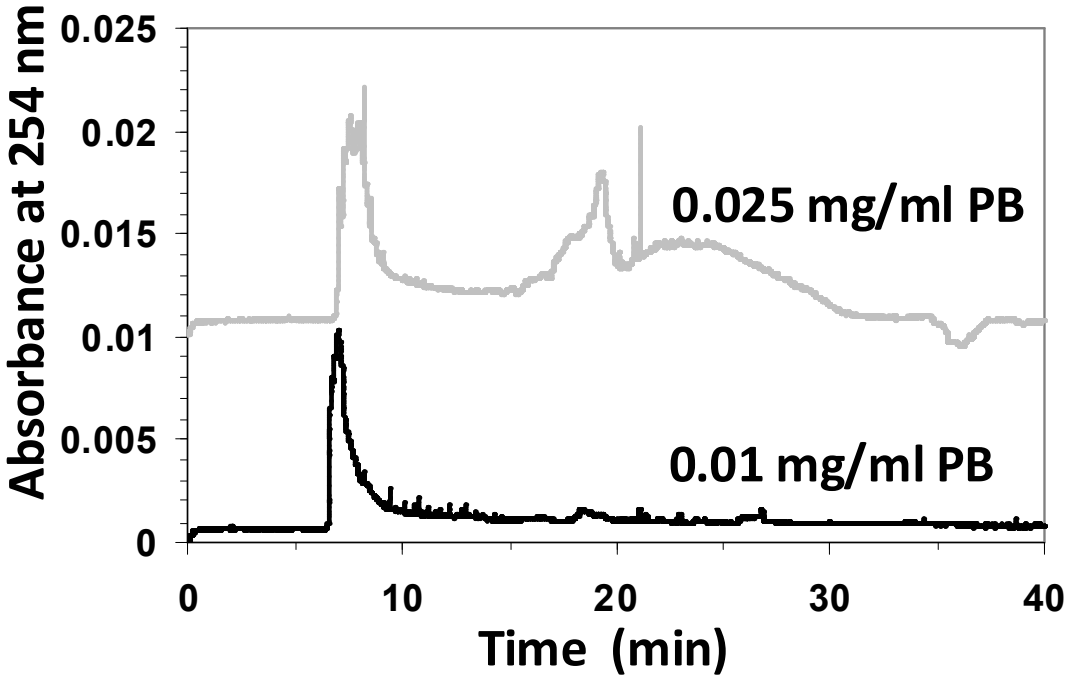

Figure 2.8: Sigma LMWH (H8537) with two concentrations of polybrene buffer additive. Run conditions: 20 mM sodium phosphate pH 3.5 with 10% DMSO, 15 kv constant voltage.

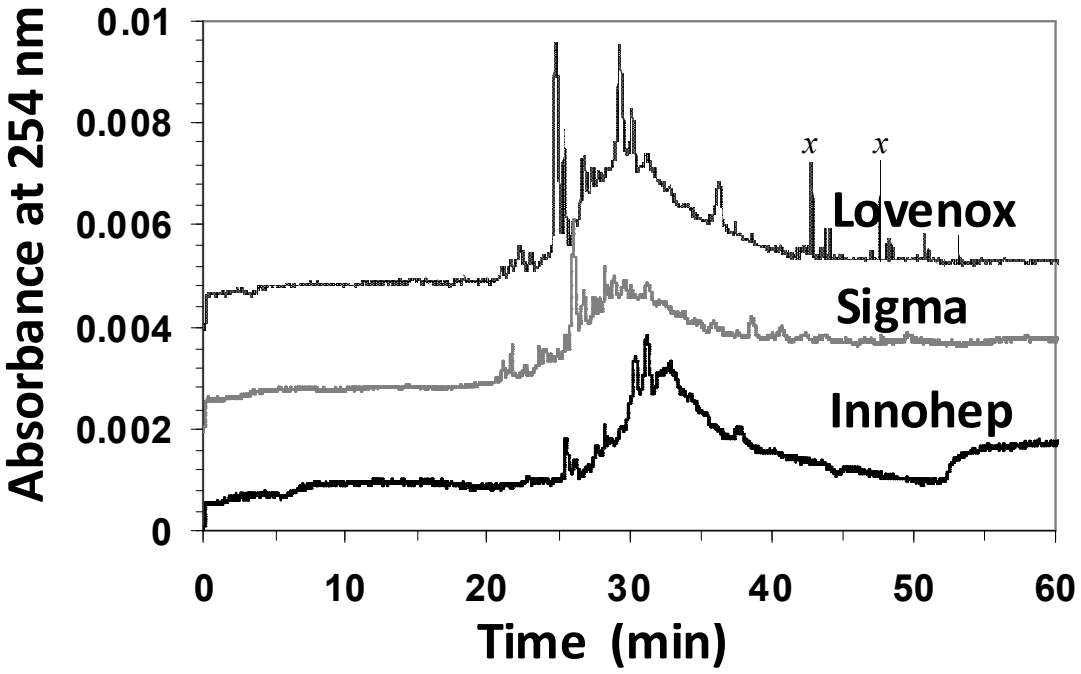

Figure 2.9: **Enoxaparin, Sigma LMWH, and tinzaparin fingerprints with 125 µM 4EP.** Peaks marked with "x" are sudden disturbances due to bubble formation during the electrophoretic run.

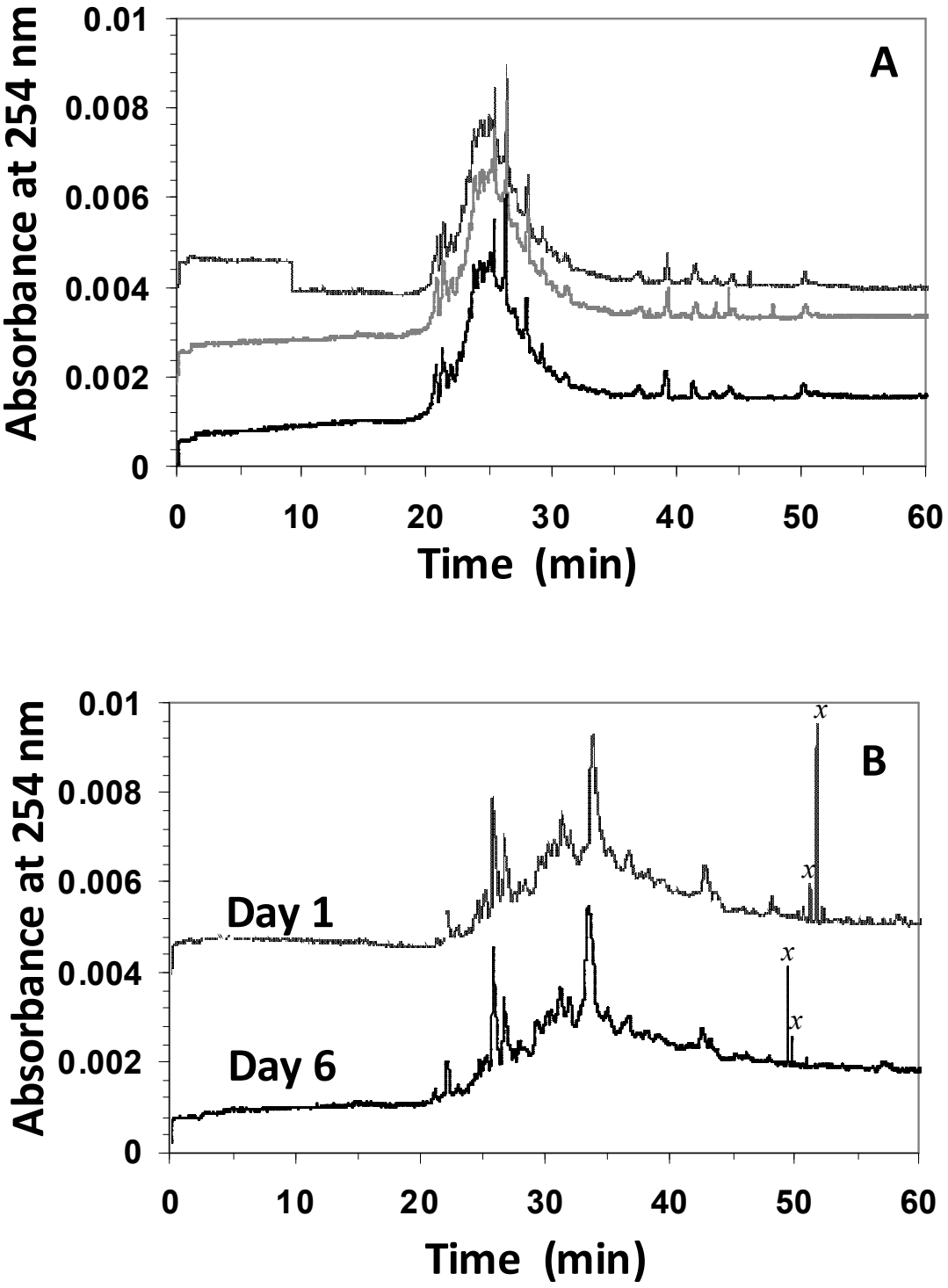

Figure 2.10: A) Same day runs of Sigma LMWH with 125 μM SPM. B) Different day runs of enoxaparin with 75 μM 5EH. Peaks marked with "x" are sudden disturbances due to bubble formation during the run.

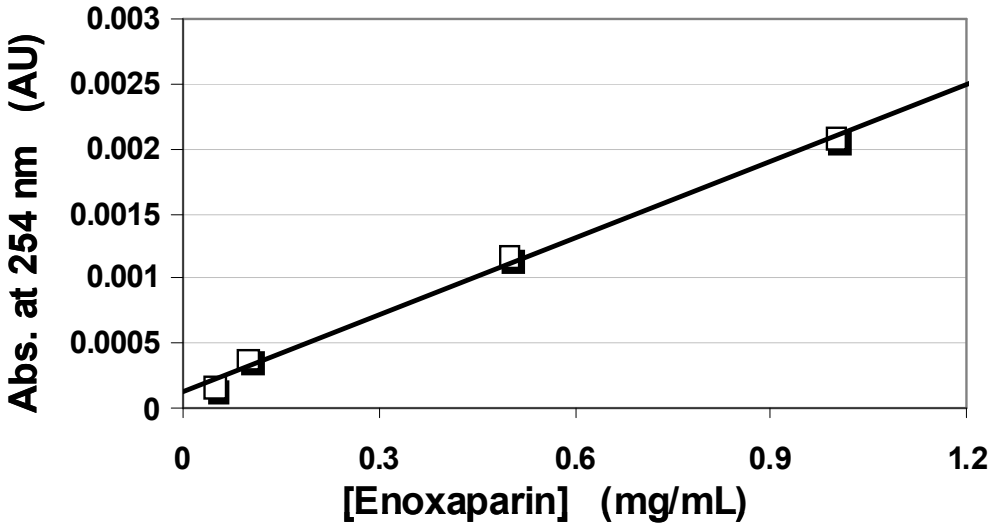

$H = 0.002 \times [LMWH] + 0.0001$ $R^2 = 0.9959$, where H = peak height

Figure 2.11: Absorption vs. enoxaparin concentration plot demonstrating the dependence of peak height on the amount of labeled LMWH. The equation obtained from the linear regression was used to calculate the LOD and LOQ (see Table 1).

Resolution of Full Length Glycosaminoglycans

3.1 Introduction

The fingerprinting of LMWHs suggested the possibility of the same with longer GAGs such as UFH. The sheer complexity of these mixtures makes their separation and characterization a difficult endeavor. Yet, the development of a reliable, high resolution fingerprinting protocol would be highly useful for a number of reasons. First, UFH is taken from animal sources, meaning that their synthesis may be affected by the environmental conditions in which the host lived. Fingerprinting would allow for detecting variation among lots of heparin and ensuring a consistent patient response [2]. Second, UFH has pharmacological properties far beyond its anticoagulant activity due to interactions with numerous proteins [141]. High resolution fingerprinting of UFH would aid in the discovery of specific sugar sequences responsible for this activity. Finally, the OSCS-heparin contamination crisis has highlighted the necessity for techniques capable of detecting unwanted contaminants as numerous protocols have appeared in the literature [26,48]. A full discussion of the issues surrounding the characterization of UFH can be found in Chapter 1.

This chapter details our efforts to use the linear polyamines to resolve and fingerprint UFH and CS. Conditions explored included wide variations in sample concentrations, buffer salt, and additives. Novel resolving agents were also explored

including poly amino acids, protamine sulfate, polybrene, and massive polyamidoamine dendrimers. These results were expected to provide insight into the nature of the interaction between positively charged small molecules and complex GAGs. This in turn will prove useful structural and functional analysis of heterogeneous polysaccharide mixtures.

We also explored the potential of our resolving agents in identifying OSCS contamination of UFH. As detailed in chapter 1, this is important for the purity of the drug and most importantly the safety of patients. While other CE protocols have been developed, we have found that 5EH provides a wider separation of the two than has been published. With improvements in sensitivity, this may become a useful technique in the analysis of UFH purity.

3.2 Methods

3.2.1 Materials

UFH lot 405492 from Abraxis Pharmaceuticals (Schaumburg, IL) was purchased from the Department of Pharmacy Services at Virginia Commonwealth University Health Systems. UFH lot 026K1554 was purchased from Sigma-Aldrich (St. Louis, MO). 2-Aminoacridone (AMAC), 2-aminoanthraquinone, 2-amino-3-hydroxyanthraquinone, CS (chondroitin sulfate A, lot # 038K1276), Polyamidoamino dendrimer generation 0 (PAMAM#0), generation 1 (PAMAM#1), polybrene, protamine sulfate, pyridine, sulfur trioxide pyridine,and dibasic sodium phosphate were purchased from Sigma-Aldrich (St. Louis, MO). DMSO and hydrochloric acid was purchased from Fisher Scientific (Pittsburgh, PA). Pentaethylenehexamine (5EH), tetraethylenepentamine (4EP), and spermine (SPM) were purchased from Acros Organics (Geel, Belgium). Fused silica

capillary (75 μm inner diameter) was purchased from Microsolv Corporation (Eatontown, NJ). Sodium cyanoborohydride and decamethonium iodide were purchased from TCI America (Portland, OR). G-10 was purchased from GE-healthcare (United Kingdom).

3.2.2 Labeling of GAGs

A representative labeling procedure involved dissolving 100 mg of CS in 800 μL of high purity water and 8 mg of AMAC in 800 μL of a 17:3 solution of water and incubation DMSO/Acetic Acid. The AMAC was then added to the dissolved UFH and the solutions were allowed to incubate at 37°C for 18-24 hours, followed by the addition of 320 mg of sodium cyanoborohydride in 350 μL water for approximately 6 more hours. The free AMAC was filtered out by a sephadex G-10 column and liopholyzed. Anthraquinone (AMAQ) based labels underwent a similar procedure to AMAC. UFH was labeled by a similar procedure to CS.

3.2.3 Oversulfation of CS

OSCS was synthesized from CS previously labeled with 2-aminoacridone. in a manner similar to that reported in the literature [43]. Briefly, AMAC-labeled CS was converted to a triethylamine salt using a AG 50W-X8 cation exchange column followed by titration to pH 5 with triethylamine. 100 mg CS and 2.5 g sulfur trioxide – pyridine complex were dissolved in 8 ml of anhydrous DMF and stirred at 50°C for 1 h. The sodium salt was regenerated by precipitation by adding cold ethanol saturated with sodium acetate as described in the literature [43].

3.2.4 Capillary Electrophoresis

CE was performed on a Beckman-Coulter P/ACE MDQ capillary electrophoresis instrument using 75 and 100 μm inner diameter fused silica capillaries. The capillary

was rinsed with 0.5 M sodium hydroxide, water, 0.5 M phosphoric acid, and water for 2 minutes each at the beginning of each round of CE runs and was briefly rinsed periodically during the day afterwards. The exact run conditions often varied between experiments and are noted in the caption of each figure or in the text.

3.3 Results

3.3.1 Fingerprinting of Unfractionated Heparin.

Initial efforts to develop high resolution fingerprints using the same conditions as LMWH as described in chapter 1 were unsuccessful. **Figure 3.1** shows electropherograms of 30 mg/ml Sigma-Aldrich UFH with increasing concentrations of 5EH. 25 μM 5EH merely resulted in the compression and sharpening of the main peak body, but higher concentrations produced a scattered peak pattern. The peaks acquired resembled the build up of air bubbles in the capillary due to joule heating, though the capillary temperature was set at 15°C. As the 50 μM runs indicate, the peaks are not reproducible from run to run, meaning they are not useful as fingerprints (**figure 3.1b**). The peaks seen did not translate into a usable fingerprint. Raising the concentration of 5EH to 150 μM further increases the number of peaks indicating that there is a vigorous interaction taking place but in an erratic manner. Decreasing the concentration of UFH to 3 mg/ml of Sigma UFH resulted in a noticeable change in the sensitivity of the GAG to 5EH, though it was not suitable as a fingerprint. 20 μM 5EH provided numerous peaks comparable to what 100-200 μM 5EH would do at much higher concentrations of UFH as displayed in **figure 3.2**. This indicates that there is likely a large number of sites for 5EH to saturate on UFH. A batch of clinically used UFH made by Abraxis Pharmaceuticals yielded the same results (not shown). Increasing the buffer

concentration from 20 to 50 mM sodium phosphate and reducing the concentration of Sigma UFH to 1 mg/ml yielded results was expected to have a moderating effect on 5EH binding and further decrease the number of possible sites as this was considered a possible reason for the erratic profiles. However, results were similar to that obtained previously though with greater sensitivity to 5EH as seen in **figure 3.3**. Since aggregation was a major problem in developing consistent LMWH fingerprints, it was thought that increasing the DMSO concentration by 50-100% would prevent aggregation that may occur with UFH. 100 mM NaCl was added to the buffer as the DMSO tended to suppress the voltage at constant current. The addition of DMSO eliminated the peaks (**figure 3.4**). The addition of 20 mM triethylamine to 30 mM phosphate buffer with 10% DMSO produced a multi-featured fingerprint of 15 mg/ml Abraxis UFH in the presence of 50 μM 5EH (**figure 3.5**). It was hoped that adding large amounts of triethylamine would have a stabilizing effect on the polyamine UFH-interaction, but it did not aid in developing useful fingerprints as the profiles acquired were not reproducible.

Buffer systems based on salts other than sodium phosphate were also explored as changes the interactions of different electrolytes with both 5EH and UFH could affect how the two interacted with each other. 10 mg/ml of Sigma Aldrich UFH was not successfully fingerprinted when pH 2.75 50 mM sodium citrate. Changing the organic additive to 5% methanol yielded similar results (not shown). 100 mM ammonium formate pH 3.46, while successfully used to fingerprint LMWH in chapter 2 (**figure 2.3**) yielded fingerprints resembling that of sodium phosphate buffer (not shown).

5EH proved unable to predictably fingerprint UFH under any set of run conditions performed in a manner similar to those used for LMWH. A novel approach to this problem was needed. 25 μM 5EH was incubated with the Abraxis UFH sample overnight at room temperature to slow and stabilize the 5EH-UFH equilibrium. CE was then performed with 25 μM 5EH in the buffer in typical fashion. The result was the most consistent UFH electropherograms acquired, with three back to back runs displaying notable similarities (**figure 3.6**). Even so, they did not display the reproducibility needed for a fingerprint useful for quality control and assurance. Runs at controlled temperature incubations of 37°C yielded similar results.

The failure of 5EH as an effective agent prompted the exploration of other polycationic compounds as means of resolution. 4EP and SPM were successful with LMWH but failed with UFH, with 4EP profiles resembling that of 5EH and SPM showing no resolutive capability (**figure 3.7**). It was thought that longer polycationic compounds would interact differently with UFH than 5EH, creating a stable interaction and a reproducible fingerprint. Poly-L-lysine with an average molecular weight of 4200 gave inconsistent results, but often resulted in a large amount of peak compression with little resolution (**figure 3.8**). Poly-L-lysine mixtures of higher average molecular weight along with poly-L-arginine mixtures proved useless as resolving agents. The quaternized, polydisperse mixtures polybrene and protamine sulfate were explored in varying mixed proportions. Like the overnight 5EH incubation results, this showed a somewhat higher run to run consistency than usual, but failed to develop useful fingerprints (**figure 3.9**). PAMAM#1 looked to be a promising agent simply because of its large size and abundance of charges like polybrene, but was also a homogeneous compound. Results

were very similar to 5EH in that the profile was not the same from one run to the next (**figure 3.10-3.11**).

3.3.2 Fingerprinting of Chondroitin Sulfate

Like heparin, CS is a glycosaminoglycan with many physiologic actions and an astonishingly high degree of heterogeneity and polydispersity [6,142]. Thus, CS was expected to behave similarly to UFH in the presence of polyamines. This however, was not the case as 5EH displayed little ability to interact with CS at 200 μM and had no resolutive capabilities with 800 μM 4EP (not shown). CS has a lower density of sulfate groups when compared to UFH (0.95 vs 2.4 sulfates per disaccharides, respectively). It is likely that there is not enough sulfate groups present on CS to effect the same response to 5EH that UFH does [143]. Poly-L-lysine provided resolution of CS (**figure 3.12**), but this could not be reproduced. Difficulties were even more prominent with polybrene. The most reproducible electrophoretic profiles for CS were obtained using PAMAM #1. **Figures 3.13** show that PAMAM #1 was able to generate surprisingly reproducible profiles of CS at 15 μM. Unfortunately, this was not consistent from day to day as subsequent runs lacked the resolution and repeatability desired for a fingerprint. As with UFH, no set of conditions explored resulted in repeatable, high resolution fingerprints of CS.

3.3.3 Separation of Oversulfated Chondroitin Sulfate from Unfractionated Heparin

While several CE protocols available for detecting oversulfated contaminants in UFH [45,46,84], we sought to use linear alkyl polyamines to improve on their resolution. Initial results CE results were confirmatory of the higher degree of sulfation pattern on OSCS when compared to CS (**figure 3.14a-b**). Both OSCS and UFH displayed affinity

for 40 μM 5EH at a sample concentration of 20 mg/ml, but yielded dramatically different profiles. OSCS showed a compressed peak that migrated very little, but UFH displayed its characteristic noisy pattern. Since the two peak bodies came out at different times, it was thought that UFH and OSCS would be easily separated in a mixture (**figure 3.14c,e**). However, this was not the case as UFH-OSCS mixtures of varying proportions were inseparable. In fact, only a single peak body was present where there should have been two of them (**figure 3.15**). The addition of 5EH to a mixture of UFH and OSCS likely causes aggregation of the two polysaccharides. However, upon sharly reducing the sample concentration, the results are dramatically different. **Figure 3.16a-b** displays UFH and OSCS electropherograms eluting separately as previously seen, with both GAGs having a sample concentration of 0.5 mg/ml and 15 μM 5EH in the run buffer. When combined to form a 1 mg/ml GAG mixture of 50% UFH and 50% OSCS, a wide separation of 10-15 minutes separation was observed (**figure 3.16c**). In comparison to other CE protocols, none have shown such a separation between OSCS and UFH. It is notable that the UFH migrated faster when mixed with OSCS than when alone. It is possible that OSCS sequesters a large proportion of 5EH and cause UFH to come out sooner than otherwise due to the reduced availability of the resolving agent. However, the low concentration of each GAG did not allow aggregation as seen with 20 mg/ml GAG. Resolution time was further shortened by applying 0.3 PSI forward pressure and switching the polarity from normal to reverse (**figure 3.16d**). This allows for OSCS to come out as normal while forcing UFH to come out in a narrow band of peaks. Unfortunately, the method suffered from an inadequate limit of detection. A 1 mg/ml solution with 10% OSCS displayed an irregular signal from run to run. Less than

10% OSCS showed little if any signal. The total GAG concentration was increased to 2 mg/ml to remedy this, but resulted in a noticable reduction in resolution (**figure 17**). It is likely the case that the increased GAG concentration was causing an aggregation similar to that of the 20 mg/ml sample in **figure 3.15**. If the concentration of the GAG were further increased, OSCS and UFH would likely become indistinguishable.

3.4 Discussion

The failure of UFH to be fingerprinted under any circumstances presents a puzzling problem. Why do LMWHs yield useful fingerprints in the presence of resolving agents while UFH does not? The answer most likely involves an abnormally high number of specific binding sites. As chapter 4 discusses in detail, enoxaparin's profile is largely due to the interaction of 5EH with high affinity sites on the GAG chain. UFH's affinity for 5EH is likely so high that a dynamic equilibrium sets in, with polyamines forming complexes with multiple UFH chains. This prevents the formation of a normal, reproducible fingerprint. Further evidence is seen in **figures 3.1-3.3**, where decreasing the UFH sample concentration 10-fold increases its response to 5EH in a noticeable manner. This indicates that whatever binding sites are available on UFH are not completely saturated at the concentrations of resolving agents used for fingerprinting. Further evidence of this phenomenon is clearly seen in the OSCS-UFH studies where the two components are only resolvable when their concentration is low. At higher concentrations, polyamines act as a "glue" that holds them together. It is highly likely that such aggregation is occurring between UFH molecules in the presence of 5EH even when OSCS is absent.

Alternatively, it is possible that the “noise” seen in most profiles is due to joule heating resulting from the high sulfate density of UFH and the concentration of polyamines. However, the data suggests otherwise. The LMWH trials in chapter 2 do not show such noisy profiles though they also contain a high density of sulfates. The fact 20 and 50 mM sodium phosphate buffers showed similar peak patterns indicates that higher ionic strength is not the cause of the irregular profiles (**figures 3.2-3.3**). Rather, it is due a tighter interaction of UFH with the resolving agents.

The best solution to the problem of UFH would be to use laser-induced fluorescence detection as this is much more sensitive than UV. This would allow the concentration of UFH to be reduced dramatically, possibly eliminating aggregation and reducing the number of binding sites. Such improvements would also allow for lowering the limit of detection of OSCS, making it a potentially viable method.

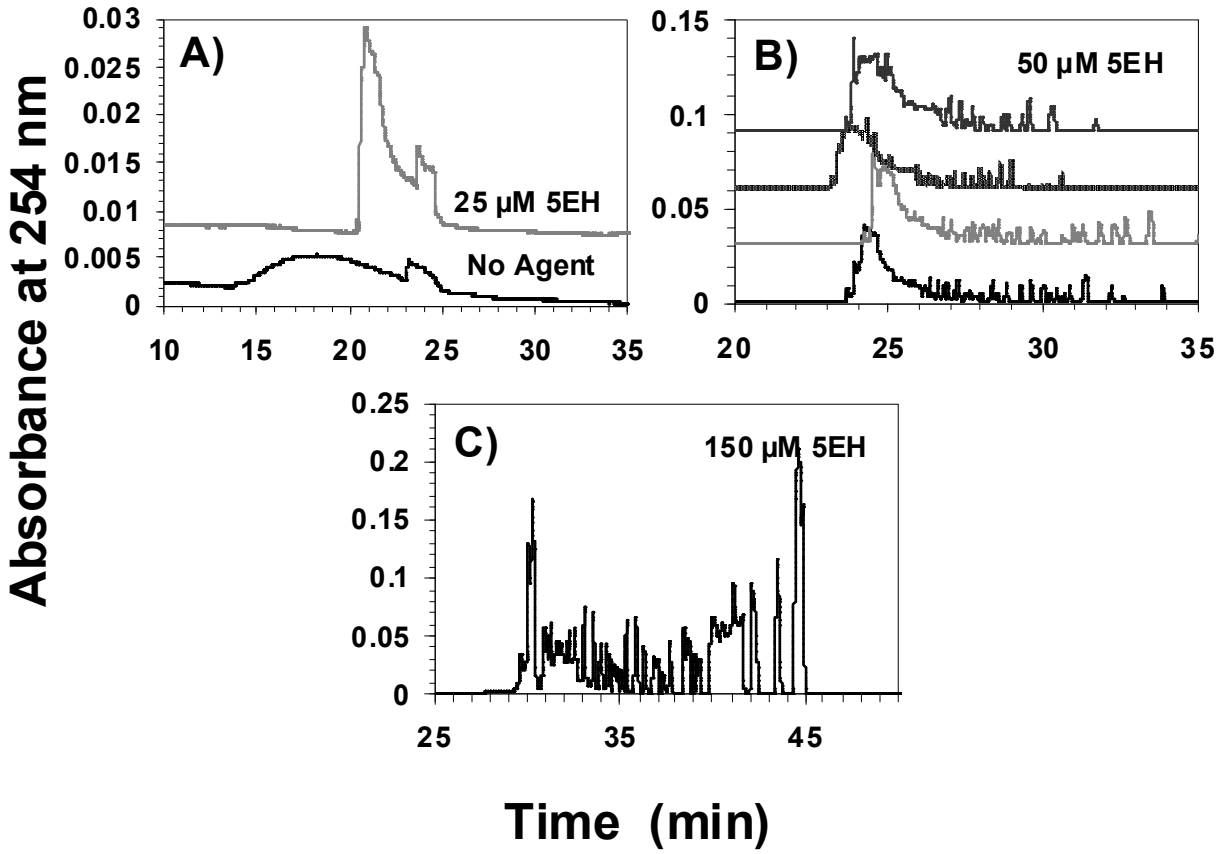

Figure 3.1: Same day fingerprints of UFH in the presence of 5EH. A) 0 and 25 µM 5EH; B) 4 repeated runs of 50 µM 5EH; C) 150 µM 5EH. Sample: 30 mg/ml Sigma UFH 026k1554 in 10% DMSO; Buffer: 20 mM sodium phosphate 10% DMSO pH 2.3; 254 nm detection; Injection: 15 seconds@1psi; temperature: 15°C; Separation: 110 µA Capillary: 100 µm ID.

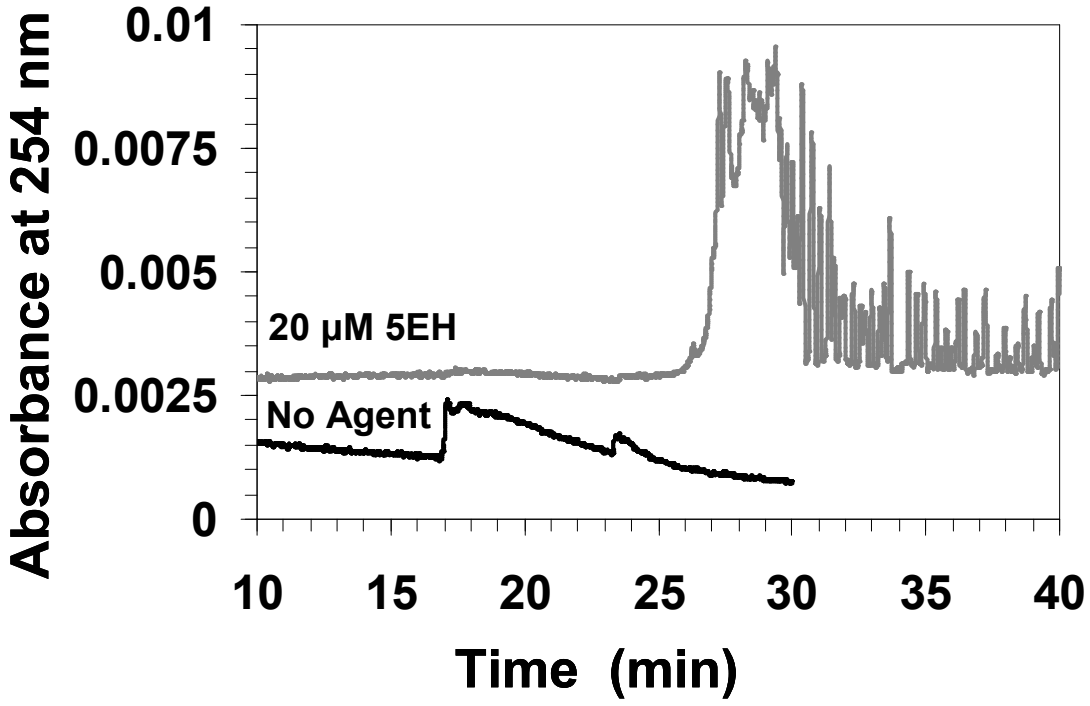

Figure 3.2: Same day fingerprints of reduced concentration UFH in the presence of 20 µM 5EH. Sample: 3 mg/ml Sigma UFH 026k1554 in 10% DMSO; Buffer: 20 mM sodium phosphate 10% DMSO pH 2.3; 254 nm detection; temperature: 15°C; Injection: 15 seconds@1psi; Separation: 110 µA; Capillary: 100 µm ID.

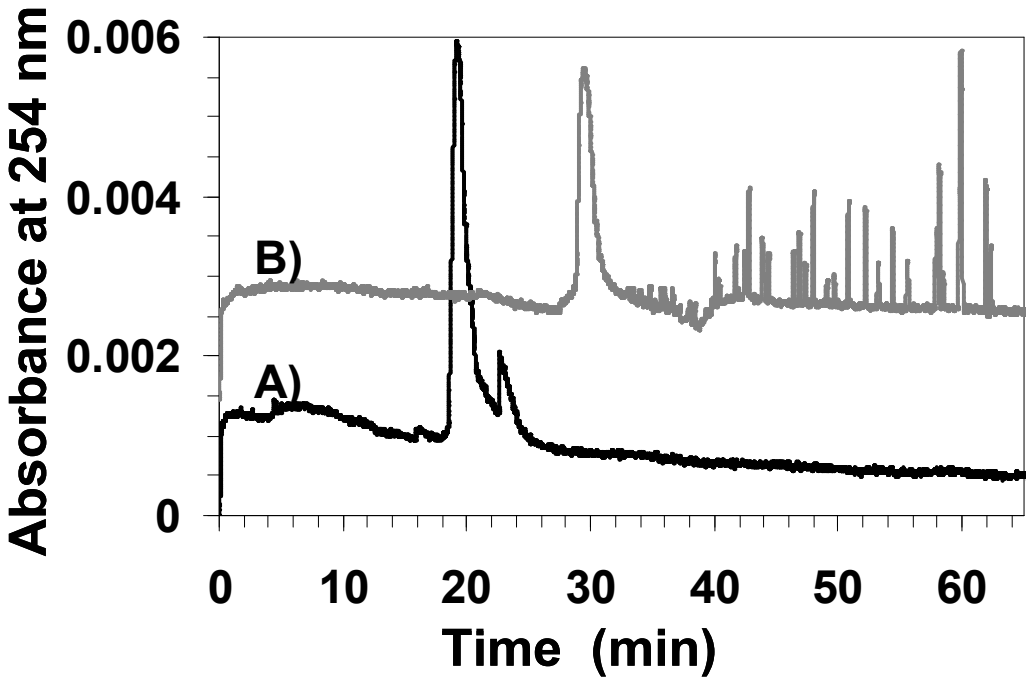

Figure 3.3: Same day fingerprints of 1 mg/ml UFH in the presence of 5EH. A) 3 µM 5EH, B) 6 µM 5EH. Sample: 1 mg/ml Sigma UFH 026K1554 in 10% DMSO; Buffer: 50 mM NaPi pH 2.3; 254 nm detection; Injection: 10 seconds@1.5psi; temperature: 15°C; Separation: 110 µA; Capillary: 100 µm ID.

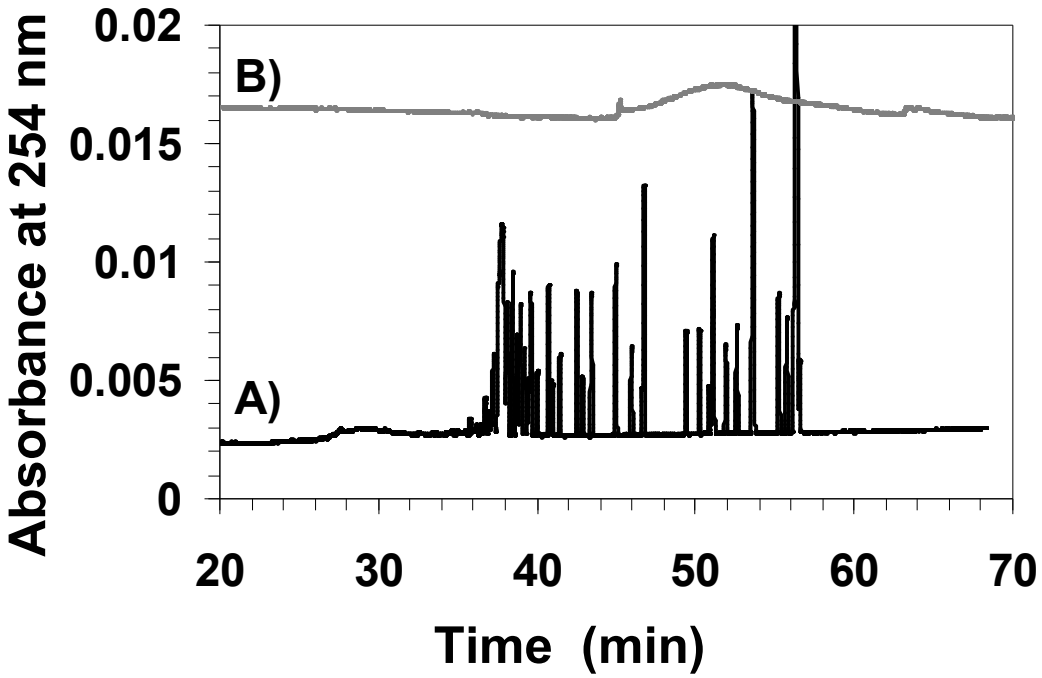

Figure 3.4: Same day fingerprints of 3 mg/ml Sigma UFH in 15 µM 5EH with differing buffer compositions. A) 20 mM sodium phosphate pH 2.3 10% DMSO, B) 20 mM sodium phosphate, 100 mM NaCl, 17.5% DMSO. Sample: 3 mg/ml Sigma UFH 026k1554 in 10% DMSO; 254 nm detection**;** Injection: 15 seconds@1psi; Separation: 110 µA; Capillary: 100 µm ID.

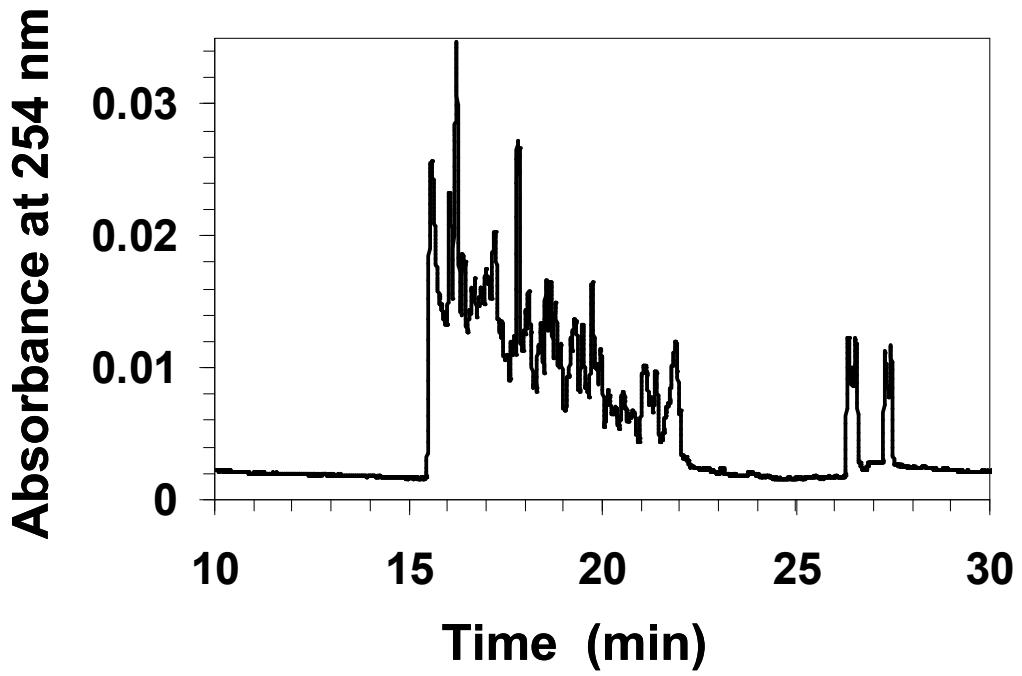

Figure 3.5: An attempt to fingerprint UFH with 50 µM 5EH and 20 mM triethylamine. Sample: 15 mg/ml Abraxis UFH 405492 10% DMSO; Buffer: 30 mM sodium phosphate 20 mM triethylamine pH 2.3 10% DMSO; 254 nm detection; Injection: 10 seconds @ 1.5 psi; temperature: 15°C; Separation: 10 kV; Capillary: 75 µm ID.

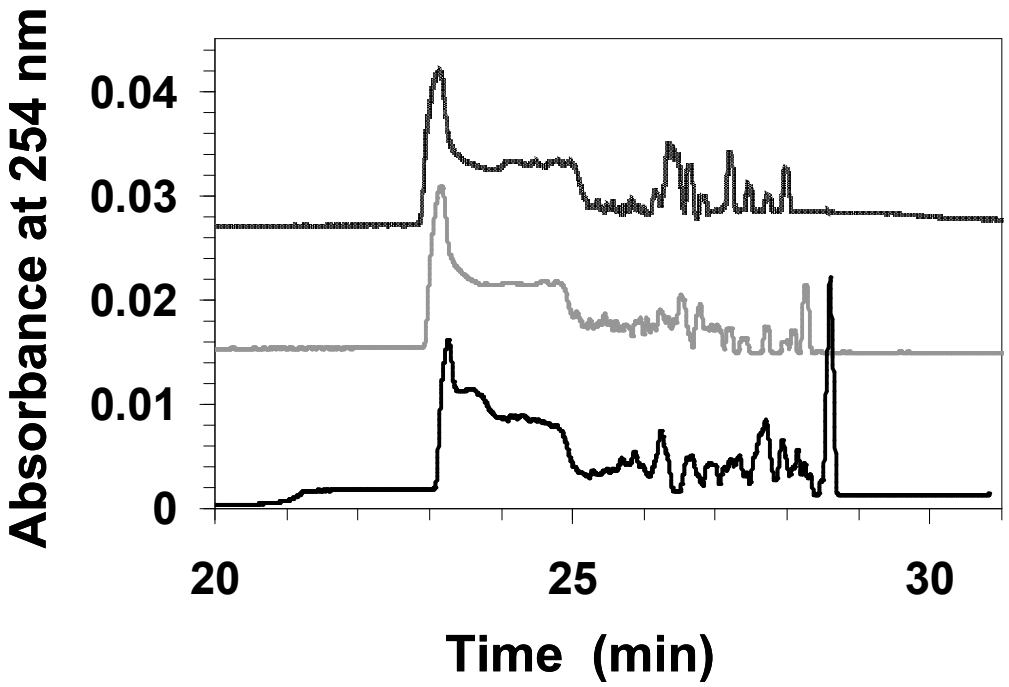

Figure 3.6: UFH sample that was incubated with 25 µM 5EH overnight. Three consecutive runs were performed. Sample: 10 mg/ml Abraxis UFH 405492 10% DMSO 25 µM 5EH; Buffer: 50 mM sodium phosphate pH 2.3 10% DMSO; 254 nm detection; Injection: 8s@1psi; temperature: 25°C; Separation: 10 kV; Capillary: 75 µm ID.

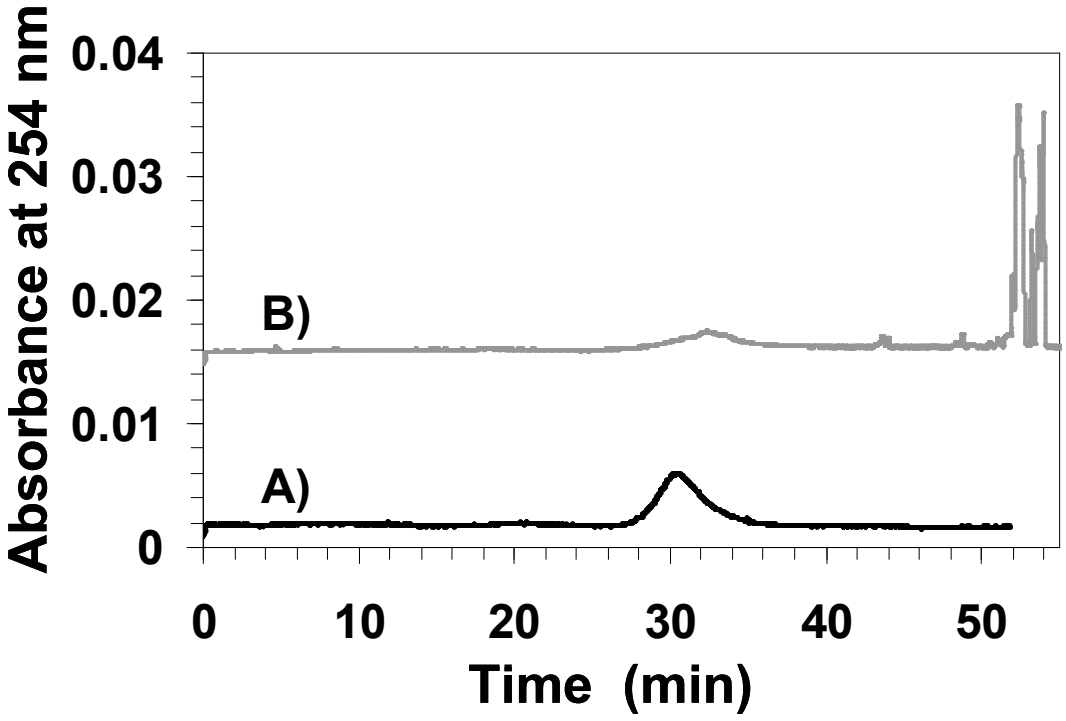

Figure 3.7: SPM and 4EP used in the resolution of UFH. A) 50 µM SPM, B) 50 µM 4EP. Sample: 2 mg/ml Sigma UFH 026K1554 10% DMSO; Buffer: 50 mM sodium phosphate pH 2.3 10% DMSO; 254 nm detection; Injection: 8 seconds@1psi; temperature: 15°C; Separation: 100 µA; Capillary: 75 µm ID.

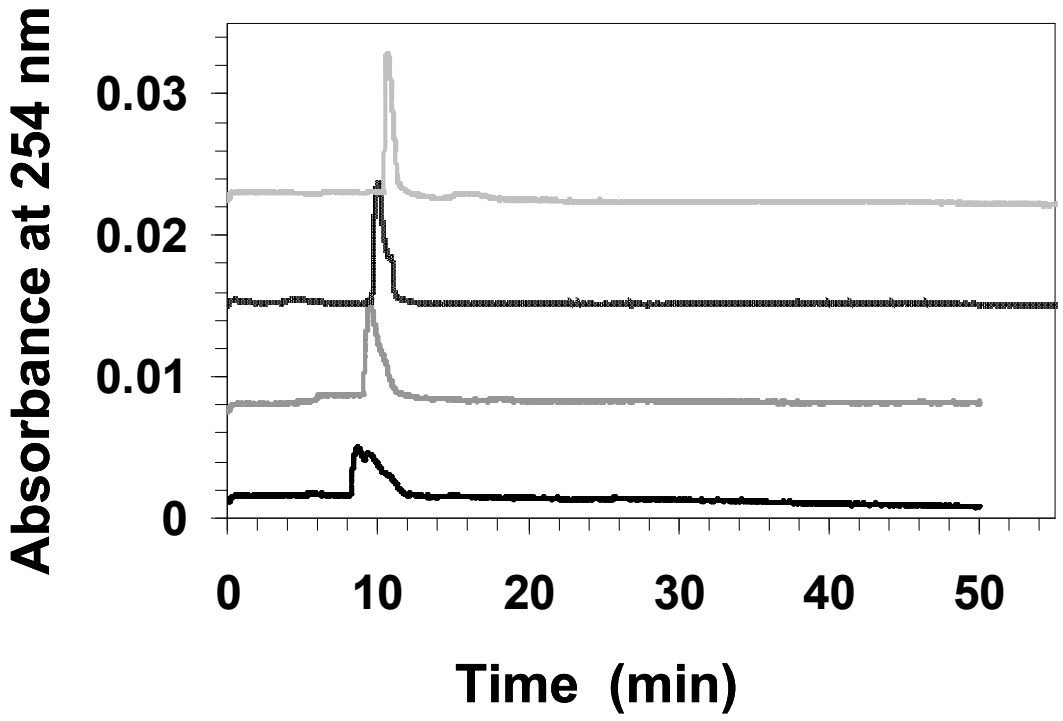

Figure 3.8: Attempt to resolve UFH with poly-L-lysine (mean MW: 4200). A) 2.5 µM PLL, B) 5 µM PLL, C) 7.5 µM PLL, D) 10 µM PLL. Sample: 10 mg/ml Abraxis UFH 405492 10% DMSO 25 µM 5EH; Buffer: 50 mM sodium phosphate pH 2.3 10% DMSO; 254 nm detection; Injection: 10 seconds@1.5psi; temperature: 25°C; Separation: 10 kV; Capillary: 75 µm ID.

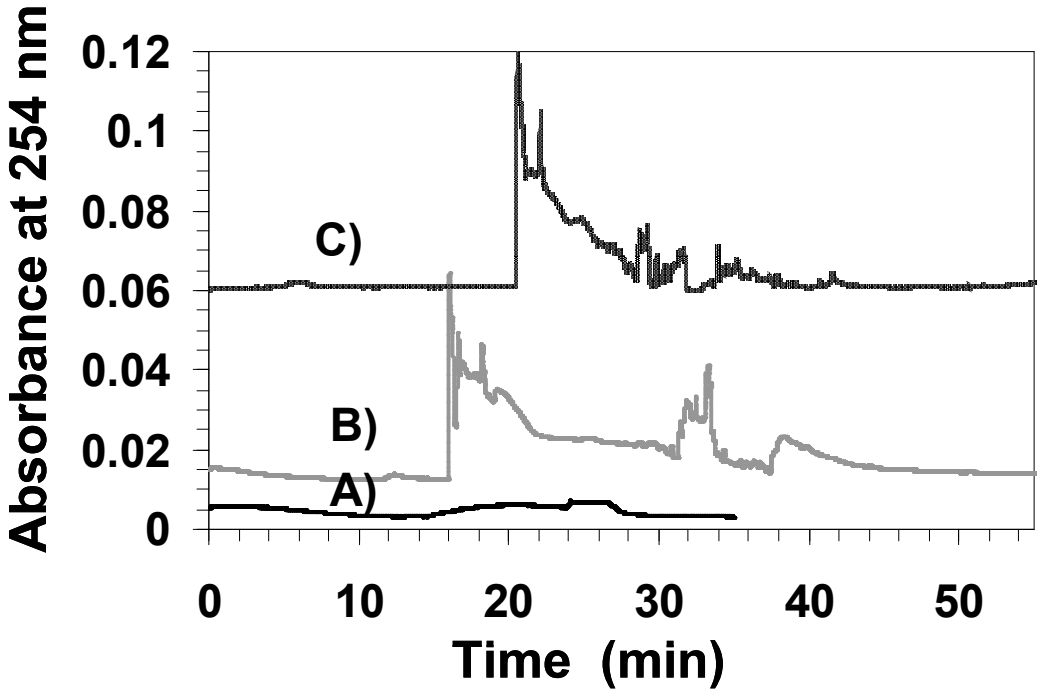

Figure 3.9: Attempt to resolve UFH a mixture of polybrene and protamine. A) No agent, B) 15 µg/ml polybrene+5 µg/ml protamine #1 C) 15 µg/ml polybrene+5 µg/ml protamine #1. Sample: 20 mg/ml Abraxis UFH 405492 10% DMSO; Buffer: 50 mM sodium phosphate pH 2.3 10% DMSO; 254 nm detection; Injection: 8 seconds@1psi; temperature: 15°C; Separation: 10 kV; Capillary: 75 µm ID.

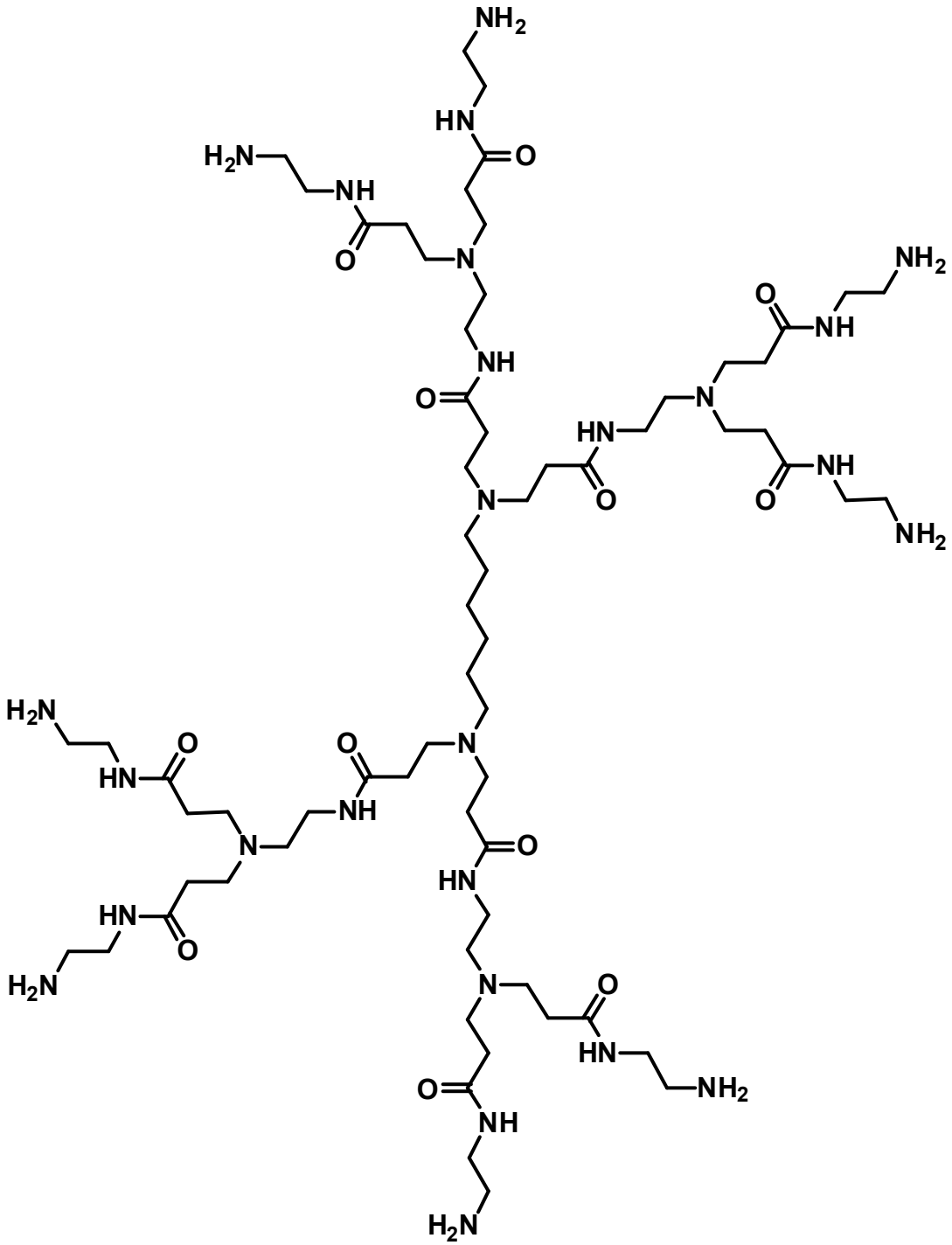

Figure 3.10: The structure of polyamidoamide #1 (PAMAM #1).

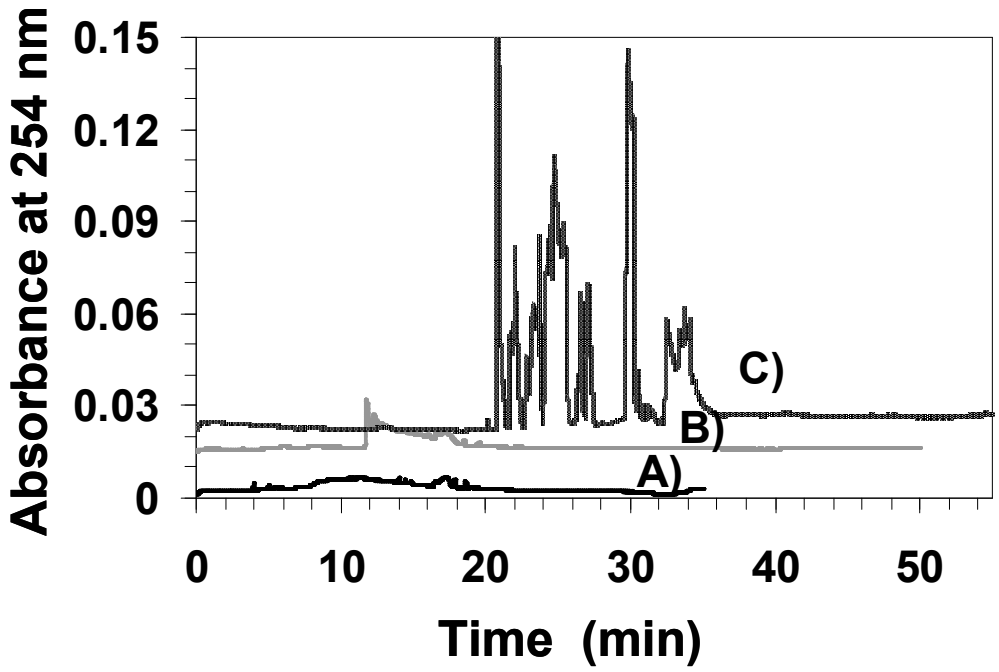

Figure 3.11: Attempt to resolve UFH with PAMAM#1. A) No agent, B) 40 μM PAMAM#1, C) 100 μM PAMAM#1. Sample: 15 mg/ml Abraxis UFH 405492 10% DMSO; Buffer: 50 mM sodium phosphate pH 2.3 10% DMSO; 254 nm detection; Injection: 10 seconds@1.5psi; temperature: 15°C; Separation: 15 kV; Capillary: 75 μm ID.

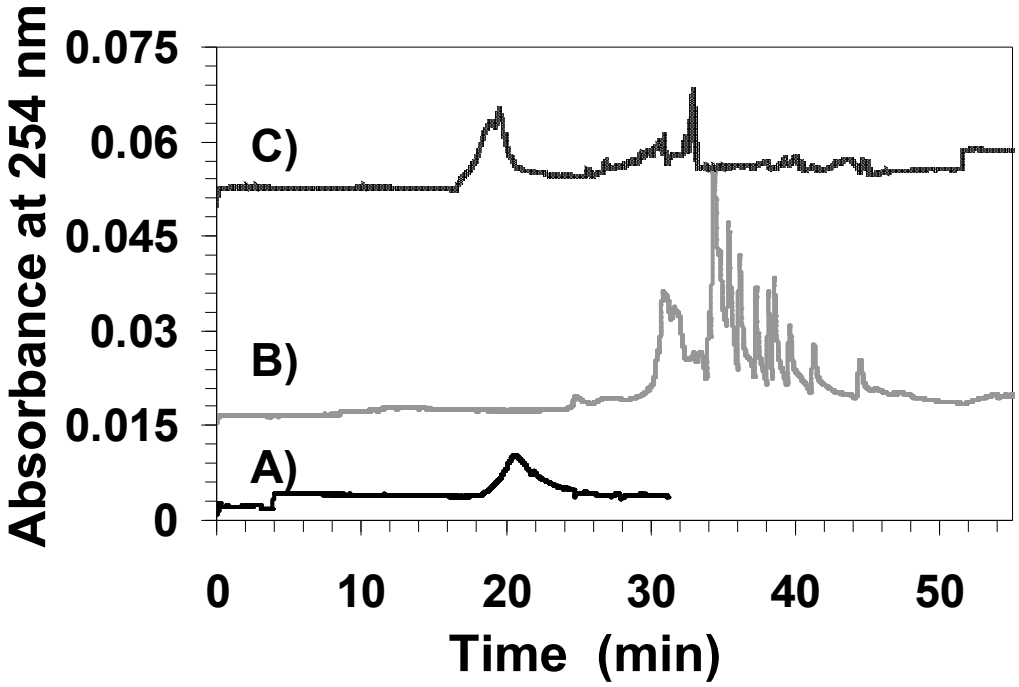

Figure 3.12: Attempt to resolve CS with poly-L-lysine (average MW: 4200) and polybrene. A) No agent, B) 25 µM poly-L-lysine, C) 25 µg/ml polybrene. Sample: CS 038K1276 10% DMSO; Buffer: 50 mM sodium phosphate pH 2.3 10% DMSO; 254 nm detection; Injection: 8 seconds@1 psi; temperature: 15°C; Separation: 14 kV; Capillary: 75 µm ID.

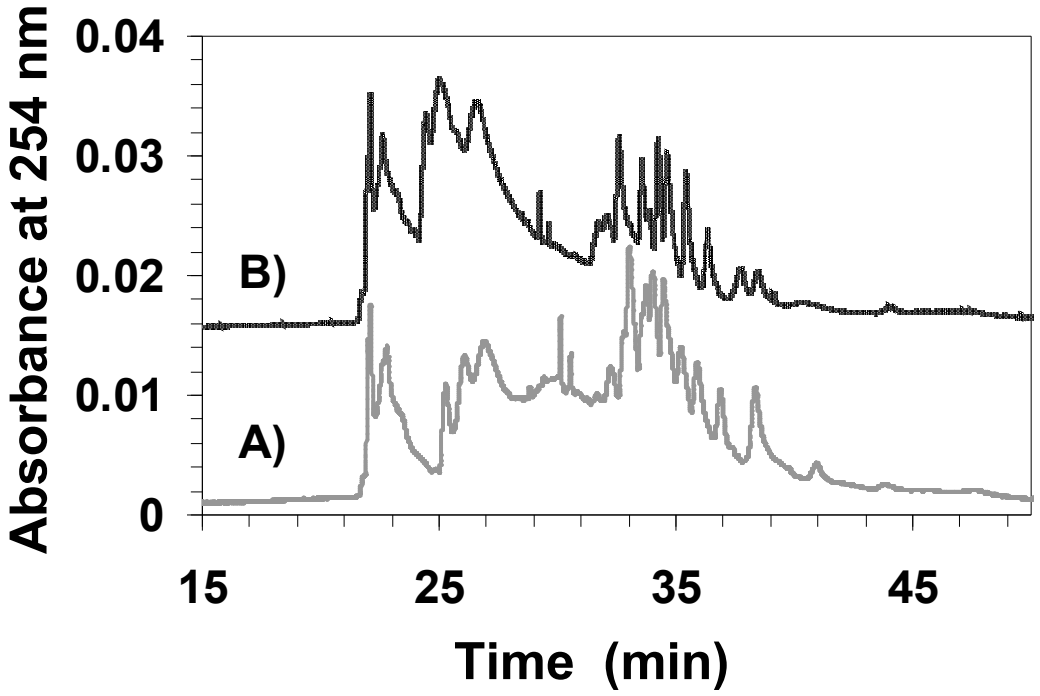

Figure 3.13: Attempt to resolve CS with back to back runs with 15 µM PAMAM #1. A) 15 µM PAMAM #1, B) 15 µM PAMAM #1. Sample: CS 038K1276 10% DMSO; Buffer: 50 mM sodium phosphate pH 2.3 10% DMSO; 254 nm detection; Injection: 8 seconds@1 psi; temperature: 15°C; Separation: 14 kV; Capillary: 75 µm ID.

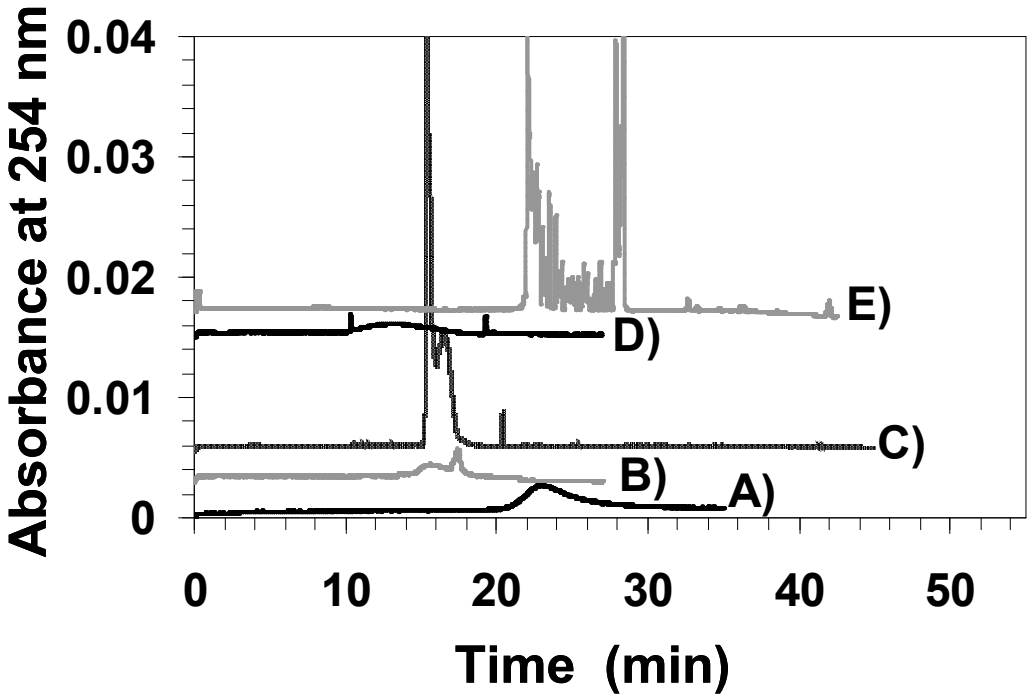

Figure 3.14: A comparison of CS, OSCS and UFH. All GAGs labeled with athraquinone and dissolved in 10% DMSO for CE. A) 9 mg/ml CS with no agent, B) 10 mg/ml OSCS with no agent, C) 20 mg/ml OSCS with 40 μM 5EH, D) 20 mg/ml Acros UFH lot B0126660 with no agent, E) 20 mg/ml Acros UFH lot B0126660 with 40 μM 5EH. Buffer: 50 mM sodium phosphate pH 2.3 10% DMSO; 300 nm detection; Injection: 8 seconds@1psi; temperature: 15°C; Separation: 85μA ; Capillary: 75 μm ID.

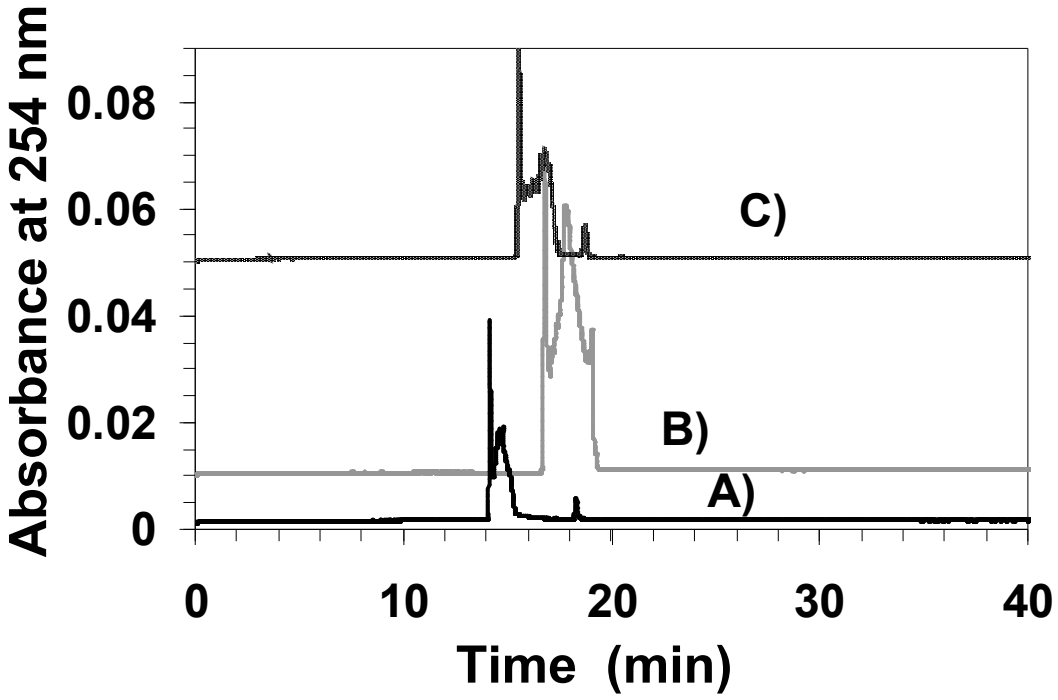

Figure 3.15: A comparison of three mixtures of OSCS and UFH. All GAGs labeled with 2-aminoanthraquinone and dissolved in 10% DMSO to a combined concentration of 20 mg/ml for CE. UFH lot: B0126660. A) 20% UFH 80% OSCS, B) 60 % UFH 40% OSCS, C) 80% UFH, 20% OSCS. Buffer: 50 mM sodium phosphate pH 2.3 10% DMSO; 300 nm detection; Injection: 8 seconds@1psi; temperature: 15°C; Separation: 85μA ; Capillary: 75 μm ID.

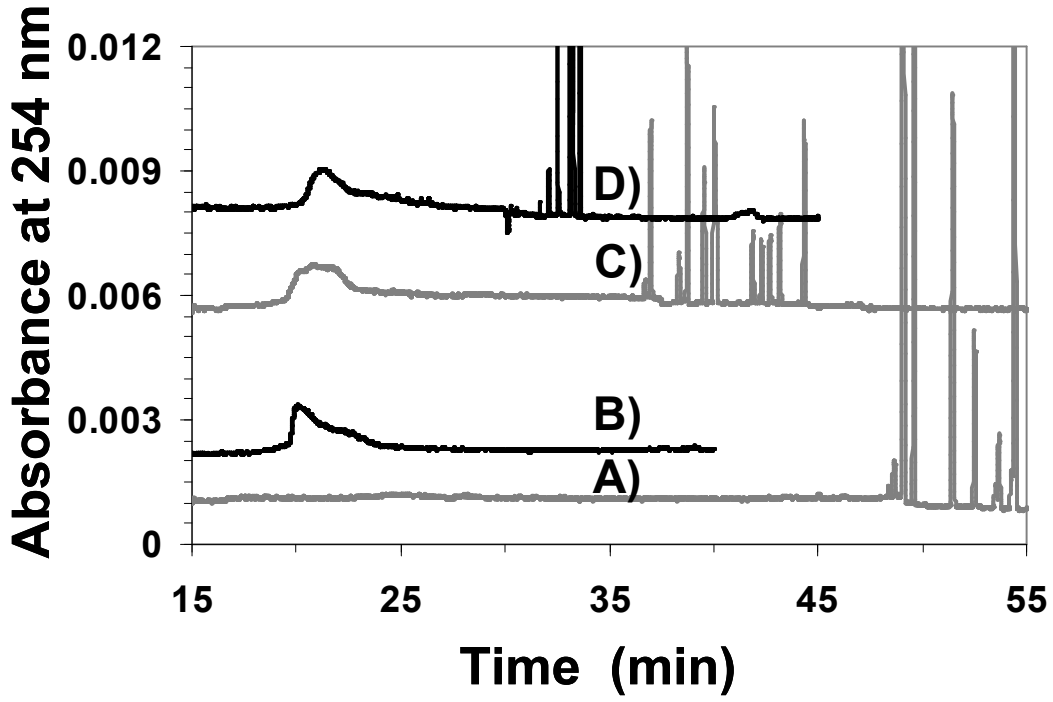

Figure 3.16: A comparison of UFH, OSCS, and a mixture of the two. All GAGs labeled with 2-aminoacridoine and dissolved in 10% DMSO. UFH lot: 026K1554. A) 0.5 mg/ml UFH, 15 µM 5EH B) 0.5 mg/ml OSCS, 15 µM 5EH , C) 1 mg/ml – 50% UFH, 50% OSCS, 15 µM 5EH. D) 1 mg/ml – 50% UFH, 50% OSCS, 15 µM 5EH w/ 0.3 PSI forward pressure and normal polarity switch at 30 minutes. Buffer: 50 mM sodium phosphate pH 2.3 10% DMSO; 254 nm detection; Injection: 8 seconds@1psi; temperature: 15°C; Separation: 85µA ; Capillary: 75 µm ID.

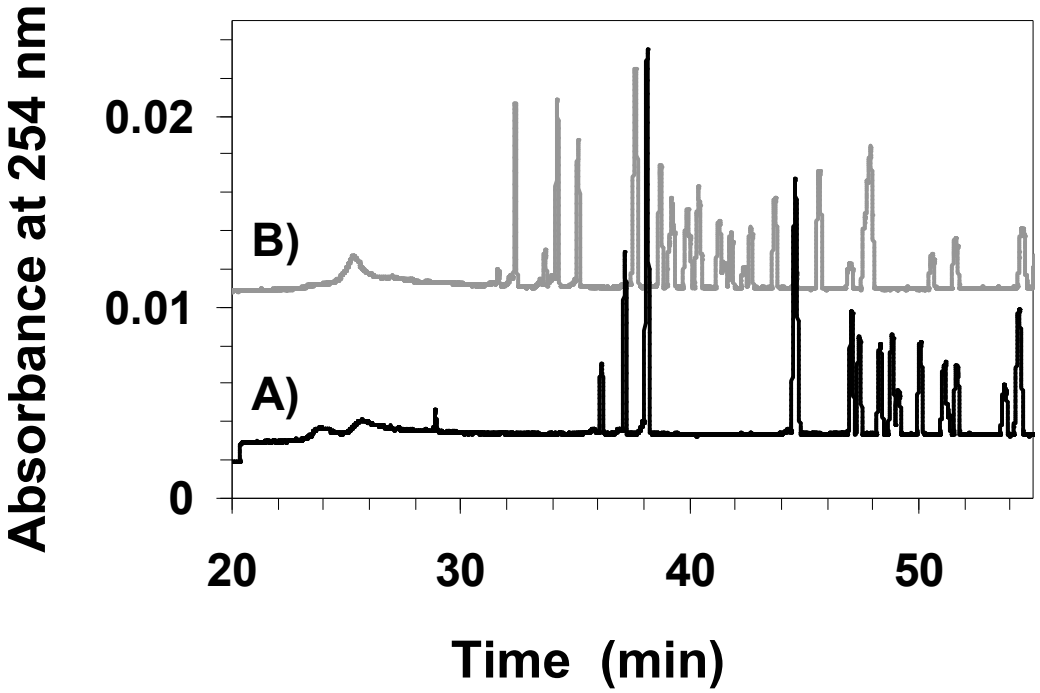

Figure 3.17: Back to back electropherograms of a 2 mg/ml GAG solution with 75% UFH and 25% OSCS in the presence of 20 µM 5EH. Buffer: 50 mM sodium phosphate pH 2.3; 254 nm detection; Injection: 8 seconds@1psi; temperature: 15°C; Separation: 85 µA; Capillary: 75 µm ID.

Insights into the Interaction of Linear Polyalkylamines with Low Molecular Weight Heparins and Glycosaminoglycans Using Capillary Electrophoresis

4.1 Introduction

GAGs are unparalleled among biomolecules in terms of their massive structural complexity, intricate and variable biosynthetic preparation, and astonishingly difficult structural, biochemical and biophysical characterization. This difficulty has inspired a large number of biophysical methods for analysis of different GAGs [68]. Further, a number of protocols relying on HPLC [100,102], NMR [45,55,144], CE [86,88], and a combination of techniques [51] have been developed for detecting UFH contaminants. We described a CE protocol that fingerprints LMWHs in chapter 2. Linear polyamines (**figure 2.2**) were used as resolving agents to produce fingerprint patterns in reverse polarity, open-tube CE from essentially featureless and unresolved profiles. These fingerprints were characteristic of the LMWH being analyzed, which afforded a major advance in profiling differences among LMWHs could prove suitable in assessing the batch-to-batch variability.

In this chapter, we address the question of why linear polyalkylamines are effective in fingerprinting LMWHs and whether these could be used in profiling other GAGs. Our work suggests that CE profile of GAGs such as DS, CS, OSCS and heparin

in the presence of polyalkylamines can be used to understand the composition of these complex mixtures. This property arises from differential recognition of micro-structures present in GAGs, which enable high affinity recognition of highly sulfated chains. These results are important because small molecule probes of GAGs are critically needed to aid in structural and functional analysis.

4.2 Methods

4.2.1 Materials

Enoxaparin (Lovenox, 40 mg syringe Lot # 09438) was purchased from the Department of Pharmacy Services at Virginia Commonwealth University Health Systems. 2-Aminoacridone (AMAC), CS (chondroitin sulfate A, lot # 038K1276), DS (lot # 118K1217), and dibasic sodium phosphate were purchased from Sigma-Aldrich (St. Louis, MO). DMSO and hydrochloric acid was purchased from Fisher Scientific (Pittsburgh, PA). Pentaethylenehexamine (5EH), tetraethylenepentamine (4EP), and spermine (SPM) were purchased from Acros Organics (Geel, Belgium) and used as received. Fused silica capillary (75 μM inner diameter) was purchased from Microsolv Corporation (Eatontown, NJ). Sodium cyanoborohydride and decamethonium iodide were purchased from TCI America (Portland, OR). Oligosaccharide species were purchased from Idruron (Manchest, UK).

4.2.2 Chromogenic Labeling of GAGs

AMAC labeling of enoxaparin was performed in a manner similar to that reported in the literature so as to enable detection of polymeric chains [145]. Briefly, LMWH (40 mg) was dissolved in 250 μL water, while AMAC (10 mg) was dissolved in 400 μL of DMSO:acetic acid (17:3 v/v). The two solutions were mixed, followed by the addition of

200 µL of sodium cyanoborohydride (100 mg) in water. The reaction was allowed to proceed for 16 hours at 37°C. The AMAC-labeled enoxaparin from the reaction mixture was purified *via* a G-10 column, the fractions lyophilized, and solid stored at 4°C until use. Samples for electrophoresis were dissolved in 10% DMSO and water just before analysis. Similar procedures were used for preparing AMAC-labeled UFH, CS, DS, and OSCS.

4.2.3 Capillary Electrophoresis

CE was performed using a Beckman-Coulter P/ACE MDQ capillary electrophoresis system using a 50 cm long fused silica capillary (40 cm to detector window, 75 µ ID). The electrophoresis buffer was composed of 50 mM sodium phosphate, pH 2.3, containing 10% DMSO. The capillary was flushed with electrophoresis buffer for two minutes, followed by injection of the analyte for 8 seconds at 1 psi. AMAC-labeled GAGs were dissolved in 10% DMSO to prevent aggregation. Separations were performed at either constant current (~85 µA) or voltage (~10 kV), temperature of 15°C and monitored at a wavelength of 254 nm. The capillary was periodically flushed with 0.5 N NaOH, 0.5 M H_3PO_4, and deionized water to maintain its resolution capability. GAG fingerprints were acquired with SPM, 5EH, 4EP and DM (**figure 2.2**, **4.1**). For the enoxaparin affinity studies, typically, 8-13 different concentrations of each resolving agent were studied within a day. Each concentration was studied at least 3 to 5 times to ensure repeatability.

For polyamine oligosaccharide affinity studies, a constant voltage of 15 kv was used at 230 nm detection.

4.2.4 Data Analysis

The affinities of LMWH and glycosaminoglycan components for linear polyalkylamines were measured from the change in electrophoretic mobility (μ^{ep}) as a function of the concentration of the resolving agent. The μ^{ep} values were calculated using equation 1, which is a modified form of that used in the literature [146].

$$\Delta\mu^{ep} = \frac{\frac{L_e}{T_{mig}}}{\frac{V}{L_t}} \qquad \textbf{(Equation 1)}$$

In this equation, L_e is the effective length of the capillary to the detector window, peak migration time is represented by t_{mig}, and V is the applied constant voltage. This equation does not include a reference migration term, i.e., the migration time of neutral marker for reducing run-to-run variations, as reported in the literature [146], because a neutral marker does not migrate under the strongly acidic conditions, which suppress electro-osmotic force. To reduce incidental run-to-run variations under reverse polarity conditions, the average current for each run (66-72 μA range) was used to normalize migration times and mobilities.

The affinity (K_D) of polyalkylamine for GAG components was calculated using equation 2, which is an adaptation of the Scatchard equation. In this equation, $\Delta\mu^{ep}$ is the change of electrophoretic mobility of a given CE peak in the presence of resolving agent (RA) as compared to that in its absence (μ_0^{ep}.) Because the resolved peaks are not distinguishable without the RA, the mobility of a peak at the start of the

electropherogram in the absence of RA (~15 min) was used as μ_0^{ep}. K_D, the equilibrium dissociation constant, was calculated from the slope of the plot.

$$\frac{\Delta\mu^{ep}}{[RA]} = -\frac{\Delta\mu^{ep}}{K_D} + \frac{\Delta\mu^{ep}_{max}}{K_D} \qquad \textbf{(Equation 2)}$$

4.3 Results

4.3.1 The Interaction of Linear Polyamines With Various Glycosaminoglycans

In chapter 2, linear polyalkylamines were used to fingerprint enoxaparin, tinzaparin and a generic LMWH [19]. Positively charged polyalkylamines (**figure 2.2**) recognize a collection of negatively charged sulfate groups on LMWH chain resulting in a fingerprint pattern. Because each LMWH is structurally distinct, its CE profile in the presence of RA was found to be characteristic of its composition (**figure 2.9**). In a manner similar to LMWHs, other GAGs are also structurally distinct in terms of constituent residues, inter-residue linkages, and the overall three dimensional organization of anionic groups. We reasoned that these features should induce differential recognition of GAGs by linear polyalkylamines. To test this hypothesis, we subjected UFH, CS and DS, the three most common available GAGs, to the fingerprinting protocol developed for LMWHs. This allowed us to discern why RA's interact with sulfated polysaccharides based on what is known about the structures of the GAGs studied.

Figure 4.2A shows CE profiles of AMAC-labeled UFH, CS and DS in the presence and absence of 5EH, a representative RA. All three polymeric GAGs gave broad peaks in the absence of 5EH. UFH eluted in about 20 mins, while CS and DS eluted between 26 – 28 mins, which was in accordance with their negative charge density. In the presence of 200 μM 5EH, a concentration found to readily fingerprint enoxaparin, the broad CS peak shifted to about 30 min indicating weak interaction with the RA that is not sufficient to induce fingerprinting. In contrast, UFH was essentially fully resolved into multiple peaks in the presence of 200 μM 5EH (**figure 2A**) indicating dramatically different interaction. Interestingly, even 10 μM 5EH resolved UFH into multiple peaks suggesting a high affinity interaction between the two molecules (not shown). DS, on the other hand, was separated into two groups of peaks – a broad peak resembling CS's broad profile and a cluster of sharp peaks resembling the UFH profile. This dual distribution profile could be transformed into single multi-peak profile at higher RA levels, e.g., 500 μM 5EH suggesting that the distribution into two major components is simply a function of affinity-governed equilibrium. To test whether CS also exhibits this phenomenon, higher 5EH levels were screened (up to 1000 μM). Although the migration time of CS gradually increased, no resolution was observed (not shown) suggesting that the fundamental structural difference between CS and DS is sensed extremely well by these linear polyalkylamines.

Changing the resolving agent to 4EP, a polyamine with potentially one less positive charge at pH 2.3 gave results similar to those obtained with 5EH, though the concentration of 4EP was four times that of 5EH (**figure 4.2B**). Thus, at 800 μM 4EP, UFH and DS resolved into multiple peaks (**figure 4.2B**). In contrast, CS continued to

display broad peak profile. Higher concentrations of 4EP were necessary to induce resolution possibly because of its lower affinity for the polymeric polyanions.

Despite the wide difference in the interaction profile of polymeric GAGs with linear polyalkylamines, it was difficult to truly fingerprint the UFH and DS. Considerable variation in peak widths, shapes and number was observed between runs for UFH as reported in chapter 3 and for DS. We theorize that as the UFH:RA multimers resolve, a dynamic equilibrium is established, which rapidly changes the electrophoretic mobilities resulting in changes in peak pattern between runs. DS was less susceptible to variation than UFH, but this changed at higher concentrations of RA. Yet overall, the observation that UFH and DS, but not CS, interact and resolve well with linear polyalkylamines indicates that these small molecules could be used as probes for direct analysis of GAGs.

4.3.2 Fingerprints of Low Molecular Weight Heparins Arises From a Two-site Interaction Phenomenon

Previous work with LMWH fingerprinting suggested that 5EH was the best RA among those tested (chapter 2). The above analysis of full-length GAGs showed that fingerprinting was not possible for CS, was minimal for DS, and unsuitable for UFH based on their interactions with the RAs. This implied that linear polyalkylamines selectively fingerprint LMWHs, i.e., shorter polysaccharide chains with high sulfate density. Between different linear polyalkylamines, however, a certain polycationic charge density was necessary as decamethonium (**figure 4.1**) failed to resolve any LMWH (as well as other GAGs) at concentrations as high 1000 μM (**figure 4.3**). To assess the fundamental basis for this phenomenon, fingerprinting profiles of enoxaparin

were studied with increasing concentrations of 5EH (**figure 4.4**). The fingerprints were highly reproducible with a day-to-day variability of < 5% (data not shown). In the absence of a mass spectrometric assignment of the peaks observed in the fingerprints, which is expected to be difficult due to lack of baseline resolution, ascertaining the change in migration time of individual LMWH chains is nearly impossible. However, the peak shape pattern remains the same as the concentration of 5EH increases. This was also found for 4EP (**figure 4.5**) as well as SPM (**figure 4.6**), enabling the monitoring of few peaks with high fidelity over a large range of RA concentration. To assess how the RAs interact with LMWHs chains, we selected two of these high fidelity, representative peaks for 5EH and 4EP, and one peak for SPM. It is important to recognize that the selected peaks do not necessarily represent one specific LMWH chain; in fact, these most probably represent many different chains, except with reasonably similar structural features that induce co-migration. Thus, for a mixture containing millions of species, the selected peaks represent chains with higher proportion of structural identity. Each peak was studied at 8-13 concentrations and electrophoretic mobilities of the peaks were calculated based on standard literature reported methods.

Figure 4.4-4.6 shows the Scatchard analysis of the interaction of 5EH, 4EP, and SPM with select peaks of enoxaparin as just described. The 5EH and SPM profiles show a biphasic interaction phenomenon for both the selected peaks. Typically, a linear Scatchard plot suggests single site binding, while a biphasic plot indicates two binding sites with sufficiently different affinities [147]. The observation of two binding modes for molecules as simple and small as 5EH and 4EP is interesting as well as challenging. Based on first principles, these LMWH peaks would be expected to display an average

single-site interaction phenomenon because the peaks are not completely homogeneous and the equilibrium status within the capillary would be dynamic. The observation of a biphasic binding mode suggests that 5EH and 4EP recognize selected chains of LMWHs in a highly specific manner. Similar results were obtained for SPM and enoxaparin, though with only a single peak and with a larger amount of error compared to 5EH and 4EP at the high affinity concentration (**figure 4.6B**). Thus, the similarity across the three RAs studied suggests that this characteristic is likely to be generally valid for most LMWH chains.

4.3.3 Fingerprinting Arises from Differential Interactions of Different Low Molecular Weight Heparin Chains

To gain quantitative information regarding the reason for the observation of fingerprints, we analyzed the observed biphasic profile as arising from two LMWH – RA equilibria that are not co-operatively linked. Typically, such biphasic profiles arise when the affinities are sufficiently distinct and thus can be analyzed using the Scatchard equation on each arm of the profile. Application of equation 2 to each arm of the 5EH – enoxaparin biphasic profile gave K_D values of 123 μM and 0.024 μM for peak 1, and 53.8 μM and <10 nM for peak 2 under the conditions of CE experiment (**table 1.1**). This corresponds to differences of 5125- and 5400-fold between the two affinities for both peaks 1 and 2, respectively. Thus, 5EH displays exceptionally strong affinity for some LMWH chains (nM), while interacting with perhaps most chains with much lower affinity (μM). The high affinity interactions most probably correspond to specific recognition of LMWH chains through the formation of one or more hydrogen bonds, while the low affinity interaction probably arises from a generalized non-specific Coulombic ion pairing

[148]. We believe that the high affinity interactions are the primary reason that polyalkylamines are able to generate fingerprints since they cause chains with similar binding profiles to group together to form peaks from which average affinity values can be obtained.

The affinity difference remains intact for the other two RAs also. **Table 4.1** lists the affinities measured for the selected peaks using Scatchard analysis. Both 4EP and SPM demonstrate a weaker interaction profile with LMWH chains as compared to that with 5EH. The high affinity interaction ranged from 0.74 μM to 5.2 μM, which is approximately 74 – 520-fold weaker than the high affinity interaction observed for 5EH. In contrast, the low affinity interactions for 4EP and SPM were 267, 308 and 414 μM, which implies a much weaker 4.9 – 7.7-fold effect. Thus, while the high affinity interactions are significantly different between the RAs, the low affinity interactions are fairly similar. These differences in the interactions, especially those of the high affinity type, generate differences in the fingerprinting profiles with each RA.

An important derivation of these observations is that it should be possible to develop powerful RAs for specific fingerprinting of these highly complex GAGs. For example, the affinity of LMWH chains increase with the number of positively charged amines on the RA. While the strength of the low affinity interaction does not decrease precipitously, the high affinity interaction is dramatically weakened through a change from 5EH and 4EP (**table 4.1**). Hence, it can be expected that longer polyalkylamines, perhaps linear and/or branched, would resolve LMWHs or GAGs better. It may even become possible to induce baseline resolution for direct structural analysis using tandem ESI-MS.

4.3.4 Tetra, Hexa, and Decasaccharide Fingerprints do not Show Two Site Binding Profiles

Theoretically, oligosaccharides of the same number of sugars would be more homogeneous and thus easier to analyze than LMWH, UFH, or other GAGs as structural diversity would be dramatically lower. To shed further light on the interaction of polycations with GAGs, the interaction purchased heparin oligosaccharides with the RA's was also studied. For hexa and decasaccharide, the electropherograms displayed remarkable homogeneity. Upon the addition of 5EH however, both profiles split into multiple peaks. This was especially prominent with decasaccharide (**figure 4.7**). Tetrasaccharide yielded similar results with 5EH and several other resolving agents (not shown). Such results were expected since oligosaccharides, while simpler than LMWH, are still not homogeneous with variation of uronic acid conformation and sulfation pattern that only increases with length. Affinity studies were unsuccessful to excessive peak blending at lower concentrations and difficulty in tracking specific peaks across higher concentrations. It was nearly impossible to identify peaks with certainty.

4.4 Discussion

Structural characterization of GAG chains is challenging because of their massive structural complexity. This work presents a rather simple protocol of resolving a group of GAGs through the use of linear polyalkylamines under strongly acidic electrophoretic conditions. The interaction of these agents with full-length heparin was found to be unusually strong. In fact, the affinity of UFH for linear polyalkylamines is likely to be lower than that of LMWH, which was found to be in the range of 10 nM. Structurally, UFH is a linear helical molecule [149] that presents its sulfate groups on

the surface resulting in greater number of polycationic recognition motifs than possible for LMWHs. Further, a three-fold longer heparin chain affords a major statistical advantage resulting in higher affinity for the RAs.

Unfortunately, UFH's significantly higher affinity did not translate into a fingerprinting advantage. Although UFH could be resolved into multiple peaks, the CE profile is not reproducible as noted for LMWHs [19]. The likely reason for this phenomenon is the possibility of high-affinity induced dynamic equilibrium between multiple equivalent binding sites on UFH chains for linear polyalkylamines and the formation bridges between GAG chains as discussed in chapter 3. While the dynamic equilibrium during electrophoresis is also present for LMWHs, the reduced affinity of RAs engineers an averaging effect resulting in high reproducibility. An alternative, less likely, explanation is that LMWHs and UFH are structurally distinct. The fact that LMWHs are derived from UFH from either chemical, enzymatic, or chromatographic means implies that the microstructures of the two species are likely to be similar. Yet, the dramatically distinct response of LMWHs and UFH to linear polyalkylamines is interesting and worth investigating. If either of the two hypotheses regarding UFH – linear polyalkylamine interaction is true, longer chains of RAs, e.g., a polyamine three times longer than 5EH, can be expected to fingerprint UFH at appropriately lower concentrations. Such polyamines are known in the literature [150-151] and may offer fingerprinting advantage, but may also carry cytotoxic and/or carcinogenic adverse effects [152-153].

Fingerprinting of LMWHs is highly dependent on the structure of the RA as demonstrated here as well in chapter 2. Affinity measurements performed here

demonstrate that optimal chain length and positive charge density are crucial for achieving resolution. Comparison of structures shows that UFH/LMWH, DS, and CS contain an average of 2.4, 1.2, and 0.95 sulfate groups per disaccharide, respectively, in their representative sequences [143]. This suggests that linear polyalkylamines studied here are effective when sulfate charge density is more than one per disaccharide (most carboxylates are expected to be protonated at pH 2.3). Yet, the ability of these RAs to interact with GAGs is not just dependent on sulfate charge density. OSCS, which is expected to possess sulfate density much greater than 1.2, does not interact strongly with linear polyalkylamines. This suggests an intricate structural component to these interactions.

Finally, the fundamental insight into the basis for fingerprinting of LMWHs by linear polyalkylamine-based resolving agents will be of value to the design of advanced resolving agents. Compounds with varying charge density, electrophoretic mobility, and conformation flexibility could be designed and screened. The possibility of baseline resolution in these profiles will facilitate direct mass spectrometric analysis for deduction of heparin sequences as well as for chemoinformatic profiling.

Table 4.1: Affinities of Selected Enoxaparin Chains for Resolving Agents.

	Peak #[a]	High Affinity Interaction (μM)[b]	Low Affinity Interaction (μM)[b]	Ratio of High to Low Affinity
5EH	1	0.024	123	5125
	2	<0.01	54	>5400
4EP	1	1.9	312	165
	2	0.74	263	355
SPM	1	5.2	417	80

[a]Peaks are identified in Figure 4. [b]The affinities of peaks were measured through Scatchard analysis. See Materials and Methods section.

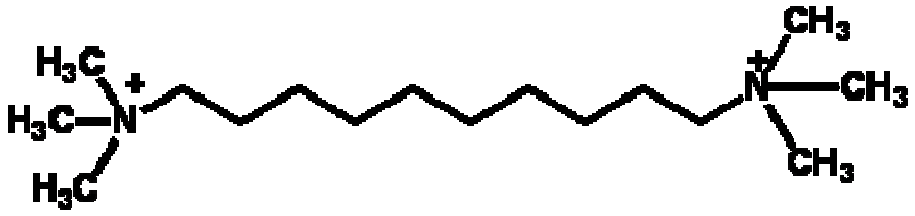

Figure 4.1: The structure of decamethonium.

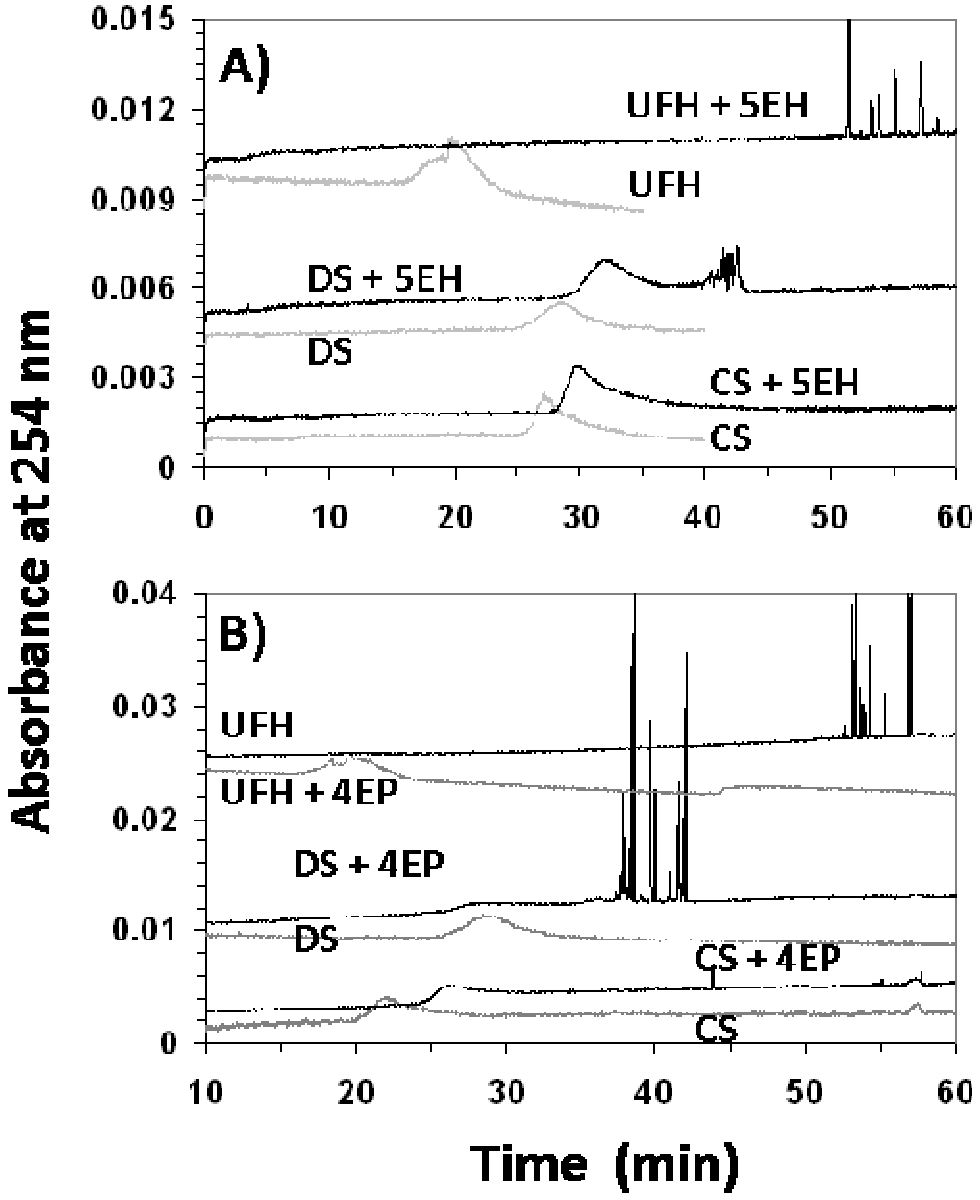

Figure 4.2: Interaction of linear polyalkylamines with glycosaminoglycans. Resolution of CS, DS, and UFH with 200 μM 5EH (A) and 800 μM 4EP (B). CE was performed in reverse polarity mode in 50 mM sodium phosphate buffer, pH 2.3, containing 10% DMSO at 10 kV and 15°C. A 75 μM (i.d.) capillary, which as 50 cm to the detector window, was used for these experiments. The profiles have been offset to enhance clarity.

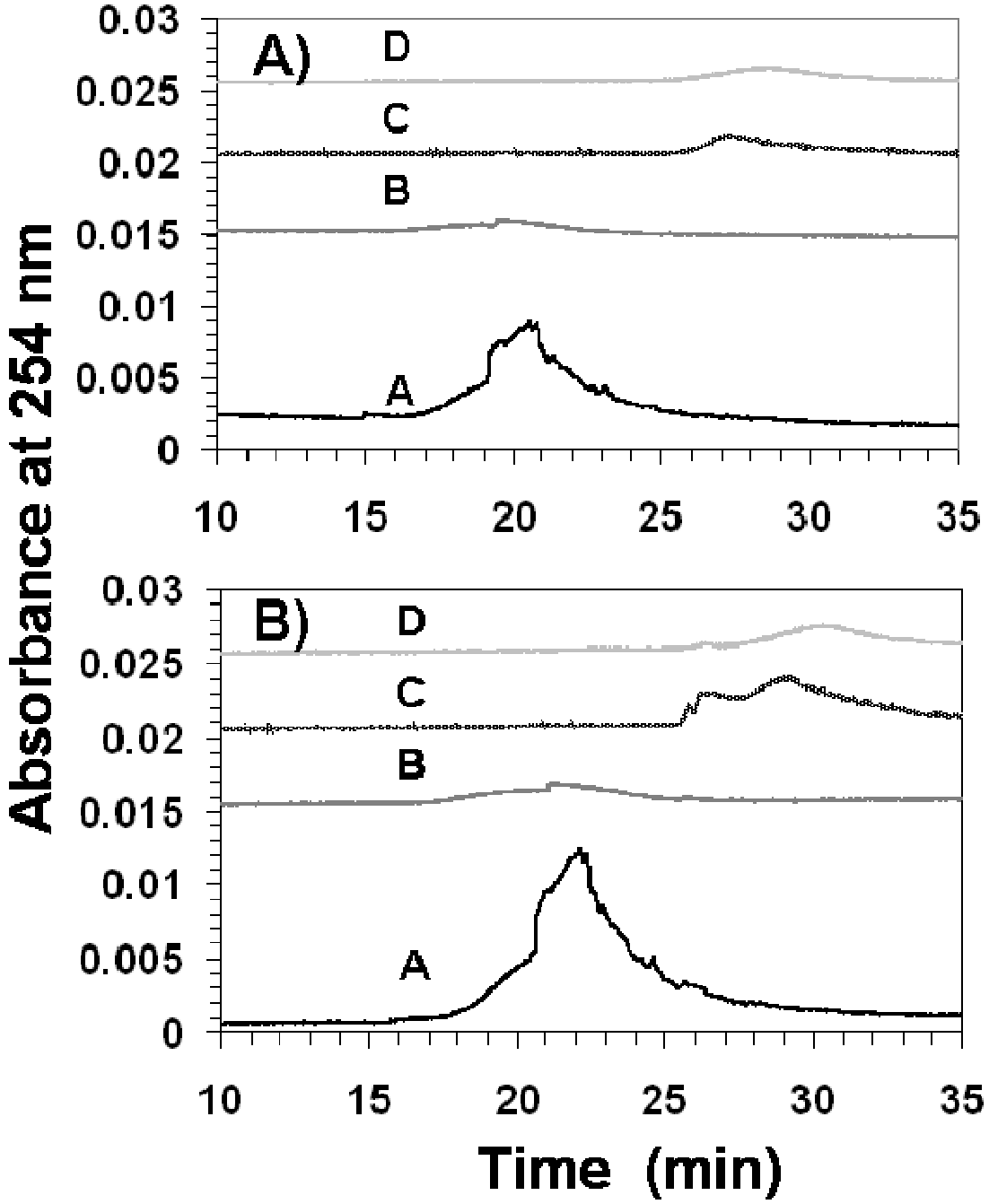

Figure 4.3: Fingerprints Enoxaparin, UFH, CS, and DS (A-D) with decamethonium. Upper diagram (A): without resolving agents. Lower diagram (B): with 500 µM decamethonium. decamethonium.

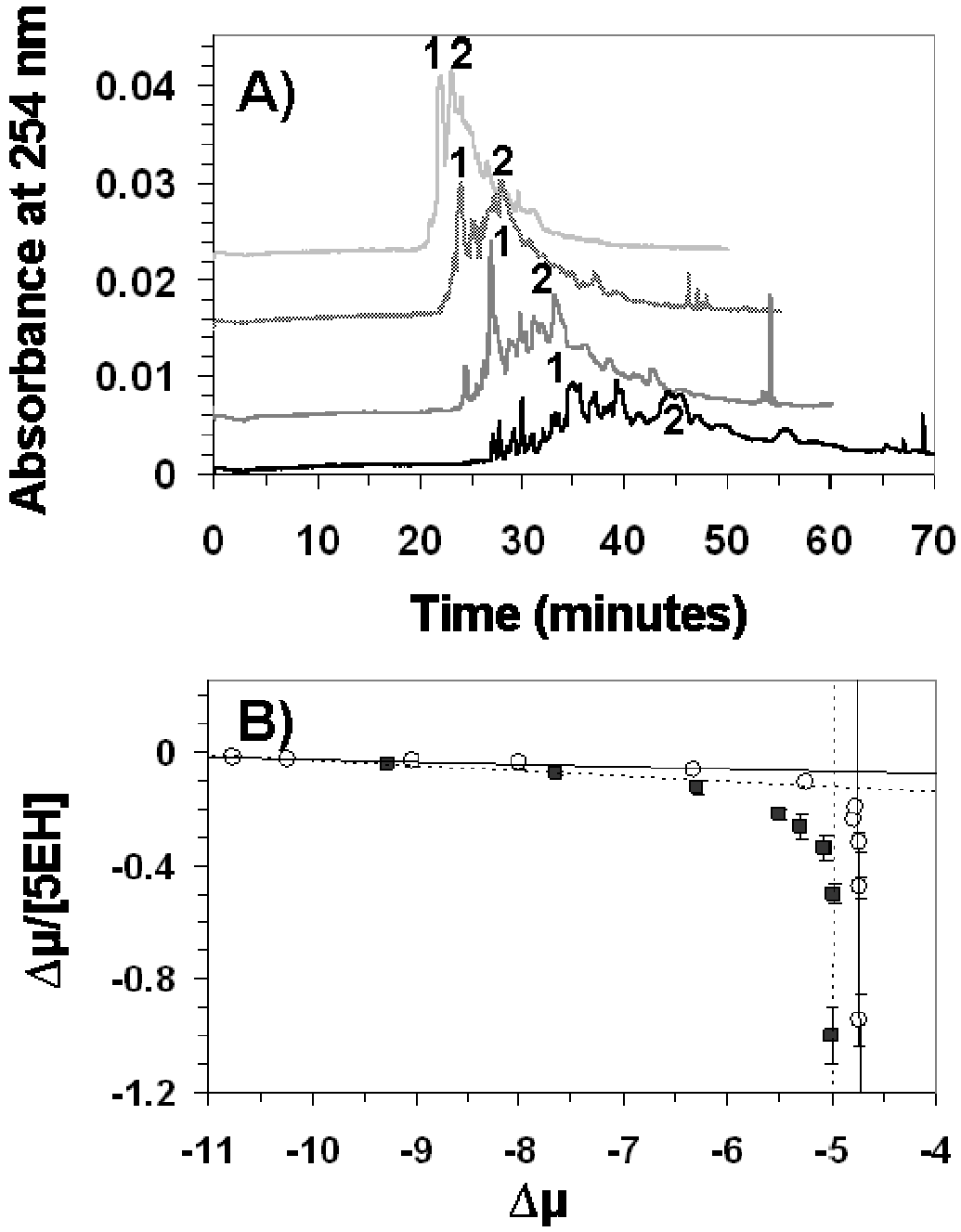

Figure 4.4: Affinity Data for 5EH and Enoxaparin. A) Resolution of LMWH with increasing concentrations of 5EH. CE was performed in 50 mM sodium phosphate buffer, pH 2.3 containing 10% DMSO and fixed concentration of the RA at 10 kV and 15°C. Only selected profiles, offset to enhance clarity, are shown. Typically 3 – 4 experiments were performed at each concentration to ensure high reproducibility. The observed fingerprint patterns are highly consistent for LMWHs. Individual peaks, e.g., 1 and 2, can be followed as a function of RA concentration. See text for details. B) Scatchard analysis of mobility data acquired from peak 1 (square) and peak (2).

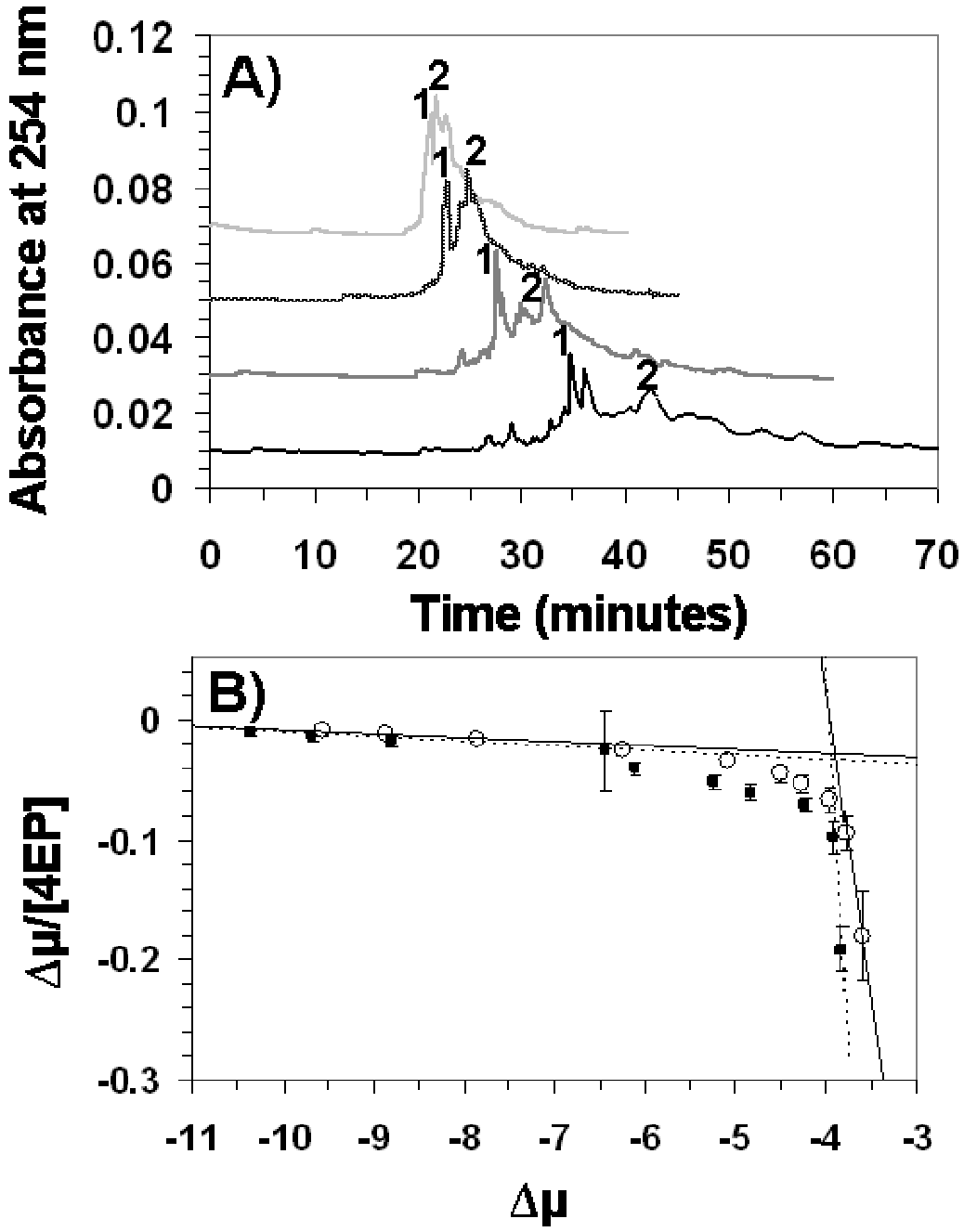

Figure 4.5: Affinity Data for 4EP and Enoxaparin. A) Resolution of LMWH with increasing concentrations of 4EP. Conditions were the same as in figure 4. The observed fingerprint patterns are highly consistent for LMWHs. Individual peaks, e.g., 1 and 2, can be followed as a function of RA concentration. See text for details.
B) Scatchard analysis of mobility data acquired from peak 1 (square) and peak 2 (circle).

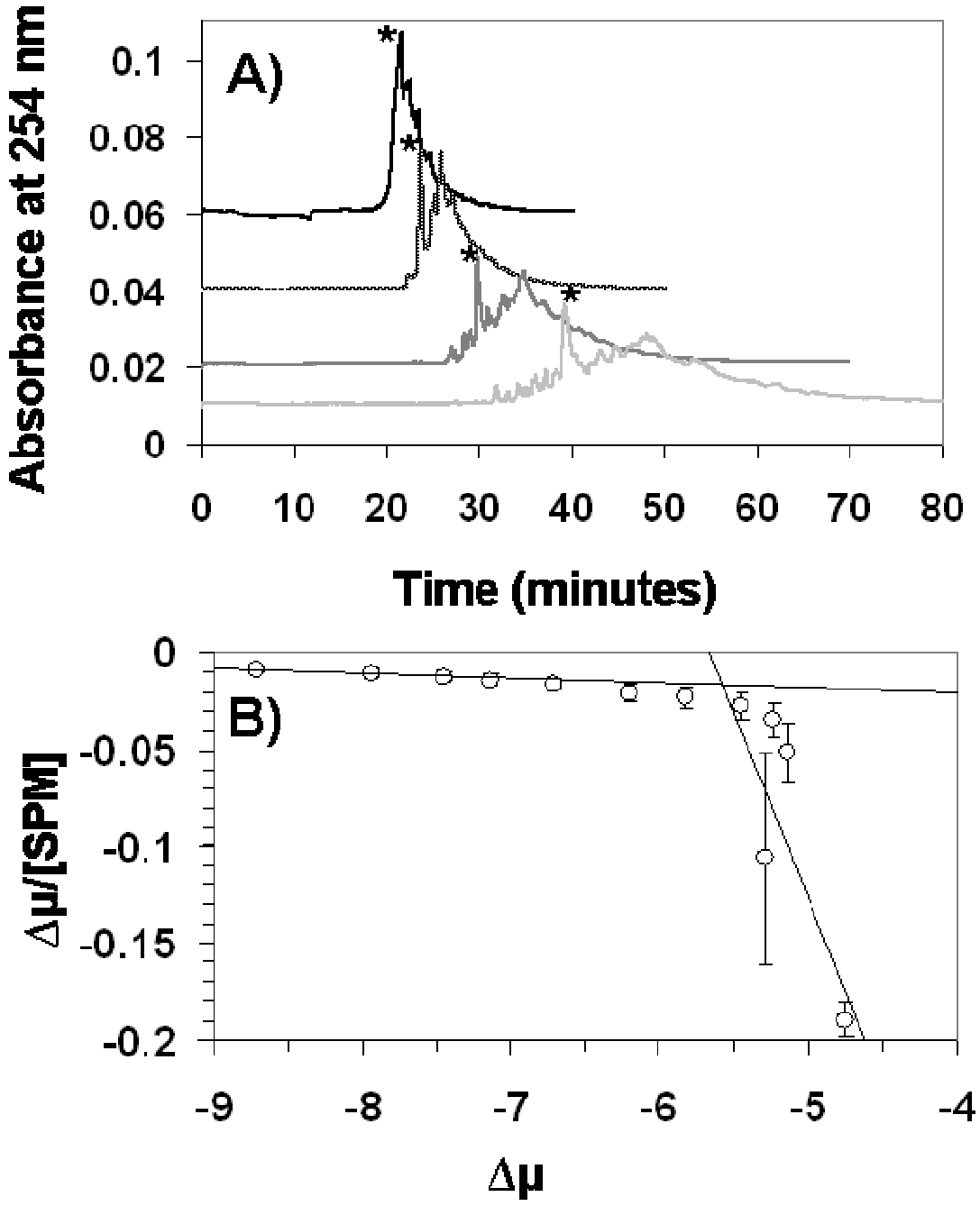

Figure 4.6: Affinity Data for SPM and Enoxaparin. A) Resolution of LMWH with increasing concentrations of SPM. Conditions were the same as in figure 4.
B) Scatchard analysis of mobility data acquired from the indicated peak.

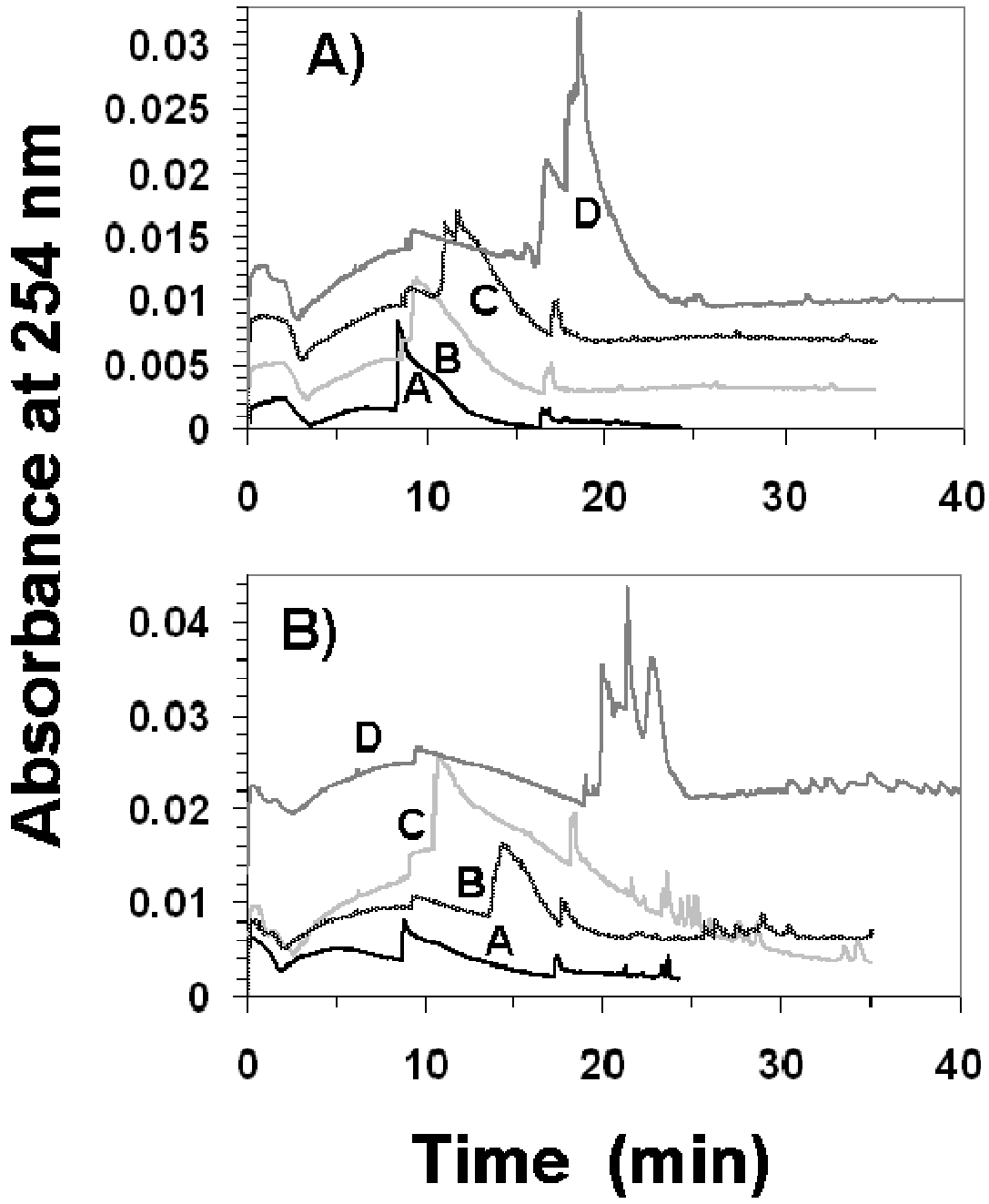

Figure 4.7: Fingerprints of decasaccharide and hexasaccharide using 5EH. The concentrations used are A) 0 μM, B) 40 μM, C) 100 μM, D) 250 μM.

A Batch to Batch Capillary Electrophoretic Analysis of Low Molecular Weight Heparins

5.1 Background

The issue of biosimilar LMWHs issue has come to prominence in recent years with the branded products approaching the end of their patent life and generics entering clinic around the world. Yet the sheer complexity of these products means that developing an equivalent product would prove very difficult. Differences between brand and generic LMWHs have been noted especially with regards to Lovenox^{TM} and generic enoxaparin products available in other countries [139]. The fundamental question is this: can a true generic formulation of LMWH be structurally identified with reasonable degree of certainty? Alternatively, can a prospective LMWH be reliably differentiated at an early stage from that used in the clinic?

In July of 2010, the FDA approved the first LMWH for use in the US as a generic equivalent of enoxaparin. While substantial *in vivo* and *in vitro* tests were performed to establish equivalence, structural equivalence was limited to molecular weight distribution and 1,6-anhydromannose ring proportion [31,32]. Considering the complexity of LMWHs, establishing biosimilarity with just two structural techniques is a dangerous proposition. Yet, structural analysis of intact LMWHs is a challenging endeavor. A wide range of electrophoretic, chromatographic, spectroscopic and mass

spectrometric techniques have been used for heparin disaccharide and oligosaccharides [76-78,101,155], but few protocols exist for intact LMWHs [101, 155-158].

Patel et al. developed a reverse phase HPLC method using tetrabutylammonium hydroxide as an ion pairing agent that produced highly resolved chromatograms of intact enoxaparin and dalteparin that displayed notably different profiles [100]. Excellent resolution of a mixture of oligosaccharides with degree of polymerization ranging from 6 to 22 was achieved using reverse phase-ion pairing UPLC coupled to mass spectrometry, which was extended to generate a tinzaparin chromatogram of over 50 peaks [101]. Outside of these methods, advanced multi-dimensional NMR spectroscopy and advanced electrospray ionization-MS methods have been developed [41,85,123], but their wide-spread applicability is doubtful.

Having developed a protocol for characterizing LMWHs with linear alkylpolyamines and capillary electrophoresis, we sought to assess whether generic enoxaparin is structurally equivalent to Lovenox as analyzed by our high-resolution CE fingerprinting protocol. Fingerprinting using multiple resolving agents shows that both generic and brand name enoxaparin behave in an essentially identical manner across a range of conditions suggesting essentially identical structural composition. More specifically, our protocol reveals that two batches of brand name enoxaparin studied are sufficiently different to accommodate generic enoxaparin within their realm. In contrast, enoxaparin and tinzaparin display widely different fingerprints suggesting that our fingerprinting protocol is extremely robust to rapidly assess compositional, and hence structural, equivalence. This work contributes to assessing the chemical equivalence of

LMWH formulations and lays the groundwork for evaluating future generics and brands expected to enter the clinic.

5.2 Materials and Methods

5.2.1 Chemicals

Lovenox™ (Lot #15146 and #29411), generic enoxaparin (Sandoz, Lot #914690), and Innohep™ (Lot #DC1863 and #DC9158) were purchased from Virginia Commonwealth University Health Systems Pharmacy. 2-Aminoacridone (AMAC), DMSO, and dibasic sodium phosphate were purchased from Sigma-Aldrich (St. Louis, MO). Pentaethylenehexamine (5EH), tetraethylenepentamine (4EP), and spermine (SPM) were purchased from Acros Organics (Geel, Belgium). Fused silica capillary was purchased from Microsolv Corporation (Eatontown, NJ). Sodium cyanoborohydride was purchased from Fisher Scientific (Pittsburgh, PA). G-10 media was purchased from GE Healthcare (Little Chalfont, UK). Cellulose ester dialysis membranes (500-1000 molecular weight cutoff) were purchased from Spectrum Laboratories (Rancho Dominguez, CA). All other chemicals and reagents were either from Sigma-Aldrich or Fisher.

5.2.2 Labeling of LMWHs with Aminoacridone

Enoxaparin and tinzaparin were labeled in a manner similar to that reported earlier. Briefly, 10 mg AMAC was dissolved in 860 µL of an 85% solution of DMSO/acetic acid and mixed with 860 µL aqueous solution containing 40-80 mg LMWH. The mixture was allowed to incubate for ~12 h at 37°C followed by addition of 200 mg of sodium cyanoborohydride in water. The reaction was allowed to proceed for

6 more hours at 37°C. The unreacted aminoacridone was removed via a G-10 column and the AMAC-labeled LMWH was dialyzed against 2 liters of water for 24 hours using membrane with a molecular weight cutoff of 500-1000. Following three changes of water, the solution lyophilized to yield pure AMAC-labeled LMWH. Each preparation of AMAC-labeled LMWH was redissolved in water to yield a stock solution of 50 mg/ml and stored at -80°C until use.

5.2.3 Capillary Electrophoresis

CE was performed using a Beckman-Coulter P/ACE MDQ capillary electrophoretic system with a fused silica capillary (I.D. 75 μM) of 50 cm length and 40 cm to the detector window. At the beginning of each day, the capillary was conditioned with 0.5 M sodium hydroxide, water, 0.5 M phosphoric acid, and finally water. The capillary was rinsed with run buffer (50 mM dibasic sodium phosphate, pH 2.3) for 2 minutes before each run and periodically with hydroxide, acid, and water. After rinsing, LMWH samples were diluted to either 4 (enoxaparin) or 1 mg/ml (tinzaparin) and injected into the capillary for 8 s at 1 PSI. Runs were performed at a constant current of 90 μA at a temperature of 15°C. Each run was completed four times to ensure reproducibility. For **figure 5.8**, all LMWH concentrations were 1 mg/ml.

5.2.4 NMR Analysis of Low Molecular Weight Heparins

^{1}H-NMR and ^{13}C-NMR spectroscopy was performed on a 400 MHz Bruker Ultrasheild plus NMR spectrometer. Unlabeled LMWH (40-50 mg) was dissolved in D_2O and lyophilized twice to remove H_2O. The sample was then re-dissolved in D_2O and ^{1}H-NMR spectrum acquired. ^{13}C-NMR spectra were taken overnight using 10,000 scans with a line broadening factor of 10 to maximize the signal to noise ratio.

5.3 Results

5.3.1 Qualitative Analysis of LMWH Fingerprints and NMR Spectra

Following the protocol developed earlier, fingerprints of two lots of Lovenox and one lot of generic enoxaparin (from Sandoz) were developed using 250, 500 and 1000 μM of three linear polyalkylamines, 5EH, 4EP and SPM, respectively. No differences were noted without resolving agents. Qualitatively, the fingerprints reveal striking similarities between the brand and generic enoxaparins as seen in **figures 5.1-5.3**, where the fingerprints have been aligned on the X-axis by designated peaks and expanded along the Y-axis to compensate for the lack of an internal standard and to enable minor peaks to be seen more easily. SPM and 4EP show the most similarities, while 5EH shows some variation (see close ups, **figures 5.1-5.3**). **Figures 5.4-5.6** show unadjusted electropherograms of the same runs. The three batches of enoxaparin displayed several major peaks in the presence of 4EP and SPM, which migrated in an essentially identical manner (within ~1.5 min). The migration times varied consistently more with 5EH, especially for later peaks (~2.5 – 4 min) of lot #29411, probably due to the higher affinity of this resolving agent. Alternatively, lot #29411 may possess a slightly altered overall sulfation pattern, which measurably affects electrophoretic mobility. Such variation is important and can be addressed with larger sample size, however, this was beyond the scope of our project.

Two batches of tinzaparin were also analyzed (generic tinzaparin is not available, as yet) with 1000 μM SPM and 200 μM 4EP **(figure 5.7**). The tinzaparin fingerprints were highly consistent across the batches with major peaks migrating at nearly identical times and no obvious difference in resolution. It is notable that at 200 μM 4EP (**figure**

5.7B), tinzaparin features “noise” peaks similar to that seen with UFH at ~45 minutes and beyond. Given that tinzaparin is acquired via enzymatic digestion of UFH, it is likely that it retains more of UFH’s basic structural features than chemically depolymerized LMWH and will thus behave in a similar manner. Interestingly, the “noise” peaks become more prominent and begin interfering with the main peak body when concentration of tinzaparin sample is raised. In spite of their similarities to each other, tinzaparin fingerprints are widely different from enoxaparin fingerprints. **Figure 5.8** shows a comparison of two tinzaparin and three enoxaparin batches in the presence of 200 μM 4EP. Major differences in group of peaks at ~22 and ~27 min are obvious. Interestingly, the ‘center of gravity’ of the tinzaparin profile is significantly delayed as compared to enoxaparin, which may indicate an average lower charge to mass ratio.

To assess whether such similarities and differences are picked up by ^{1}H and ^{13}C NMR spectroscopy, we recorded the spectra for all LMWH batches. While expected peaks such as those representing the N-acetyl protons at ~ 2-2.05 ppm were seen, none of the spectra demonstrated any difference for the enoxaparin or the tinzaparin batches (**figure 5.9-12**). Between enoxaparin and tinzaparin, both ^{1}H and ^{13}C NMR spectra were noted to be different, but the differences were not as obvious as revealed by fingerprinting protocol. This indicates that the structural heterogeneity of these LMWH preparations is so high that the resulting peak broadening in NMR spectra accommodates minor structural differences.

5.3.2 Quantitative Analysis of LMWH Fingerprints

To more accurately compare the LMWH fingerprints, detailed analysis was performed for each profile. Notable differences emerged for several peaks in terms of

both area and height. For example, peak 2 for enoxaparin resolved with 5EH (**figure 5.4**) displayed different areas of $(2.9\pm0.2)\times10^6$, $(3.1\pm0.2)\times10^6$, and $(1.7\pm0.05)\times10^6$ for one generic and two batches of Lovenox. Similar differences were also calculated for enoxaparins with 4EP and SPM (**figure 5.5-5.6**). However, considering the absence of a fixed reference in these fingerprints, such differences could possibly be explained by non-structural or compositional reasons. Thus, relative changes in the proportions of the resolved components were evaluated using peak 1 as a reference point as this would allow the comparison of enoxaparin lots while correcting for differences in percent labeling. **Table 5.1** shows the ratio of area for peaks 2 as a proportion of peak 1 for enoxaparin fingerprints in the presence of 250 μM 5EH, resulting in values of 4.7, 6.98 and 2.98 for generic batch 914690 and Lovenox^{TM} 15146 and 29411 respectively. The differences between these are substantial and reaches over 100% when comparing the brand batches to one another, differences in each ratio can be noted between the two batches of Lovenox. In fact, the ratios of various peaks displayed substantial variation across the two batches of Lovenox. Generic enoxaparin displayed ratios different from either Lovenox lots, but within the range defined by the two batches of the brand enoxaparin (see **figure 5.4 and table 5.1**). These conclusions remained the same when peak area ratios were evaluated with 4EP or SPM fingerprints (see **figure 5.5-5.6 and table 5.2-5.3**).

5.4 Discussion

Our earlier work on the mechanistic basis of LMWH fingerprinting indicated that each linear polyalkylamine studied, i.e., 5EH, 4EP and SPM, interacted with the polyanionic polysaccharide with high affinity (chapters 2 and 4). More importantly, a

biphasic interaction phenomenon was observed, thus explaining the highly specific fingerprint achieved with each polyalkylamine. This led to the idea that as a group these polybasic molecules might help identify small differences between different LMWHs and especially pinpoint differences between different batches of the same LMWH, if any. This idea is exciting because high resolution fingerprints coupled with nano-MS technology may provide a robust, operational platform for quick assessment of 'biosimilarity' [101].

To our knowledge, rigorous comparison of brand and generic enoxaparin has not been reported in the literature, although it has been widely recognized that generic LMWH may be technologically difficult to achieve [139,154,159]. Our effort is the first bioanalytical comparison of Lovenox with its generic version. Using the three molecule toolbox, our analysis suggests that the two enoxaparins are remarkably similar within limits of experimental error. In fact, the two batches of Lovenox display greater variance between them for all three polyalkyamine resolving agents, which accommodates the generic enoxaparin reasonably well. This result is striking and appears to indicate that the variation in the manufacture of the brand LMWH may be sufficiently high to accommodate several versions of generic.

Given that the fingerprints are the results of structure-specific interactions of the resolving agents with LMWH chains, the variations in the fingerprints imply detectable differences in the chemical composition of Lovenox from batch to batch. This difference is less with regard to the type of polysaccharide species and more with regard to the proportion of species. This work provides a stimulus for a wider study with much higher sample size so as to define the limits better. Yet, whether these structural differences

necessarily imply functional (beneficial and adverse) differences remains unevaluated, although theoretically a direct correlation is predicted.

Our study demonstrated a higher level of consistency between the two batches of tinzaparin studied here. More importantly, the resolution with polyalkylamines was so high that massive differences were evident between tinzaparin and enoxaparin. This was in striking contrast to one-dimensional ^{1}H and ^{13}C NMR spectra that failed to display much differences. The work, therefore, highlights the limitations of one-dimensional NMR spectroscopy in such analysis, while showcasing the power of linear polyalkylamine-based CE fingerprinting.

Finally, although limited in scope our effort provides a glimpse into the inter-batch variability and puts forward a robust platform for assessing structural biosimilarity of LMWHs. The use CE-MS could greatly expand this protocol. The bioanalytical fingerprinting is no substitute for clinical and epidemiological data, but could form an inexpensive method for rapid evaluation of ‘biosimilarity’. Considering that more generic LMWHs are being prepared for clinical entry, our protocol would be handy.

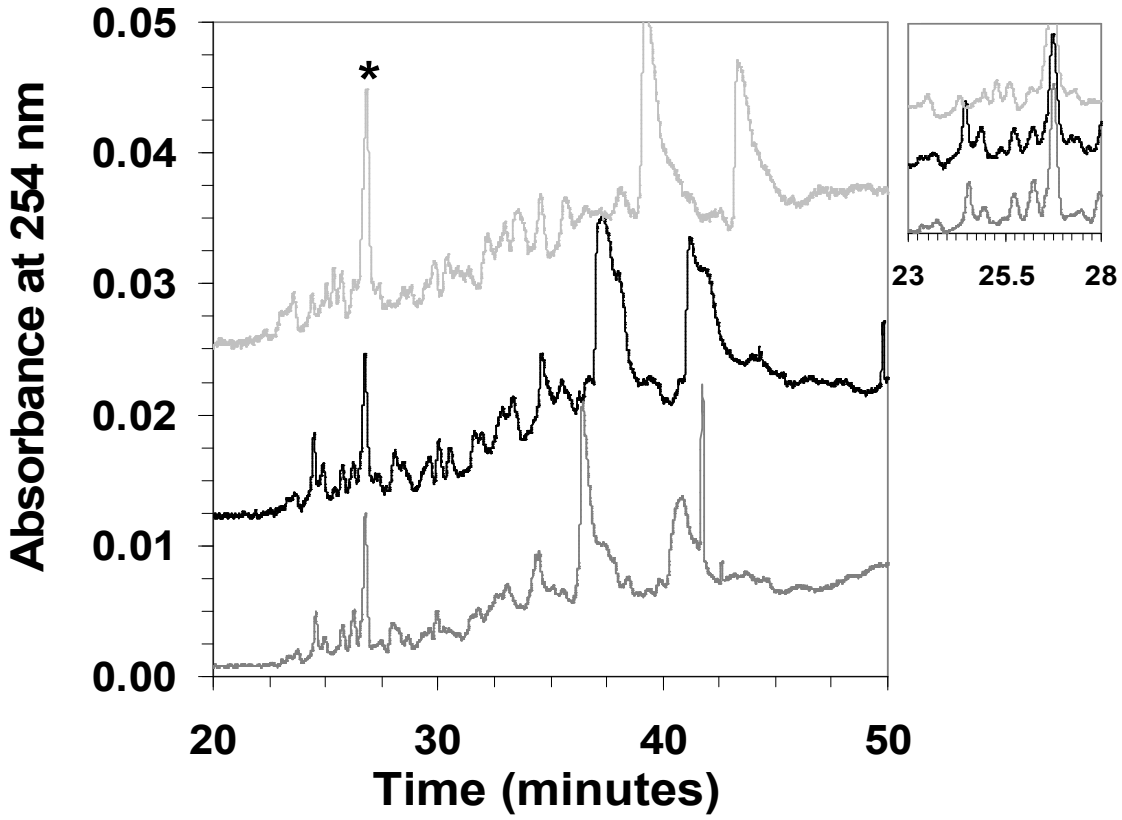

Figure 5.1: Comparison of enoxaparin fingerprints in the presence of 250 µM 5EH. Lot numbers from the bottom: 914690, 15146, 29411. Electropherograms have been aligned by peaks aligned with the peak marked by (*) for ease of comparison. Y-values have been multiplied for optimum to increase peak height.

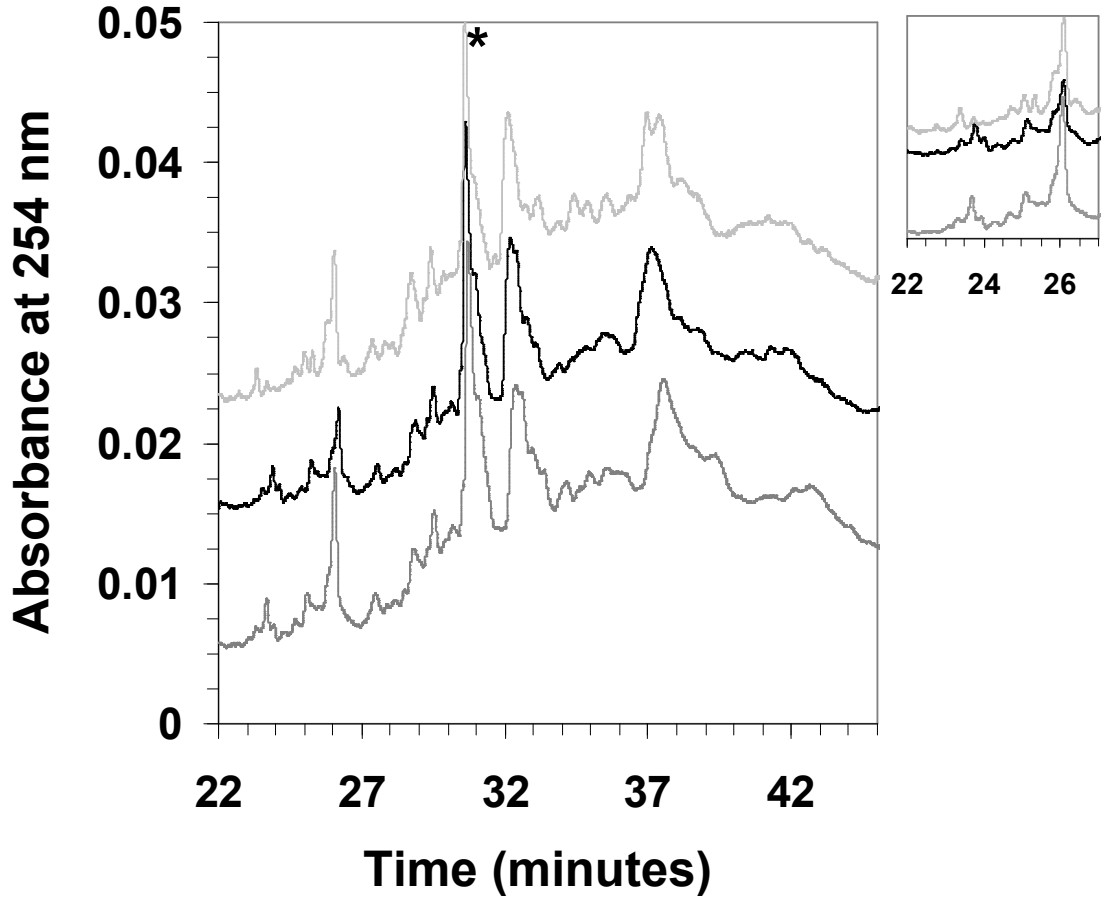

Figure 5.2: Comparison of enoxaparin fingerprints in the presence of 500 µM 4EP. Lot numbers from the bottom: 914690, 15146, 29411. Electropherograms have been aligned by peaks aligned with the peak marked by (*) for ease of comparison. Y-values have been multiplied for optimum to increase peak height.

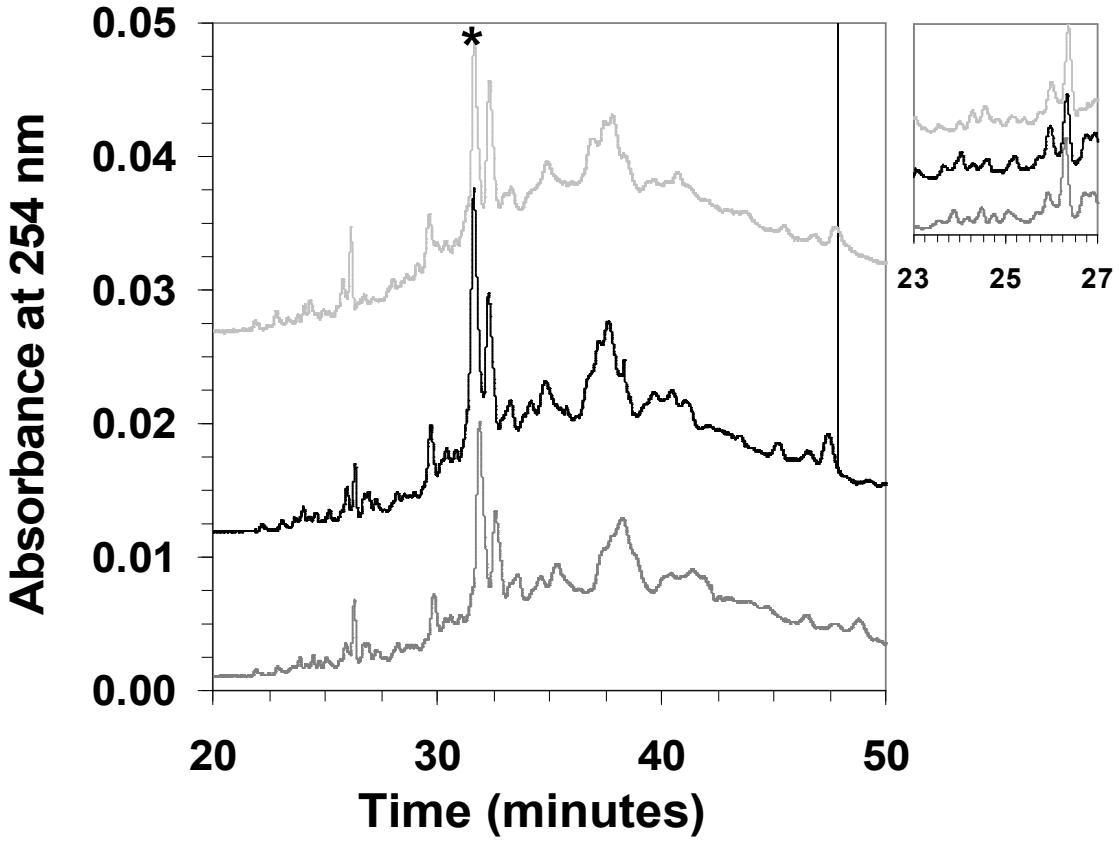

Figure 5.3: Comparison of enoxaparin fingerprints in the presence of 1000 µM SPM. Lot numbers from the bottom: 914690, 15146, 29411. Electropherograms have been aligned by peaks aligned with the peak marked by (*) for ease of comparison. Y-values have been multiplied for optimum to increase peak height.

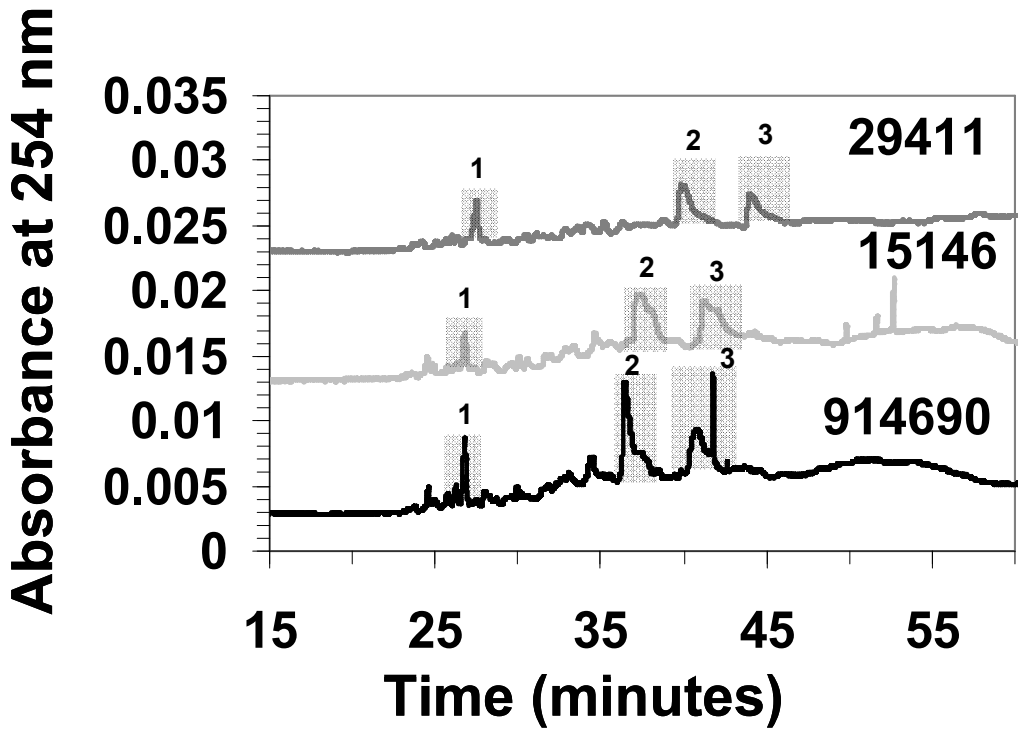

Figure 5.4: Unmodified enoxaparin batch fingerprints acquired with 250 µM 5EH. Analysis of the highlighted and numbered peaks are seen in table 5.1.

Table 5.1: Peak area analysis of enoxaparin batches with 250 µM 5EH.

			Enoxaparin 914690		Lovenox 15146		Lovenox 29411	
			Mean	Stdev	Mean	Stdev	Mean	Stdev
Area	Area	Pk 1	63377	7267	44530	2792	59336	7739
		Pk 2	297710	22649	310995	16863	176577	5099
		Pk 3	274201	25475	250014	19755	144012	5355
	Peak Ratio	Pk 2:1	4.70	0.90	6.98	0.82	2.98	0.47
		Pk 3:1	4.33	0.90	5.61	0.80	2.43	0.41
		Pk 3:2	0.92	0.16	0.80	0.11	0.82	0.05

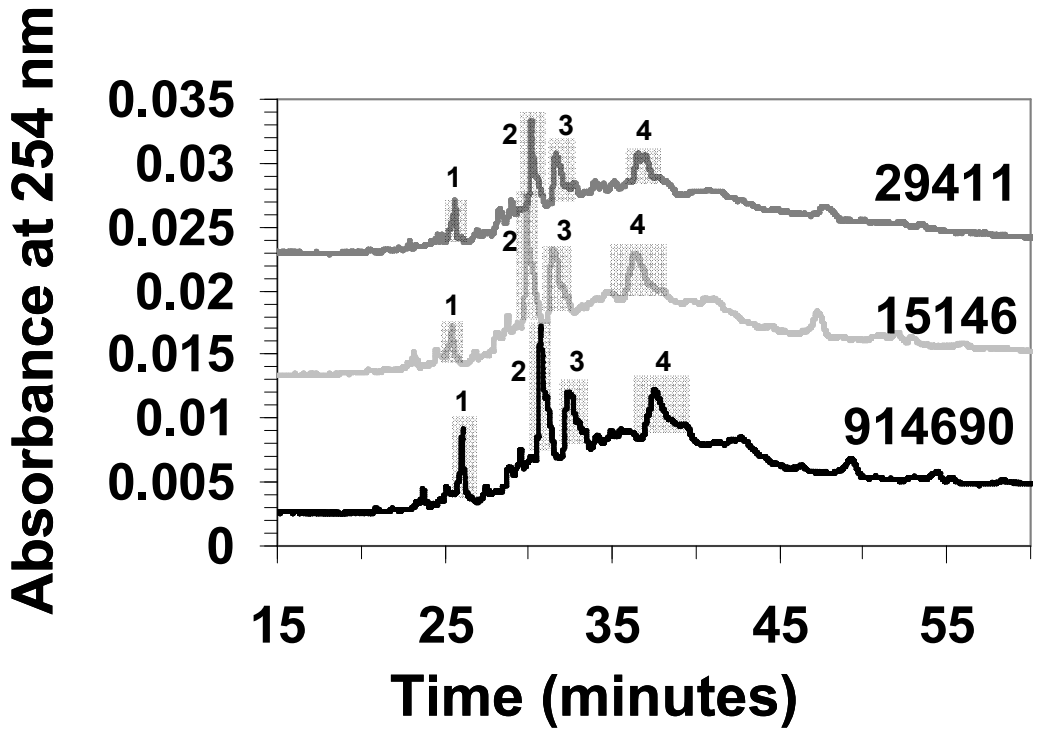

Figure 5.5: Unmodified enoxaparin batch fingerprints acquired with 500 µM 4EP. Analysis of the highlighted and numbered peaks are seen in table 5.2.

Table 5.2: Peak area analysis of enoxaparin batches with 500 µM 4EP.

			Enoxaparin 914690		Lovenox 15146		Lovenox 29411	
			Mean	Stdev	Mean	Stdev	Mean	Stdev
Peak Area	Area	Pk 1	68187	11706	36841	4653	44525	1857
		Pk 2	272719	20369	251961	11216	135537	13891
		Pk 3	236724	20613	235613	11080	124493	16653
		Pk 4	356554	24984	275923	10681	215826	19855
	Peak Ratio	Pk 2:1	4.00	0.985	6.84	1.168	3.04	0.439
		Pk 3:1	3.47	0.898	6.40	1.108	2.80	0.491
		Pk 3:2	0.87	0.140	0.94	0.086	0.92	0.217
		Pk 4:1	5.23	1.264	7.49	1.236	4.85	0.648
		Pk 4:2	1.31	0.420	1.10	0.236	1.59	0.393

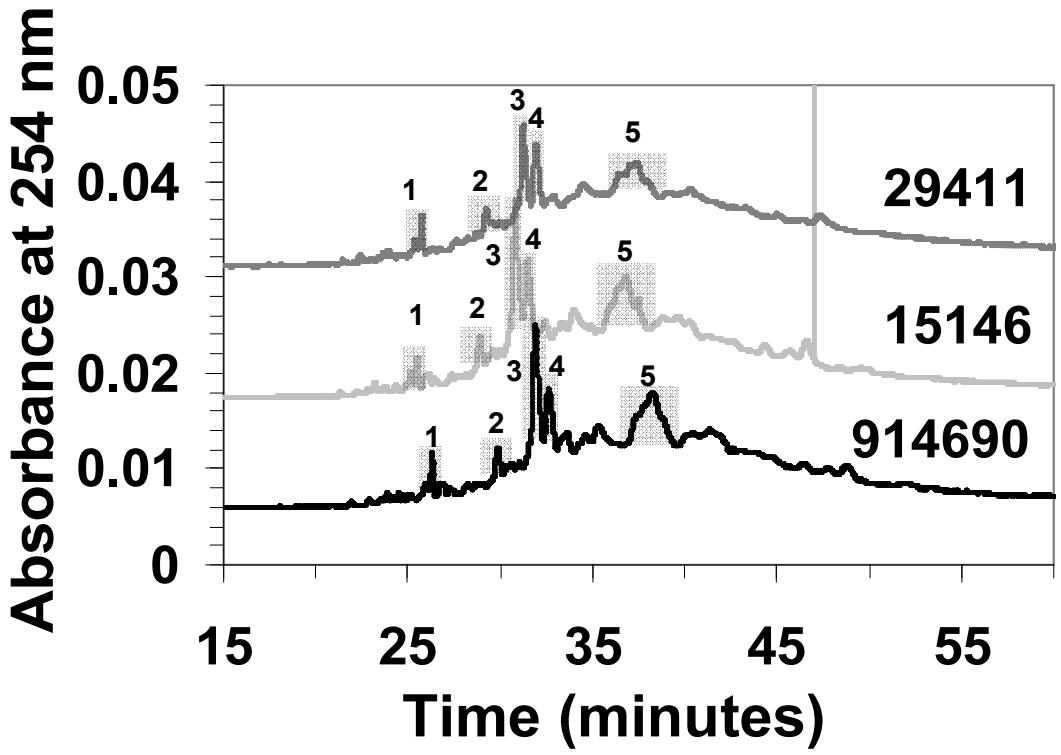

Figure 5.6: Unmodified enoxaparin batch fingerprints acquired with 1000 µM SPM. Analysis of the highlighted and numbered peaks are seen in table 5.3.

Table 5.3: Peak area analysis of enoxaparin batches with 1,000 µM SPM.

			Enoxaparin 914690		Lovenox 15146		Lovenox 29411	
			Mean	Stdev	Mean	Stdev	Mean	Stdev
Peak Area	Area	Pk 1	79393	2768	62632	4400	61453	7766
		Pk 2	41337	1299	41846	1389	33194	7514
		Pk 3	242483	8371	216374	10043	141178	6794
		Pk 4	109210	5231	94834	13114	115188	5279
		Pk 5	457733	19401	461615	23927	296239	16357
	Peak Ratio	Pk 2:1	0.52	0.03	0.67	0.07	0.54	0.19
		Pk 3:1	3.05	0.21	3.45	0.40	2.30	0.40
		Pk 4:1	1.38	0.11	1.51	0.32	1.87	0.32
		Pk 5:1	5.77	0.45	7.37	0.90	4.82	0.88
		Pk 5:2	11.07	0.82	11.03	0.94	8.92	2.51
		Pk 3:2	5.87	0.39	5.17	0.41	4.25	1.17
		Pk 4:3	0.45	0.04	0.44	0.08	0.82	0.08
		Pk 5:3	1.89	0.15	2.13	0.21	2.10	0.22

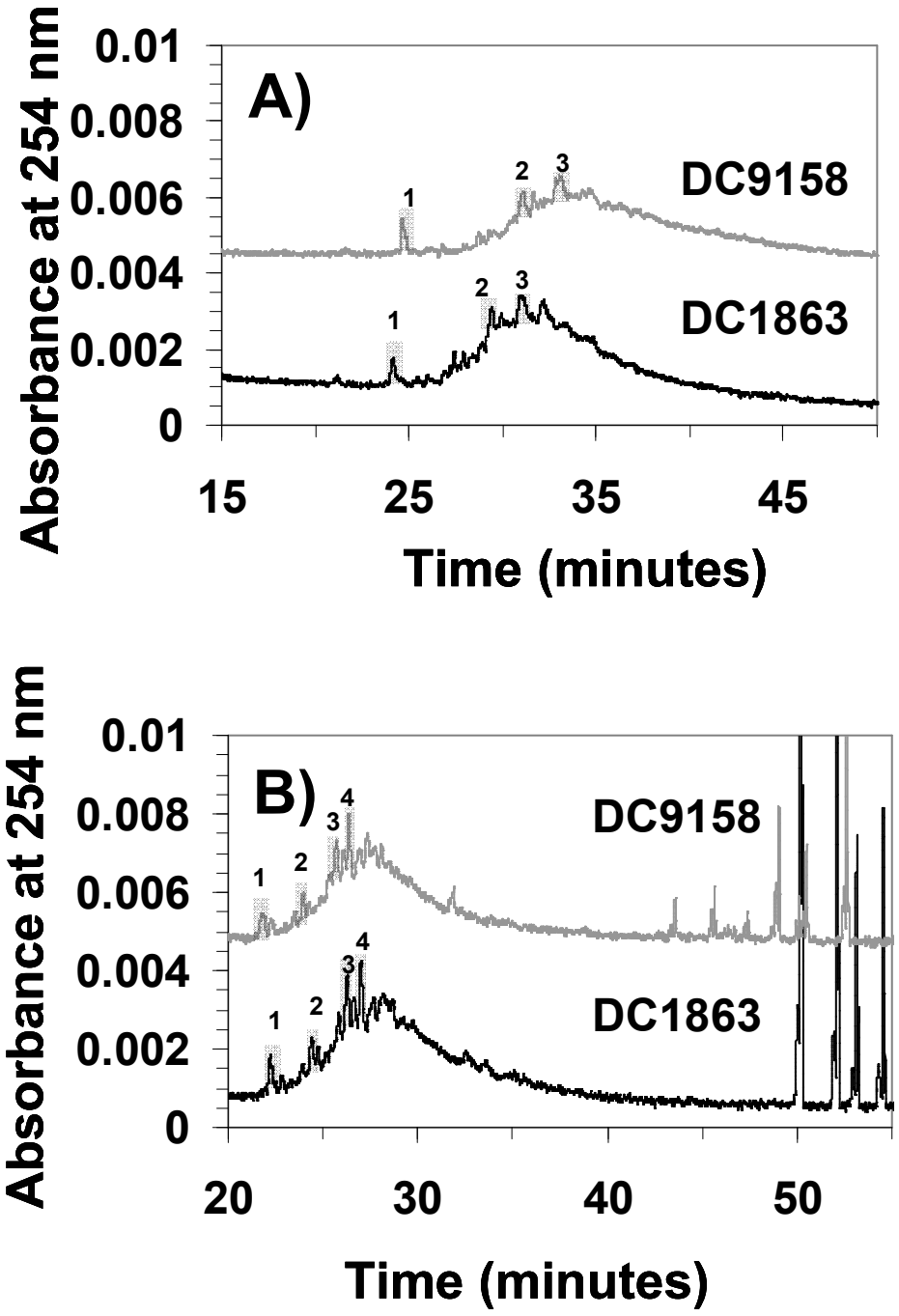

Figure 5.7: Batch to batch tinzaparin comparison. A) 1000 µM SPM, B) 200 µM 4EP. No adjustments made to data.

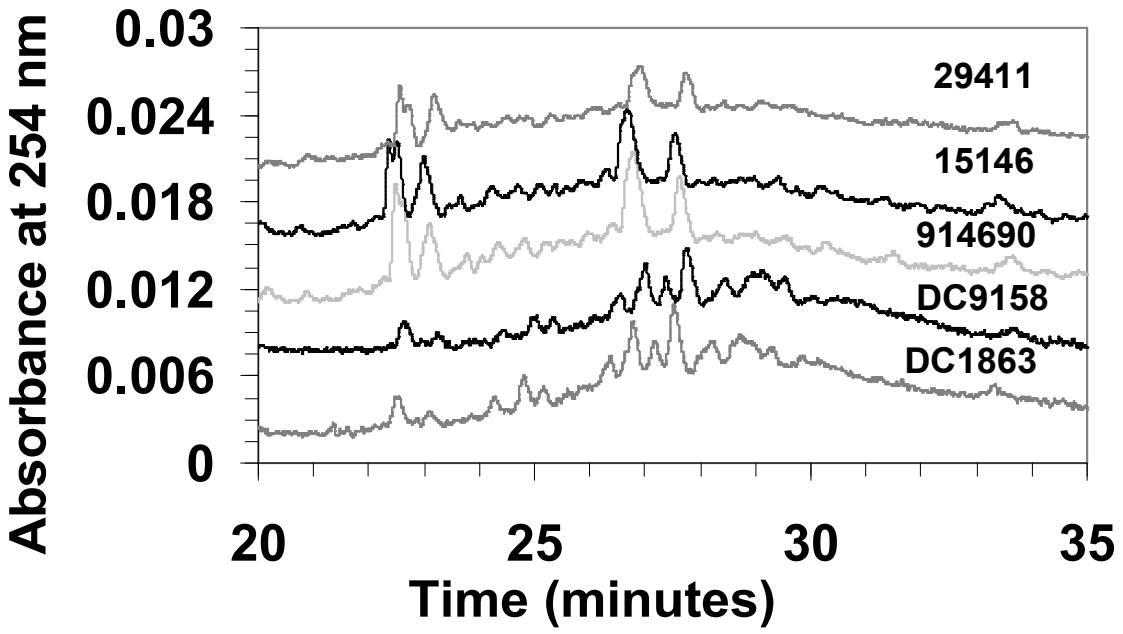

Figure 5:8: Tinzaparin and enoxaparin batches in the presence of 200 µM 4EP. All GAG concentrations 1 mg/ml. Batches beginning with DC are tinzaparin. The data points have been multiplied on the Y axis to increase peak height and allow for easy comparisons. No adjustment made on the X-axis.

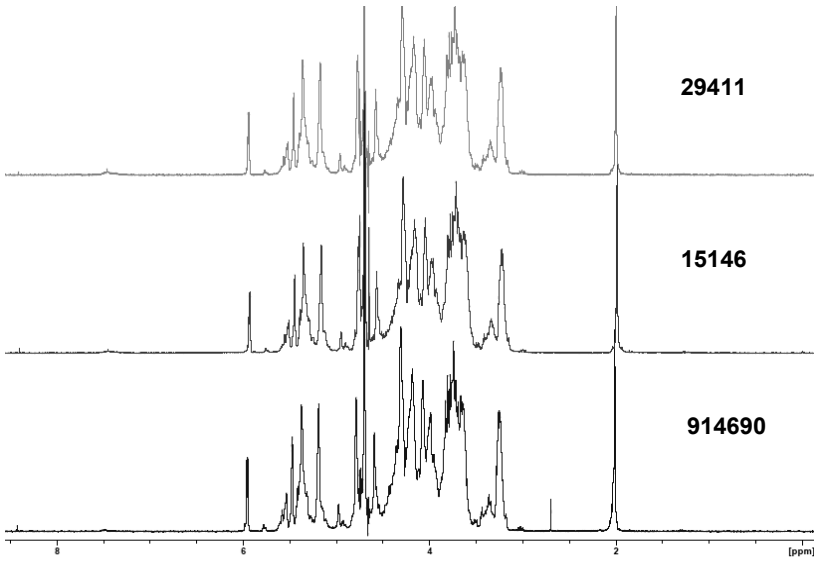

Figure 5:9: ^{1}H-NMR of enoxaparin batches in D_2O.

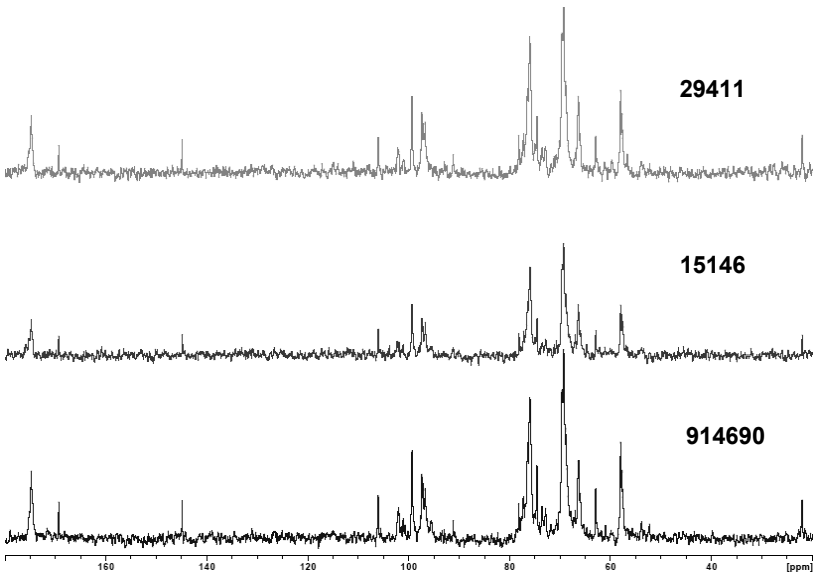

Figure 5:10: ^{13}C-NMR of enoxaparin batches in D_2O. A line broadening factor of 10 was used to maximize the signal to noise ratio.

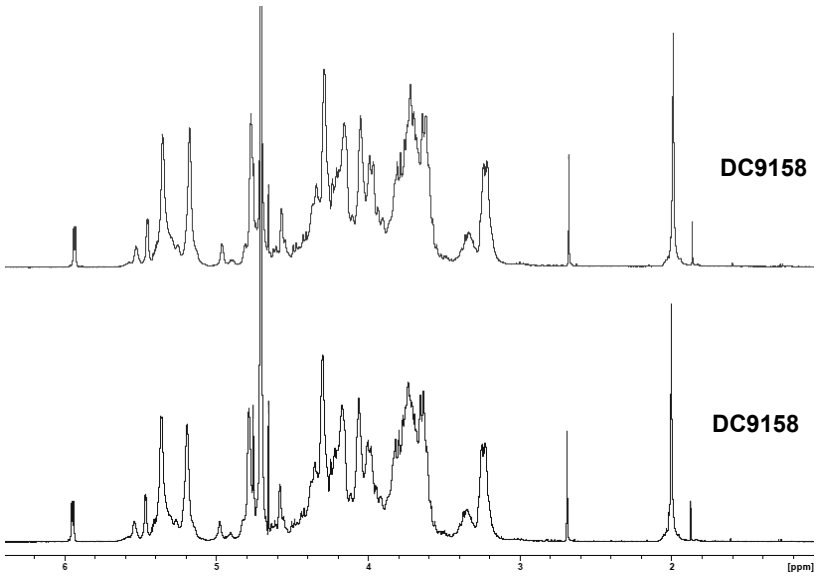

Figure 5:11: ^{1}H-NMR of tinzaparin batches in D_2O.

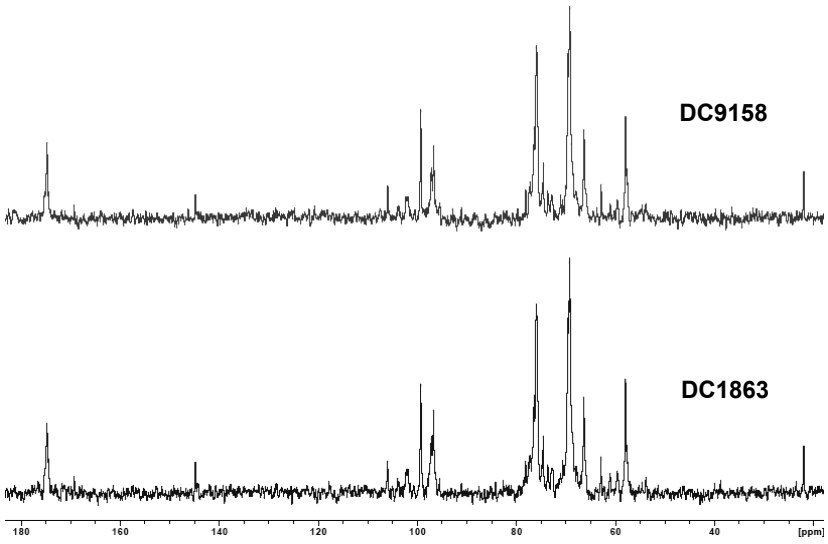

Figure 5.12: 13C-NMR of tinzaparin batches in D_2O. A line broadening factor of 10 was used to maximize the signal to noise ratio.

References

1. G.F. Medeiros, A. Mendes, R.A.B. Castro, E.C. Baú, H.B. Nader, C.P. Dietrich, Distribution of sulfated glycosaminoglycans in the animal kingdom: widespread occurrence of heparin-like compounds in invertebrates, Biochim. Biophys. Acta 1475 (2000) 287-294.

2. R.J. Linhardt, N.S. Gunay. Production and Chemical Processing of Low Molecular Weight Heparins, Semin. Thromb. Hemost. 25 (1999) 5-16.

3. H.L. Messmore, W.H. Wehrmacher, E. Coyne, J. Fareed, Heparin to pentasaccharide and beyond: the end is not in sight, Semin. Thromb. Hemost. 30 (2004) 81-88.

4. A. Liang, X. He, Y. Du, K. Wang, Y. Fung, B. Lin, Capillary zone electrophoresis investigation of the interaction between heparin and granulocyte-colony stimulating factor, Electrophoresis 25 (2006) 870-875.

5. I. Capila, R.J. Linhardt, Heparin-Protein interactions, Angew. Chem. Int. Ed. 41 (2002) 390-412.

6. N.S. Gandhi, R.L. Mancera, The structure of glycosaminoglycans and their interactions with proteins, Chem. Biol. Drug Des. 72 (2008) 455-482.

7. D.L. Rabenstein, Heparin and heparin sulfate: structure and function, Nat. Prod. Rep. 19 (2002) 312-331.

8. J.M. Whitelock, RV Iozzo, Heparan Sulfate: A Complex Polymer Charged with Biological Activity, Chem. Rev. 105 (2005) 2745-2746.

9. R.J. Linhardt, J.S. Dordick, P.L. Deangelis, J. Liu. Enzymatic Synthesis of Glycosaminoglycan Heparin, Semin. Thromb. Hemost. 33 (2007) 453-465.

10. H.L. Messmore, W.H. Wehrmacher, E. Coyne, J. Fareed, Heparin to pentasaccharide and beyond: the end is not in sight, Semin Thromb Hemost. 30 (2004), 81-88.

11. U.R. Desai, Antithrombin activation and designing novel heparin mimics, in: B.D. Jones, R.Z. Smith (Eds.) Chemistry and Biology of Heparin and Heparan Sulfate, New York: Elsevier Ltd. 2005, pp. 483-512.

12. J. Hirsh, K.A. Bauer, M.B. Donati, M. Gould, M.M. Samama, J.I. Weitz, Parenteral anticoagulants: American College of Chest Physicians evidenced-based guidelines (8^{th} edition), Chest 133 (2008) 141S-159S.

13. E. Racine, Differentiation of low-molecular-weight heparins, Pharmacotherapy 21 (2001) 62S-70S.

14. U.R. Desai, Antithrombin activation and designing novel heparin mimics, in: H.G. Garg, R.J. Linhardt, C.A. Hales eds., Chemistry and biology of heparin and heparan sulfate, London: Elsevier Ltd. (2005) 483-512.

15. ^{1}S. Laporte, J. Liotier, L. Bertoletti, F.X. Kleber, G.F. Pineo, C. Chapelle, N. Moulin, P. Mismetti, Individual patient data meta-analysis of enoxaparin vs

unfractionated heparin for venous thromboembolism prevention in medical patients, J. Thromb. Haemost. 9 (2011) 454-472.

16. W.H. Geerts, D. Bergqvist, G.F. Pineo, J.A. Heit, C.M. Samama, M.R. Lassen, C.W. Colwell, Prevention of venous thromboembolism: American College of Chest Physicians evidence-based clinical practice guidelines (8th edition), Chest 133 (2008) 381S-453S.

17. A.F. Shorr, E.A. Nutescu, E. Farrelly, R. Horblyuk, L.E. Happe, M. Franklin, Post discharge oral versus Injectable anticoagulation following major orthopedic surgery, Ann. Pharmacother. 42 (2008) 1222-1228.

18. J.I. Weitz, Low molecular weight heparins, N. Engl. J. Med. 337 (1997) 688-698.

19. Lovenox (enoxaparin sodium) injection. Sanofi-Aventis 2009 ; http://products.sanofi-aventis.us/lovenox/lovenox.html#section-14, Acessed : 3/21/2011

20. E. Gray, B. Mulloy, Biosimilar low molecular weight heparin products, J. Thromb. Haemost. 7 (2009) 1218-1221.

21. J. Fareed, W.L. Leong, D.A. Hoppensteadt, W.P. Jeske, J. Walenga, R. Wahi, R.L. Bick, Generic low-molecular-weight heparins: some practical considerations, Semin. Thromb. Hemost. 6 (2004) 703-713.

22. M. Gomes, E. Ramacciotti, D. Hoppensteadt, J.M. Walenga, B. Lewis, I. Thethi, J. Fareed, An open label, non-randomized, prospective clinical trial evaluating the immunogenicity of branded enoxaparin versus biosimilars in healthy volunteers, Clin. Appl. Thromb. Hemost. 17 (2011) 66-69.

23. T.K. Kishimoto, K. Viswanathan, T. Ganguly, S. Elankumaran, S. Smith, K. Pelzer, J.C. Lansing, N. Sriranganathan, G. Zhao, Z. Galcheva-Gargova, A. Al-Hakim,

G.S. Bailey, B. Fraser, S. Roy, T. Rogers-Cotrone, L. Bushe, M. Whary, J. Fox, M. Nasr, G.J. Dal Pan, Z. Shriver, R.S. Langer, G. Venkataraman, K.F. Austen, J. Woodcock, R. Sasisekharan, Contaminated heparin associated with adverse clinical events and activation of the contact system, N. Engl. J. Med. 358 (2008) 2457-2467.

24. D.B. Blossom, A.J. Kallen, P.R. Patel, A. Elward, L. Robinson, G. Gao, R. Langer, K. Perkins, J.L. Jaeger, K.M. Kurkijian, M. Jones, S.F. Schillie, N. Shehab, D. Ketterer, G. Venkataraman, T.K. Kishimoto, Z. Shriver, A.W. McMahon, K.F. Austen, S. Kozlowski, A. Srinivasan, G. Turabelidze, C.V. Gould, M.J. Arduino, R. Sasisekharan, Outbreak of adverse reactions associated with contaminated heparin, N. Engl. J. Med. 359 (2008) 2674-2684.

25. J. McKee, S. Bairstow, C. Szabo, J. Ray, T. Wielgos, P. Hu, E. Chess, M. Nordhaus, T. Hai, J. Campbell, S. Donovan, N. Viseux, N. Riedel, J. Cammack, R. Johnson, Structure elucidation and biological activity of the oversulfated chondroitin sulfate contaminant in Baxter heparin, J. Clin. Pharmacol. 50 (2010) 1159-1170.

26. M. Guerrini, D. Beccati, Z. Shriver, A. Naggi, K. Viswanathan, A. Bisio, I. Capila, J.C. Lansing, S. Guglieri, B. Fraser, A. Al-Hakim, N.S. Gunay, Z. Zhang, L. Robinson, L. Buhse, M. Nasr, J. Woodcock, R. Langer, G. Venkataraman, R.J. Linhardt, B. Casu, G. Torri, R. Sasisekharan, Oversulfated chondroitin sulfate is a contaminant in heparin associated with adverse clinical events, Nat. Biotech. 26 (2008) 669-675.

27. A. Adam, N. Montpas, D. Keire, A. Désormeaux, N.J. brown, F. Marceau, B. Westenberger, Bradykinin forming capacity of oversulfated chondroitin sulfate contaminated heparin in vitro, Biomaterials 31 (2010) 5741-5748.

28. C. Hai, Airway smooth muscle cell as therapeutic target of inflammation, Curr. Med. Chem. 14 (2007) 67-76.

29. Heparin Sodium. Pharmacopeial forum. The United States Pharmacopeal Convention. Sept-oct 2009, 35.

30. D.A. Keire, H. Ye, M.L. Trehy, W. Ye, R.E. Kolinski, B.J. Westenberger, L.F. Buhse, M. Nasr, A. Al-Hakim, Characterization of Currently Marketed Heparin Products: Key Tests for Quality Assurance, Anal Bioanal Chem. 399 (2011) 581-591.

31. C.A. Thompson, FDA approves first generic enoxaparin product, Am. J. Health Syst. Pharm. 67 (2010) 1486-1488.

32. The identity problem. Nat Biotech 2010;28:877.

33. L.B. Jaques, L.W. Kavanagh, M. Mazurek, A.S. Perlin, The Structure of Heparin Proton Magnetic Resonance Spectral Observations, Biochem. Biophys. Res. Commun. 24 (1966) 447-451.

34. S. Inoue, Y. Inoue, Nuclear Magnetic Resonance Study of Sulfated Mucopolysaccharides, Biochem. Biophys. Res. Commun. 23 (1966) 513-517.

35. A.S. Perlin, D.M. Mackie. Evidence for a (1→4)-Linked 4-O-(α-L-Idopyranosyluronic Acid 2-Sulfate)-(2-Deoxy-2-Sulfoamino-D-Glucopyranosyl 6-Sulfate) sequence in heparin, Carbohyd. Res. 18 (1971) 185-194.

36. A. Pervin, C. Gallo, K.A. Jandik, X.J. Han, R.J. Linhardt, Preparation and Structural Characterization of Large Heparin-Derived Oligosaccharides, Glycobiology 5 (1995) 83-95.

37. A. Larnkjaer, S.H. Hansen, P.B. Østergaard, Isolation and characterization of hexasaccharides derived from heparin, Analysis by HPLC and elucidation of structure by 1H NMR, Carbohyd. Res. 266 (1995) 37-52.

38. H.B. Nader, M.A. Porcionatto, L.S.I. Tersariol, M.A.S. Pinhal, F.W Oliveira, C.T. Moraes, C.P. Dietrich, Purification and Substrate Specificity of Heparitinase I and Hparitinase II from Flavobacterium heparinum, J. Biol. Chem. 265 (1990) 16807-16813.

39. P. Bigler, R. Brenneisen, Improved impurity fingerprinting of heparin by high resolution 1H NMR, J. Pharm. Biomed. Anal. 49 (2009) 1060-1064.

40. G.A. Neville, F. Mori, K.R. Holme, A.S. Perlin, Monitoring the purity of pharmaceutical heparin preparations by high-field 1H-Nuclear magnetic resonance spectroscopy, J. Pharm. Sci. 78 (1989) 101-104.

41. M. Guerrini, A. Bisio, G. Torri, Combined quantitative 1H and 13C nuclear magnetic resonance spectroscopy for characterization of heparin preparations, Semin. Thromb. Hemost. 27 (2001) 473-482.

42. K.R. Holme, A.S. Perlin, Nuclear magnetic resonance spectra of heparin in admixture with dermatan sulfate and other glycosaminoglycans. 2-D spectra of the chondroitin sulfates, Carb. Res. 186 (1989) 301-312.

43. T. Maruyama, T. Toida, T. Imanari, G. Yu, R.J. Linhardt, Conformational changes and anticoagulant activity of chondroitin sulfate following its O-sulfonation, Carb. Res. 306 (1998) 35-43.

44. T. Beyer, B. Diehl, G. Randel, E. Humpfer, H. Schäfer, M. Spraul, C. Schollmayer, U Holzgrabe, Quality Assessment of Unfractionated Heparin Using 1H Nuclear Magnetic Resonance Spectroscopy, J. Pharm. Biomed. Anal. 48 (2008) 13-19.

45. Z. Zhang, B. Li, J. Suwan, F. Zhang, Z. Wang, H. Liu, B. Mulloy, R.J. Linhardt, Analysis of Pharmaceutical Heparins and Potential Contaminants Using 1H-NMR and PAGE, J. Pharm. Biomed. Anal. 98 (2009) 4017-4026.

46. D.A. Keire, M.L. Trehy, J.C. Reepmeyer, R.E. Kolinski, W. Ye, J. Dunn, B.J. Westenberger, L.F. Buhse, Analysis of crude heparin by 1H-NMR, Capillary Electrophoresis, and strong-anion-exchange-HPLC for contamination by oversulfated chondroitin sulfate, J. Pharm. Biomed. Anal. 51 (2010) 921-926.

47. A.K. Korir, V.K. Almeida, D.S. Malkin, C.K. Larive, separation and analysis of nanomole quantities of heparin oligosaccharides using on-line capillary isotachophoresis coupled with NMR detection, Anal. Chem. 77 (2005) 5998-6003.

48. J.F.K. Limtiaco, C.J. Jones, C.K. Larive, Characterization of heparin impurities with HPLC-NMR using weak anion exchange chromatography, Anal. Chem. 81 (2009) 10116-10123.

49. T. Beyer, M. Matz, D. Brinz, O. Rädler, B. Wolf, J. Norwig, K. Baumann, S. Alban, U. Holzgrabe, Composition of OSCS-contaminated heparin occurring in 2008 in batches on the german market, Eur. J. Pharm. Sci. 40 (2010) 297-304.

50. M.A. Lima, T.R. Rudd, E.H.C. de Farias, L.F. Ebner, T.F. Gesteira, L.M. de Souza, A. Mendnes, C.R. Córdula, J.R.M. Martins, D. Hoppensteadt, J. Fareed, G.L. Sassaki, E.A. Yates, I.L.S. Tersariol, H.B. Nader, A new approach for heparin standardization: Combination of scanning UV spectroscopy, nuclear magnetic resonance and principle component analysis, Analayst 6 (2011) 1-9.

51. Q. Zang, D.A. Keire, R.D. Wood, L.F. Buhse, C.M.V. Moore, M. Nasr, A. Al-Hakim, M.L. Trehy, W.J. Welsh, Combining 1H NMR spectroscopy and chemometrics

to identify heparin samples that may possess dermatan sulfate DS impurities or oversulfated chondroitin sulfate (OSCS) contaminants, J. Pharm. Biomed. Anal. 54 (2011) 1020-1029.

52. T.R. Rudd, D. Gaudesi, M.A. Skidmore, M. Ferro, M. Guerrini, B. Mulloy, G. Torri, E.A. Yates, Construction and use of a library of bona fide heparins employing 1H NMR and multivariate analysis, Analyst 36 (2011) 1380-1389.

53. M. Ringnér, What is principal component analysis, Nat. Biotech. 26 (2008) 303-304.

54. E. Bednarek, J. Sitkowski, W. Bocian, B. Mulloy, L. Kozerski, An assessment of polydispersed species in unfractionated and low molecular weight heparins by diffusion ordered nuclear magnetic resonance spectroscopy method, J. Pharm. Biomed. Anal. 53 (2010) 302-308.

55. J. Sitowski, E. Bednarek, W. Bocian, L. Kozerski, Assessment of oversulfated chondroitin sulfate in low molecular weight and unfractionated heparins diffusion ordered nuclear magnetic resonance spectroscopy method, J. Med. Chem. 51 (2008) 7663-7665.

56. T.R. Rudd, D. Gaudesi, M.A. Lima, M.A. Skidmore, B. Mulloy, G. Torri, H.B. Nader, M. Guerrini, E.A. Yates, High-sensitivity visualization of contaminants in heparin nsamples by spectral filtering of 1H NMR spectra, Analyst 136 (2011) 1390-1398.

57. P. Bigler, R. Brenneisen, Improved impurity fingerprinting of heparin by high resolution 1H NMR spectroscopy, J. Pharm. Biomed. Anal. 49 (2009) 1060-1064.

58. J.A. Spencer, J.F. Kauffman, J.C. Reepmeyer, C.M. Gryniewicz, W. Ye, D.Y. Toler, L.F. Buhse, B.J. Westenberger, Screening of heparin API by near infrared reflectance and raman spectroscopy, J. Pharm. Sci. 98 (2009) 3541-3547.

59. C. Sun, H. Zang, X. Liu, Q. Dong, L. Li, F. Wang, L. Sui, Determination of potency of heparin active pharmaceutical ingredient by near infrared reflectance spectroscopy, J. Pharm. Biomed. Anal. 51 (2010) 1060-1063.

60. T.R. Rudd, S.E. Guimond, M.A. Skidmore, L. Duchesne, M. Guerrini, G. Torri, C. Cosentino, A. Brown, D. T. Clarke, J.E. Turnbull, D. G. Fernig, E.A. Yates,Influence of substitution pattern and cation binding on conformation and activity in heparin derivatives, Glycobiology 17 (2007) 983-993.

61. I. McEwen, T. Rundlöf, M. Ek, B. Hakkarainen, G. Carlin, T. Arvidsson, Effects of Ca^{2+} on the 1H NMR chemical shift off the methyl signal of oversulphated chondroitin sulfate, a heparin contaminant, J. Pharm. Biomed. Anal. 49 (2009) 816-819.

62. E.C. Stevens, E.R. Morris, D.A. Rees, J.C. Sutherland, Synchrotron light source applied to measuring the vacuum ultraviolet circular dichromism of heparin, J. Am. Chem. Soc. 107 (1985) 2982-2983.

63. R.B.C. Jagt, R.F. Gomez-Biagi, M. Nitz, Pattern-based recognition of heparin contaminants by an array of self-assembling fluorescent receptors, Angew. Chem. Int. Ed. Engl. 48 (2009) 1995-1997.

64. C.P. Dietrich, H.B. Nader, L.R.G. Britto, M.E. Silva. Fractionation and Characterization of four acidic mucopolysaccharides in heparitin sulfate from beef lung tissue, Biochim. Biophys. Acta. 237 (1971) 430-441.

65. K.G. Rice, M.K. Rottink, R.J. Linhardt, Fractionation of heparin-derived oligosaccharides by gradient polyacrylamide-gel electrophoresis, Biochem. J. 244 (1987) 515-522.

66. W. Mao, C. Thanwiroon, R.J. Linhardt, Capillary electrophoresis for the analysis of glycosaminoglycan-derived oligosaccharides, Biomed. Chromatogr. 16 (2002) 77-94.

67. M. Dantuluri, U.R. Desai, Capillary electrophoresis of sulfated molecules, Recent Res. Devel. Anal. Biochem. 3 (2003) 1-18.

68. A.K. Korir, C.K. Larive, Advances in the separation, sensitive detection, and characterization of heparin and heparan sulfate, Anal. Bioanal. Chem. 393 (2009) 155-169.

69. P. Gebauer, Z. Malá, P. Boček, Recent progress in analytical capillary isotachophoresis, Electrophoresis 32 (2011) 83-89.

70. S. E. Deeb, M. A. Iriban, R. Gust, MECK as a powerful growing analytical technique, Electrophoresis 32 (2011) 166-183.

71. C. Heller, Principles of DNA separation with capillary electrophoresis, Electrophoresis 22 (2001) 629-643.

72. K. Shimura, Recent advances in IEF in capillary tubes and microchips, Electrophoresis 30 (2009) 11-28.

73. F. Yang, J. Zhao, S. Li, CEC of phytochemical bioactive compounds, Electrophoresis 31 (2010) 260-277.

74. K. Salomon, D.S. Burgi, J.C. Helmer, Evaluation of fundamental properties of a silica capillary used for capillary electrophoresis, J. Chromatogr. A. 559 (1991) 69-80.

75. R. Weinberger, Practical Capillary Electrophoresis 2nd ed, Academic Press, New York, 2000, 31-35.

76. A. Pervin, A. Al-Hakim, R.J. Linhardt, Separation of glycosaminoglycan-derived oligosaccharides by capillary electrophoresis using reverse polarity, Anal. Biochem. 221 (1994) 182-188.

77. U.R. Desai, H. Wang, S.A. Ampofo, R.J. Linhardt, Oligosaccharide composition of heparin and low-molecular-weight heparins by capillary electrophoresis, Anal. Biochem. 213 (1993) 120-127.

78. M. Militsopoulou, C. Lecomte, C. Bayle, F. Couderc, N.K. Karamanos, Laser-induced fluorescence as a powerful detection tool for capillary electrophoretic analysis of heparin/heparan sulfate disaccharides, Biomed. Chromatogr. 17 (2003) 39-41.

79. T. Toida, R.J. Linhardt, Detection of glycosaminoglycans as a copper (II) complex in capillary electrophoresis, Electrophoresis 17 (1996) 341-346.

80. I. Ramasamy, J. Kennedy, K. Tan, Capillary electrophoresis for characterization of low molecular weight heparins, Lab. Hematol. 9 (2003) 64-66.

81. R.P. Patel, C. Narkowicz, J.P. Hhutchinson, E.F. Hilder, G.A. Jacobson, A simple capillary electrophoresis method for the rapid separation and determination of intact low molecular weight and unfractionated heparins, J. Pharm. Biomed. Anal. 46 (2008) 30-35.

82. R. Domanig, W. Jöbstl, S. Gruber, T. Freudemann, One-dimensional cellulose acetate plate electrophoresis - A feasible method for analysis of dermatan sulfate and other glycosaminoglycan impurities in pharmaceutical heparin, J. Pharm. Biomed. Anal. 49 (2009) 151-155.

83. D.A. Keire, M.L. Trehy, J.C. Reepmeyer, R.E. Kolinski, W.Ye, J. Dunn, B.J. Westenberger, L.F. Buhse, Analysis of crude heparin by 1H NMR, capillary electrophoresis, and strong-anion-exchange-HPLC for contamination by oversulfated chondroitin sulfate, J. Pharm. Biomed. Anal. 51 (2010) 921-926.

84. T. Wielgos, K. Havel, N. Ivanova, R. Weinberger, Determination of impurities in heparin by capillary electrophoresis using high molarity phosphate buffers, J. Pharm. Biomed. Anal. 49 (2009) 319-326.

85. S. Beni, J.F.K. Limtiaco, C. K. Larive, Analysis and characterization of heparin impurities, Anal. Bioanal. Chem. 399 (2011) 527-539.

86. G.W. Somsen, Y.H. Tak, J.S. Torano, P.M.J.M. Jongen, G.J. de Jong, Determination of oversulfated chondroitin sulfate and dermatan sulfate impurities in heparin by capillary electrophoresis, J. Chrom. A. 1216 (2009) 4107-4112.

87. V. Tripodi, S. Flor, C. Dobrecky, M. Continn, S. Lucangioli, Novel and highly sensitive mixed-polymeric electrokinetic chromatography system for determination of contaminants and impurities of heparin samples, Electrophoresis 31 (2010) 3606-3612.

88. N. Volpi, F. Maccari, R.J. Linhardt, Quantitative capillary electrophoresis determination of oversulfated chondroitin sulfate as a contaminant in heparin preparations, Anal. Biochem. 388 (2009) 140-145.

89. M.D. Bischel, J.H. Austin, M.D. Kemeny, C.M. Hubble, R.K. Lear, Separation and identification of acid polysaccharides by thin-layer chromatography, J. Chromatogr. 21 (1966) 40-45.

90. J.A. Cifonelli, Reactions of heparitin sulfate with nitrous acid, Carbohydr. Res. 8 (1968) 233-242.

91. M.J. Bienkowaki, H.E. Conrad, Structural characterization of oligosaccharides formed by depolymerization of heparin with nitrous acid, J. Biol. Chem. 260 (1985) 356-365.

92. C. Thanawiroon, R.J. Linhardt, Separation of a complex mixture of heparin-derived oligosaccharides using reversed-phase high performance liquid chromatography, J. Chromatogr. A. 1014 (2003) 215-233.

93. J. Henriksen, P. Roepstorff, L.H, Ringborg, Ion-pairing reversed-phased chromatography/mass spectrometry of heparin, Carbohydr. Res. 31 (2006) 382-387.

94. B. Kuberan, M. Lech, L. Zhang, Z.L. Wu, D.L. Beeler, R.D. Rosenberg, Analysis of heparan sulfate oligosaccharides with ion pair-reverse phase capillary high performance liquid chromatography-microelectrospray ionization time-of-flight mass spectrometry, J. Am. Chem. Soc. 124 (2002) 8707-8718.

95. J.E. Camamra, M.B. Satterfield, B.C. Nelson, Quantitative determination off disaccharide content in digested unfragmented heparin and low molecular weight heparin by direct-infusion electrospray mass spectrometry, J. Pharm. Biomed. Anal. 43 (2007) 1706-1714.

96. J. Henriksen, P. Roepstorff, L.H. Ringborg, Ion-pairing reversed-phased chromatography/mass spectrometry of heparin, Carbohydr. Res. 31 (2006) 382-387.

97. B. Kuberan, M. Lech, L. Zhang, Z.L. Wu, D.L. Beeler, R.D. Rosenberg, Analysis of heparan sulfate oligosaccharides with ion pair-reverse phase capillary high performance liquid chromatography-microelectrospray ionization time-of-flight mass spectrometry, J. Am. Chem. Soc. 124 (2002) 51-56.

98. N.K. Karamanos, P. Vanky, G.N. Tzanakakis, T. Tsegenidis, A. Hjerpe, Ion-pair high-performance liqueid chromatography for determining disaccharide composition in heparin and heparan sulphate, J. Chromatogr. A. 765 (1997) 169-179.

99. A.K. Korir, J.F.K. Limtiaco, S.M. Gutierrez, C.K. Larive, Ultraperfornace ion-pair liquid chromatography coupled to electrospray time-of-flight mass spectrometry for compositional profiling and quantification of heparin and heparan sulfate, Anal. Chem. 80 (2008) 1297-1306.

100. R.P. Patel, C. Narkowics, G.A. Jacobson, Effective reverse-phase ion pair high-performance liquid chromatography method for the separation and characterization of intact low-molecular-weight heparins, Anal. Biochem. 387 (2009) 113-121.

101. C.E. Doneanuk, W. Chen, J.C. Gebler, Analysis of oligosaccharides derived from heparin by ion-pair reversed-phase chromatography/mass spectrometry, Anal. Chem. 81 (2009) 3485-3499.

102. M.L. Trehy, J.C. Reepmeyer, R.E. Kolinski, B.J. Westenberger, L.F. Buhse, Analysis of heparin sodium by SAX/HPLC for contaminants and impurities, J. Pharm. Biomed. Anal. 49 (2009) 670-673.

103. D.A. Keire, D.J. Mans, H. Ye, R.E. Kolinski, L.F. Buhse. Assay of possible economimcally motivated additives or native impurities levels in heparin by 1H NMR, SAX-HPLC, and anticoagulation time approaches. J. Pharm. Biomed. Anal. 52 (2010) 656-664.

104. N. Hashii, N. Kawasaki, S. Itoh, Y. Quin, N. Fujita, T. Hattori, K. Miyata, A. Bando, Y. Sekimoto, T. Hama, M. Kashimura, M. Tatsumi, K. Mabuchi, H. Namekawa, T. Sakai, M. Hirose, S. Dobashi, H. Shimasashi, S. Koyama, S. O. Herr, K. Kawai, H.

Yoden, T. Yamaguchi, Heparin identification test and purity test for OSCS in heparin sodium and heparin calcium by weak anion-exchange high-performance liquid chromatography, Biologicals 38 (2010) 539-543.

105. T. E. Turnbull, J. T. Gallagher, Oligosaccharide mapping of heparan sulphate by polyacrylamide-gradient-gel electrophoresis and electrotransfer to nylon membrane, Biochem. J. 251 (1988) 597-608.

106. R. J. Linhardt, D. Loganathan, A. al-Hakim, H. M. Wang, J. M. Walenga, D. Hoppensteadt, J. Fareed, Oligosaccharide mapping of low molecular weight heparins: structure and activity differences, J. Med. Chem. 33 (1990) 1639-1645.

107. R. E. Edens, A. al-Hakim, J. M. Weiler, D. G. Rethwisch, J. Fareed, R. J. Linhardt, Gradient polyacrylamide gel electrophoresis for determination of molecular weights of heparin preparations and low-molecular-weight heparin derivatives, J Pharm. Sci. 81 (1992) 823-827.

108. R. Malsch, J. Harenberg, L. Piazolo, G. Huhle, D. L. Heene, Chromatographic and electrophoretic applications for the analysis of heparin and dermatan sulfate, J. Chromatogr. B Biomed. Appl. 685 (1996) 223-231.

109. N. Volpi, Characterization of heparins with different relative molecular masses (from 11,600 to 1600) by various analytical techniques, J. Chromatogr. 622 (1993) 13-20.

110. H. Komatsu, K. Yoshii, S. Ishimitsu, S. Okada, T. Takahata, Molecular mass determination of low-molecular-mass heparins. Application of wide collection angle measurements of light scattering using a high-performance gel permeation

chromatographic system equipped with a low-angle laser light-scattering photometer, J. Chromatogr. 644 (1993) 17-24.

111. H. Komatsu, T. Takahata, M. Tanaka, S. Ishimitsu, S. Okada, Determination of the molecular-weight distribution of low-molecular-weight heparins using high-performance gel permeation chromatography, Biol. Pharm. Bull. 16 (1993) 1189-1193.

112. R. Malsch, J. Harenberg, High-performance size exclusion chromatography and polyacrylamide gel electrophoresis for characterization of unfractionated and low molecular mass glycosaminoglycans, Semin. Thromb. Hemost. 20 (1994) 135-143.

113. U. R. Desai, R. J. Linhardt, Molecular weight of low molecular weight heparins by 13C nuclear magnetic resonance spectroscopy, Carbohydr. Res. 255 (1994) 193-212.

114. B. Mulloy, C. Gee, S. F. Wheeler, R. Wait, E. Gray, T. W. Barrowcliffe, Molecular weight measurements of low molecular weight heparins by gel permeation chromatography, Thromb. Haemost. 77 (1997) 668-674.

115. K. G. Rice, Y. S. Kim, A. C. Grant, Z. M. Merchant, R. J. Linhardt, High-performance liquid chromatographic separation of heparin-derived oligosaccharides, Anal. Biochem. 150 (1985) 325-331.

116 L. Rosenfeld, M. T. Prior, L. M. Girardi, Comparison of the separation of bovine heparin by strong anion exchange and by gel filtration chromatography, Thromb. Res. 64 (1991) 203-211.

117. R. E. Hileman, A. E. Smith, T. Toida, R. J. Linhardt, Preparation and structure of heparin lyase-derived heparan sulfate oligosaccharides, Glycobiology 7 (1997) 231-239.

118. J. E. Turnbull, Analytical and preparative strong anion-exchange HPLC of heparan sulfate and heparin saccharides, Methods Mol. Biol. 171 (2001) 141-147.

119. W. L. Chuang, H. McAllister, L. Rabenstein, Chromatographic methods for product-profile analysis and isolation of oligosaccharides produced by heparinase-catalyzed depolymerization of heparin, J. Chromatogr. A. 932 (2001) 65-74.

120. R. R. Vivès, S. Goodger, D. A. Pye, Combined strong anion-exchange HPLC and PAGE approach for the purification of heparan sulphate oligosaccharides, Biochem. J. 354 (2001) 141-147.

121. B. Casu, M. Guerrini, A. Naggi, G. Torri, L. De-Ambrosi, G. Boveri, S. Gonella, A. Cedro, L. Ferró, E. Lanzarotti, M. Paterno, M. Attolini, M. G. Valle, Characterization of sulfation patterns of beef and pig mucosal heparins by nuclear magnetic resonance spectroscopy. Arzneimittelforschung 46 (1996) 472-477.

122. M. Sudo, K. Sato, A. Chaidedgumjorn, H. Toyoda, T. Toida, T. Imanari, (1)H nuclear magnetic resonance spectroscopic analysis for determination of glucuronic and iduronic acids in dermatan sulfate, heparin, and heparan sulfate, Anal. Biochem. 297 (2001) 42-51.

123. M. Guerrini, S. Guglieri, A. Naggi, R. Sasisekharan, G. Torri, Low molecular weight heparins: structural differentiation by bidimensional nuclear magnetic resonance spectroscopy. Semin. Thromb. Hemost. 33 (2007) 478-487.

124. J. Sitkowski, E. Bednarek, W. Bocian, L. Kozerski, Assessment of oversulfated chondroitin sulfate in low molecular weight and unfractionated heparins diffusion ordered nuclear magnetic resonance spectroscopy method, J. Med. Chem. 51, 7663-7665.

125. W. Chai, J. Luo, C. K. Lim, A. M. Lawson, Characterization of heparin oligosaccharide mixtures as ammonium salts using electrospray mass spectrometry, Anal. Chem. 70 (1998) 2060-2066.

126. R. M. Pope C. S. Raska, S. C. Thorp, J. Liu, Analysis of heparan sulfate oligosaccharides by nano-electrospray ionization mass spectrometry, Glycobiology 11 (2001) 505-513.

127. O. M. Saad, J. A. Leary, Compositional analysis and quantification of heparin and heparan sulfate by electrospray ionization ion trap mass spectrometry, Anal. Chem. 75 (2003) 2985-2995.

128. C. Thanawiroon, K. G. Rice, T. Toida, R. J. Linhardt, Liquid chromatography/mass spectrometry sequencing approach for highly sulfated heparin-derived oligosaccharides, J. Biol. Chem. 279 (2004) 2608-2615.

129. O. M. Saad, H. Ebel, K. Uchimura, S. D. Rosen, C. R. Bertozzi, J. A. Leary, Compositional profiling of heparin/heparan sulfate using mass spectrometry: assay for specificity of a novel extracellular human endosulfatase, Glycobiology 15 (2005) 818-826.

130. S. A. Ampofo, H.-M. Wang, R. J. Linhardt, Disaccharide compositional analysis of heparin and heparan sulfate using capillary zone electrophoresis, Anal. Biochem. 199 (1991) 249-255.

131. F. N. Lamari, M. Militsopoulou, T. N. Mitropoulou, A. Hjerpe, N. K. Karamanos, Analysis of glycosaminoglycan-derived disaccharides in biologic samples by capillary electrophoresis and protocol for sequencing glycosaminoglycans, Biomed. Chromatogr. 16 (2002) 95-102.

132. H. Kitagawa, A. Kinoshita, K. Sugahara, Microanalysis of glycosaminoglycan-derived disaccharides labeled with the fluorophore 2-aminoacridone by capillary electrophoresis and high-performance liquid chromatography, Anal. Biochem. 232 (1995) 114-121.

133. M. Militsopoulou, F. N. Lamari, A. Hjerpe, N. K. Karamanos, Determination of twelve heparin- and heparan sulfate-derived disaccharides as 2-aminoacridone derivatives by capillary zone electrophoresis using ultraviolet and laser-induced fluorescence detection, Electrophoresis 23 (2002) 1104-1109.

134. V. Ruiz-Calero, E. Moyano, L. Puignou, M. T. Galceran, Pressure-assisted capillary electrophoresis-electrospray ion trap mass spectrometry for the analysis of heparin depolymerised disaccharides, J. Chromatogr. A. 914 (2001) 277-291.

135. D. A. Armbruster, M. D. Tillman, L. M. Hubbs, Limit of detection (LOD)/Limit of quantitation (LOQ): Comparison of the empirical and the statistical methods exemplified with GC-MS assays of abused drugs, Clin. Chem. 40 (1994) 1233-1238.

136. J. B. Damm, G. T. Overklift, B. W. Vermeulen, C. F. Fluitsma, G. W. van Dedem, Separation of natural and synthetic heparin fragments by high-performance capillary electrophoresis, J. Chomatogr. 608 (1992) 297-309.

137. V. Duchemin, I. le Potier, C. Troubat, D. Ferrier, M. Taverna, Analysis of intact heparin by capillary electrophoresis using short end injection configuration, Biomed. Chromatogr. 16 (2002) 127-133.

138. T. Toida, R. J. Linhardt, Detection of glycosaminoglycans as a copper (II) complex in capillary electrophoresis, Electrophoresis 17 (1996) 341-346.

139. J Maddineni, J. M. Walenga, W. P. Jeske, D. A. Hoppensteadt, J. Fareed, R. Wahi, R. L. Bick, Product individuality of commercially available low-molecular-weight heparins and their generic versions: therapeutic implications, Clin. Appl. Thromb. Hemost. 12 (2006) 267-276.

140. U. R. Desai, New antithrombin-based anticoagulants, Med. Res. Rev. 24 (2004) 151-181.

141. Lever R, Page CP, Novel drug development opportunities for heparin, Nat Rev Drug Disc. 1 (2002) 140-149.

142. TN Wright, MG Kinsella, EE Qwarnström, The role of proteoglycans in cell adhesion, migration, and proliferation, Curr Op Cell Bio 4 (1992) 793-801.

143. M. Schuksz, M.M. Fuster, J.R. Brown, B.E. Crawford, D.P. Ditto, R. Lawrence, C.A. Glass, L. Wang, Y. Tor, J.D. Esko, Surfen, a small molecule antagonist of heparan sulfate, Proc. Natl. Acad. Sci. USA. 105 (2008) 13075-13080.

144. M Guerrini, Z. Zhang, Z, Shriver, A. Naggi, S. Masuko, R. Langer, B. Casu, R.J. Linhardt, G. Torri, R. Sasisekhran, Orthogonal analytical approaches to detect potential contaminants in heparin, Proc. Natl. Acad. Sci. USA 106 (2009) 16956-16961.

145. A.F. Portmann, W.D. Holden, Protamine Suplphate, heparin, and blood coagulation, 28 (1949) 1451-1458.

146. A. Liang, A. Raghuraman, U.R. Desai, Capillary electrophoretic study of small, highly sulfated, non-sugar molecules interacting with antithrombin, Electrophoresis 30 (2009) 1544-1541.

147. G.W. Dombi, Constructing nonlinear scatchard plots, J. Chem. Educ. 61 (1984) 527-528.

148. R.A. Al-Horani, U.R. Desai, Chemical Sulfation of Small Molecules - Advances and Challenges, Tetrahedron 66 (2010) 2907-2918.

149. S. Khan, J. Gor, B. Mulloy, S.J. Perkins, Semi-rigid solution structures of heparin by constrained X-ray scattering modelling: new insight into heparin-protein complexes, J. Mol. Biol. 395 (2010) 504-521.

150. J. Kloeckner, E. Wagner, M. Orgis, Degradable gene carriers based on oligomers, Eur. J. Pharm. Sci. 29 (2006) 414-425.

151. W. Fischer, B. Brissault, S. Prevost, M. Kopaczynska, I. Andreou, A. Janosch, M. Gradzielski, R. Haag, Synthesis of linear polyamines with different amine spacings and their ability to form dsDNA/siRNA complexes suitable for transfection, Macromol. Biosci. 10 (2010) 1073-1083.

152. T. Thomas, T.J. Thomas, Polyamine Metabolism and Cancer, J. Cell. Mol. Med. 7 (2003) 113-126.

153. D. Fischer, Y. Li, B. Ahlemeyer, J. Krieglstein, T. Kissel, In vitro cytotoxicity testing of polycations: influence of polymer structure on cell viability and hemolysis, Biomaterials 24 (2003) 1121-1131.

154. J. Fareed, O. Iqbal, H. Nader, S. Mousa, R. Wahi, E. Coyne, R.L. Bick, Generic low molecular weight heparins: a significant dilemma, Clin. Appl. Thromb. Hemostas. 11 (2005) 363-366.

155. W. Mao, C. Thanawiroon, R.J. Linhardt, Capillary electrophoresis for the analysis of glycosaminoglycans and glycosaminoglycan-derived oligosaccharides, Biomed. Chromatogr. 16 (2002) 77-94.

156. B. Yang, K. Solakyildirim, Y. Chang, R.J. Linhardt, Hyphenated techniques for the analysis of heparin and heparan sulfate, Anal. Bioanal. Chem. 399 (2011) 541-57.

157. N. Volpi, F. Maccari, Electrophoretic approaches to the analysis of complex polysaccharides, J. Chromatogr. B. Analyt. Technol. Biomed. Life Sci. 834 (2006) 1-13.

158. J. Zaia, On-line separations combined with MS for analysis of glycosaminoglycans, Mass. Spectrom. Rev. 28 (2009) 254-72.

159. W.P. Jeske, J.M. Walenga, D.A. Hoppensteadt, C. Vandenberg, A. Brubaker, C. Adiguzel, M. Bakhos, J. Fareed, Differentiating low-molecular-weight heparins based in chemical, biological, and pharmacologic properties: implications for the development of generic versions of low-molecular-weight heparins, Semin. Thromb. Hemost. 34 (2008) 74-85.

Vita

Joseph “Tim” King was born on July 21, 1983 in Athens, GA. Tim graduated from Grayson County High School in 2002 and completed his pre-pharmacy studies at Wytheville Community College and the University of Virginia’s College at Wise. He entered the doctor of pharmacy program at Virginia Commonwealth University’s School of Pharmacy in 2005 and subsequently enrolled in the combined PharmD/PhD program in 2006. He was the recipient of the J. Doyle Smith Award for excellence in teaching, research, and service from the department of medicinal chemistry and the Research Excellence Award for combined degree students in 2011.